CHALMERS
UNIVERSITY OF TECHNOLOGY

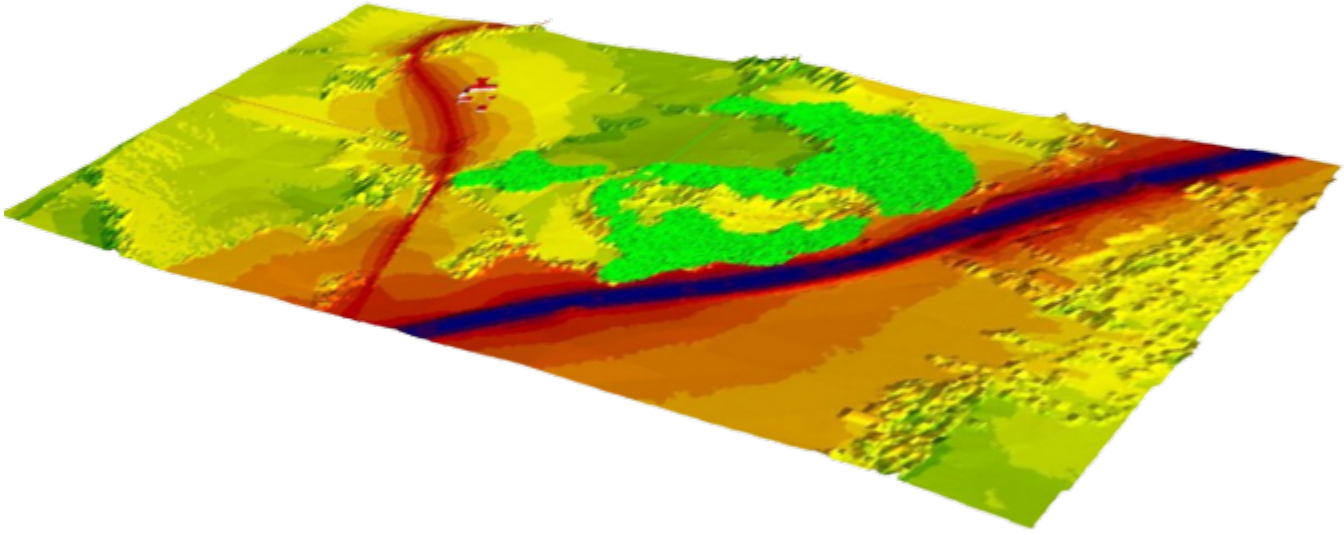

Assessment of noise from motorway E18 Tønsberg – Sandefjord in Norway

Master of Science Thesis in Applied Acoustics

Ehsan Hosseni

Department of Architecture and Civil Engineering
CHALMERS UNIVERSITY OF TECHNOLOGY
Master's thesis ACEX30
Gothenburg, Sweden 2022

MASTER'S THESIS ACEX30

Assessment of noise from E18 Tønsberg – Sandefjord in Norway

Ehsan Hosseini

CHALMERS
UNIVERSITY OF TECHNOLOGY

Department of Architecture and Civil Engineering
Division of Applied Acoustics
CHALMERS UNIVERSITY OF TECHNOLOGY
Gothenburg, Sweden 2022

Assessment of noise from E18 Tønsberg – Sandefjord in Norway

EHSAN HOSSEINI

Supervisor: Jorge Torres, Senior Advisor in Vibroacoustics at Brekke & Strand
Supervisor: Professor Jens Forssén, Department of Architecture and Civil Engineering
Examiner: Professor Jens Forssén, Department of Architecture and Civil Engineering

Department of Architecture and Civil Engineering
Division of Applied Acoustics
Chalmers University of Technology
SE-412 96 Gothenburg
Telephone +46 31 772 1000

Cover: An illustration of noise mapping at Kodalveien 31 using SoundPLAN 8.2.

Department of Architecture and Civil Engineering
Gothenburg, Sweden 2022

Assessment of noise from E18 Tønsberg– Sandefjord in Norway.
EHSAN HOSSEINI
Department of Applied Acoustics
Chalmers University of Technology

Abstract

In 2014, a motorway was established between Tønsberg and Sandefjord in Norway, with a speed limit of 110 km/h. However, residents living near the E18 have complained of disturbing noise. To increase understanding of the impact of noise generated by the E18, this study employed a series of measurement techniques. Long-term (24-hour) measurements of traffic noise levels were taken on the facades of buildings during the day and night. Short-term (1-hour) measurements of noise levels were taken in surrounding houses using four receiver positions. Additionally, noise mapping and simulated results by SoundPLAN 8.2 were correlated with the short-term monitoring measurements based on two prediction models, RLS-90 and Nord2000, in both winter and summer conditions. The findings suggest that Solbergveien 37 is prone to high sound levels due to temperature inversion. Specifically, sound pressure levels increased by more than 10 dB(A) at 8:00 in the wintertime. The study correlated the measured results with the prediction models at the designated locations. Furthermore, the analysis also focused on the formation of the traffic noise spectrum and its magnitudes at three specific measurement locations.

Keywords: Noise mapping, Nord2000, RLS-90, SoundPLAN, Short-term measurement, Long-term measurement, Traffic noise spectrum, E18.

Acknowledgements

I would like to take the opportunity to thank my supervisor at Brekke & Strand Jorge Torres for his consistent support and guidance during the running of this project. Also, Sigmund Olafsen for all the supervision and sharing of important materials which were really influential in shaping my measurement methods and critiquing my results. Additionally, I would like to express gratitude to Professor Jens Forssén in the division of Applied Acoustics at Chalmers University of Technology for his treasured support.

Ehsan Hosseini, Gothenburg, May 2022

Contents

List of Figures

List of Tables

1
Introduction

Noise is an undesired sound that can be produced by various sectors like transportation, manufacturing and utilities, and construction; the sound sources are automotive, train, airplane, and industrial machines. Transportation noise has always been a significant problem for humans, especially near highways, airports, or rials.
Community noise continues to grow by the increasing number of cars in the cities and the highways; human health can be affected by prolonged or excessive noise and it provides some issues such as stress, poor concentration, and sleep disturbance.
Norway is sparsely populated, but the cities and towns are densely populated, and traffic noise is the primary source that affects people in Norway. The Norwegian statistics has been estimated that about 30% of the total population is adversely affected by noise that exceeds 55 dB [1].
Also, road noise was the largest source of noise pollution in Norway in 2014, when 1.9 million of the population was affected. Traffic noise is a combination of propulsion noise by the engine, rolling noise from the tires, and the sound from the exhaust.
E18 has been on the current route between Tønsberg and Sandefjord since the 1990s. It has been a two-lane road with level crossings for a long time. In 2014, two new fields were opened in parallel with the old road, and the speed limit has now been set at 110 km/h. Some residents believe there is too much noise from E18 now, which set a study to increase the understanding of E18.
The noise assessments have included:

- Measurement of traffic noise levels during periods of the day and night-long term measurement (24-hour) using Norsonic 140
- Measurement of noise levels in the surrounding three houses at various locations using HEAD Acoustics (Squadriga)-short-term measurement (1-hour)
- Preparation of a computerized noise model and comparing to the field measurement (short-term measurements)

The theoretical background and noise prediction methods applied in the study are treated in Chapters 2 and 3; fundamental parameters of outdoor sound propagation explain in Chapter 2 as geometric spreading, atmospheric absorption, ground effect, diffraction by barriers, and atmospheric effects divided into refraction and turbulence, and reflection.
Chapter 3 discusses the theory of sound prediction methods, Nordic noise prediction Nord2000 and German noise prediction RLS-90, which the methods prescribe the calculation method for road noise mapping, and the Nord2000 propagation model can be applied for a variety of weather conditions.
Chapter 4 includes the material of measurement sites, measurement equipment, measurement techniques, the analysis of short and long measurements, and how to pre-

pare the model-building process in SoundPLAN 8.2.
Most of the discussions in Chapter 5 are devoted to interpreting the obtained results in various parts, for instance, the connection between the measurement and the simulated results.

2

Theoretical background

In this chapter, the fundamental parameters of outdoor sound propagation are explained; sound propagation in the atmosphere is an exciting topic in environmental acoustics related to predicting and controlling noise in an outdoor environment.
Outdoor sound propagation is affected by various parameters, namely wind, temperature, spreading, absorption, obstacles, humidity, pressure, ground type, terrain profile, turbulence, etc.

2.0.1 Geometric spreading

When a sound wave spreads from an omnidirectional source, by increasing the radius of the wave, the sound intensity decays which the intensity $I[w^2]$ at a distance of r in meter from the source power $I[w^2]$ is given as Equation 2.1 [2].

$$I = \frac{P}{4\pi r^2} \tag{2.1}$$

A point source creates a spherical wave that the sound level has a reduction of 6 dB by doubling the distance from the start; the relation between the sound power L_w and the sound pressure L_p is shown in Equation 2.2 [2].

$$L_p = L_w - 20\log r - 11dB \tag{2.2}$$

An infinite line source can be modeled as a cylindrical source. The cylindrical wavefront increases by radius, and by doubling the distance from the source, the sound pressure level reduces 3 dB.

2.0.2 Atmospheric absorption

Sound energy is converted to heat when it travels through the air. The atmospheric absorption is caused by heat conduction, shear viscosity, and molecular relaxation losses. The losses vary with the air's temperature, humidity, and atmospheric pressure; those losses are highest at high frequencies and in hot, dry weather [2].

2.0.3 Ground effect

A propagating sound wave can reach the receiver point directly and be reflected or absorbed by the ground. Hence, the sound pressure level of the receiver point can be mixed with the direct and reflected sound waves. The amount of ground attention

depends on the ground type, the frequency of the sound, the heights of the source and receiver, the propagation distance, and the angle of incidence.
The ground is an acoustically hard or soft surface; the incident sound energy is almost fully reflected on the hard surface. The asphalt surface is an example of a hard surface. For the soft ground as grass, only a tiny portion of incident sound energy reflected [4].

2.0.4 Diffraction by Barriers

Barriers are used along highways to help reduce the noise of streets in nearby neighborhoods. The effectiveness of noise barriers is related to the distance of obstacles to the source, and the noise barriers are most effective at short distances. Refraction limits the effectiveness of the walls, especially at more considerable distances in which the sound is bending to the ground into the shadow zone of the barrier. Figure 2.1 shows the effectiveness of the noise barrier [3].

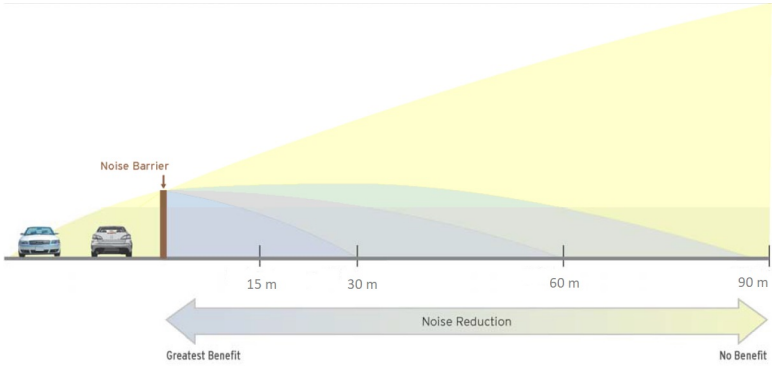

Figure 2.1: Diffraction by a barrier.

2.1 Atmospheric effects

2.1.1 Refraction

Sound propagation is affected by changes in atmospheric conditions such as air temperature, air velocity, relative humidity, wind, etc. The sound waves can be bent by wind and temperature variations and sound levels can be influenced by them, especially when the propagation distance is more significant than a few hundred meters [4].
In neutral atmospheric conditions, a sound source on the ground emits sound waves in all directions and leading sound rays in straight lines.

The speed of the sound changes with the temperature variations; at higher temperatures, the speed of the sound is also higher. The direction of the outdoor sound propagation changes once sound propagates at various velocities; then, the sound waves can be bent upwards or downwards.

Moreover, the land is heated by the sun, which makes the air warmer near the ground during the day, and the temperature decreases with height; the condition is called the temperature lapse which the sound waves are refracted upward and never reach the receiver point, besides, upward refraction creates an acoustics shadow zone with lower than usual sound levels.

The earth's surface begins to cool after sunset. The air is cooler on the ground than above, and the temperature increases with height; this condition is a temperature inversion. Hence, the sound waves are bent, and sound levels can be enhanced and higher than usual.

As mentioned earlier, wind also influences sound propagation, and the effects can be the same as temperature effects. Wind velocity increases with height caused by the air being denser near the ground and the presence of blockages, therefore wind closer to the ground moves slower, and sounds are reflected towards the ground; this can happen at an approximate distance of 300 m between source and receiver or more. When sound propagates against the wind (upwind), the velocity decreases with height, and the sound waves are reflected upwards. It creates an acoustical shadow zone near the ground [3] [4].

2.1.2 Turbulence

Outdoor sound propagation is affected by irregular air motions by winds that fluctuations in amplitude and phase are caused by sound propagating through a turbulent atmosphere. The speed of the sound increases by the turbulence in some locations and decreases in others, and those locations with high and low sound speed continuously change their positions with time. Also, more sound is in the shadow zones due to the turbulence, which acts as a collection of randomly positioned reflectors that reflect a part of the sound. The result of sound propagating through a turbulent atmosphere fluctuates in amplitude and phase, caused by temperature and wind fluctuations. The amplitude changes in sound level due to turbulence increases with increasing distance of propagation [5] [6].

2.2 Reflection

Acoustical reflection is divided into four phenomena: specular reflection, diffuse reflection, fraction, and diffraction, which are indicated in Figure 2.2. Specular reflection is the sound at the same angle as the incidence sound; diffuse reflection happens when the sound energy is scattered into non-specular directions, as shown in Figure 2.2.

The diffuse reflection can be divided into three mechanisms as the acoustical waves are speared out in all directions due to the roughness of an acoustic reflecting surface; the second is called the edge reflection, and the third mechanism of diffuse reflection, is known as a numerical diffuser which is a wall treatment, and wells of different depths produce non-specular reflections [7].

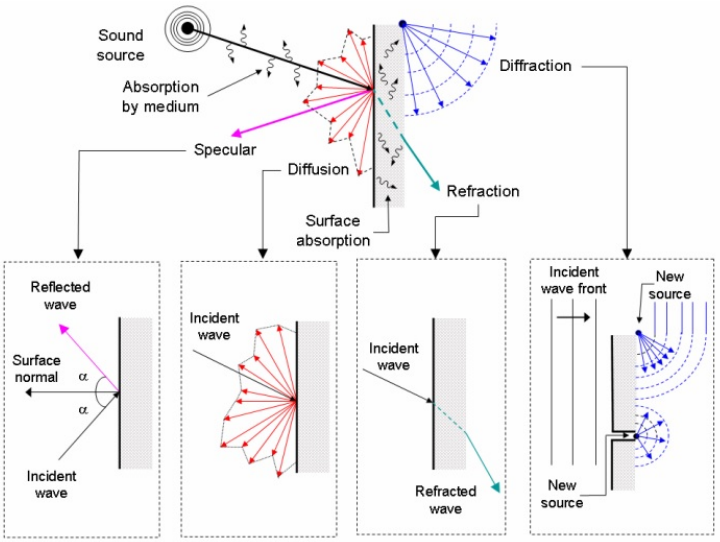

Figure 2.2: Specular reflection, diffuse reflection, fraction and diffraction phenomena [7].

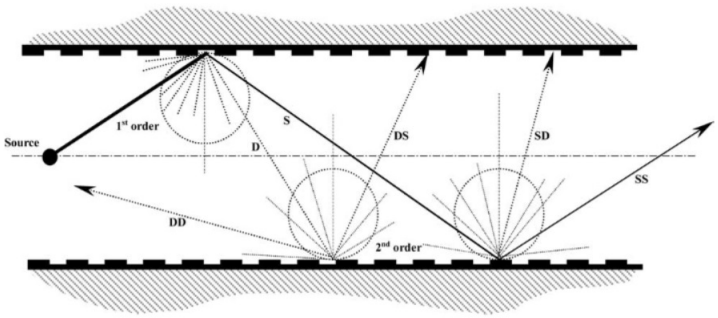

Figure 2.3: Specular and diffuse reflection between two facade [8].

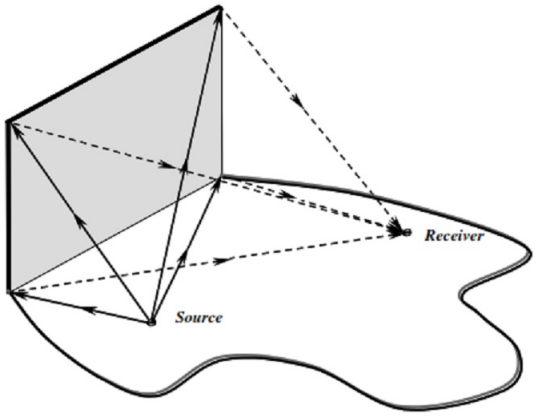

Figure 2.4: Radiation from a point source to a point receiver via a diffusing surface [8].

Figure 2.3 shows a point source of sound between two facades in the second reflection order. Figure 2.4 indicates a first-order diffuse reflection for a point source to the receiver position in which the coming sound for the source meets the diffusing surface, and some of its energy is scattered to the receiver. Moreover, the amount of the energy scattered to the receiver point is a function of the position, and the size of the scattering surface relative to the receiver and source [8].
The incident power P_i is divided into four elements as illustrated in Figure 2.5. Where P_r is reflected power, P_t is transmitted power, P_s is related to structure-borne sound and P_a is absorbed power [9].

$$P_i = P_r + P_t + P_s + P_a \tag{2.3}$$

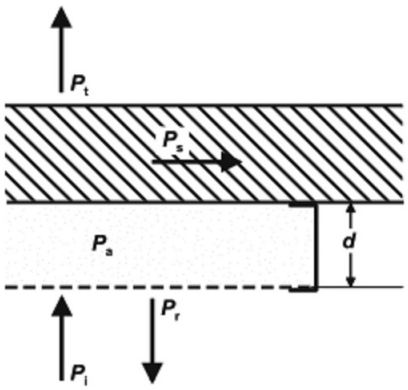

Figure 2.5: The four components of the incident power [9].

In a condition, if the mass per unit area of the obstacle which is a wall m''_w is larger than the oscillating mass per area of the air m''_a as stated in Equation 2.4, hence the major part of sound power is reflected the source and only a tiny portion of the sound power is transmitted [9].

$$m''_w >> m''_a = \frac{1}{\omega}\frac{p_i}{v_i} = \frac{1}{\omega}Z_0 = \frac{\rho_0 \lambda}{2\pi} \tag{2.4}$$

Where $\omega = 2\pi f$, λ is the wavelength, p_i is sound pressure, v_i is sound velocity, ρ_0 is the density of the air.
The absorption coefficient α of an absorber can be defined concerning its effectiveness; therefore, P_t and P_s can be added to P_a on the side of the source, as written in Equation 2.5 [9].

$$\alpha = \frac{P_a + P_t + P_s}{P_i} = \frac{P_i - P_r}{P_i} = 1 - \rho \tag{2.5}$$

Where ρ is the sound power reflection coefficient and the value of ρ, and α is between 0 to 1. Also, the effect of reflection can be stated as the ratio of amplitudes of the reflected sound wave and the incident sound wave, which is shown in Equation 2.6 based on sound pressure reflection factor r [9].

$$\rho = \frac{P_r}{P_i} = \frac{P_r^2}{P_i^2} = \mid r \mid^2 = 1 - \alpha \tag{2.6}$$

Besides, the wall impedance W can be obtained by real part W' and the imaginary part W'' of W, for normal incidence using the sound velocity v_w and the sound pressure p_w in the front of the wall, the wall impedance is written in following Equations below [9]:

$$W = \frac{p_w}{v_w} = W' + jW'' \tag{2.7}$$

$$r = \frac{W - \rho_0 c_0}{W + \rho_0 c_0} \tag{2.8}$$

$$\alpha = 1 - \mid r \mid^2 = \frac{4W'\rho_0 c_0}{(W' + \rho_0 c_0)^2 + W''^2} \tag{2.9}$$

Equation 2.9 is known as matching low when the imaginary part of the wall impedance is zero, then the absorption coefficient α achieves its maximum. If the real part of the wall impedance is equal to $\rho_0 c_0$, the maximum unity can be reached. In the opposite case for mismatched, the absorbers with partial reflection ($\rho < 1$), the sound field in the front of the wall or reflector consists of a forward progressive wave and a reflected wave in x-direction as written in Equation 2.10 [9].

$$p = p_0 e^{-jkx} + r\, p_0 e^{jkx} = (1 - r)\, p_0 e^{-jkx} + r\, p_0 (e^{-jkx} + e^{jkx}) \tag{2.10}$$

According to the given value for r, which is zero or one, two types of waves can be observed; for matching with the value of $r = 0$, only the forward progressing wave with a spatially constant level distribution happens, and for total reflected with the value of $r = 1$, the sound field consists of standing waves with a strongly fluctuating level in x-direction. Moreover, $k = \frac{\omega}{c_0}$ is the wave number [9].
Two parallel surfaces (walls) with a distance w [m] can confront acoustic phenomena called flutter echo that repetitive reflections with $\Delta t = \frac{nw}{c}$ in second between each reflection give a perceived tone with a frequency of $f_0 = \frac{1}{\Delta t}$ in Hz which is in the low-frequency range, for gradually higher frequencies, the harmonics of this resonance as $2f_0$, $3f_0$, $4f_0$, etc. can be noticed [10].
Δt can be obtained by the distance between two surfaces w in m, the order of reflection n occur for n =1, 2, 3, ..., and the velocity of the sound $c_0 = 343\ \frac{m}{s}$.
As stated in the study by Halmrast [11] with examples for a distance of 3.43 m between two surfaces and the velocity of the sound $c_0 = 343\ \frac{m}{s}$, the resonance peak f_0 is 100 Hz for the first order of reflection and the second-order of reflection is 50 Hz. It is happened due to standing waves between the surfaces; flutter echo is in mid/high frequency around 1-2 kHz. Additionally, the wall distance is altered to 12 m. The resonance peak f_0 for the second-order of reflection is 14 Hz and flutter echo is more than 2 kHz, which is shown by increasing the distance between two surfaces the resonance or repetition peak is taken lower values in the lower frequency range. However, the flutter echo takes a higher value than the short distance between two surfaces.

3

Noise prediction methods

3.1 Noise prediction method

Accurate noise prediction methods are required to estimate the environmental impact and the realistic design of new roads or buildings. The Nordic noise prediction method, Nord2000 has been used as a calculation method for predicting traffic noise compared with the standard German RLS-90.

3.1.1 Nord 2000

Nord2000 sound propagation module is based on geometrical ray theory, which consists of source models for road and rail traffic and a sound propagation model. The model works at a 1/3 octave band in the frequency range of 25 Hz- 10 kHz for various weather conditions in which the terrain shape and ground type in the path between the source and the receiver are taken to the account for sound attenuation.
The sound pressure level at the receiver point, L_R, is predicted by Equation 3.1:

$$L_R = L_W + \Delta L_d + \Delta L_a + \Delta L_t + \Delta L_s + \Delta L_\Gamma \tag{3.1}$$

L_w is the sound power within the considered frequency band, ΔL_d is the propagation effect of spherical divergence of the sound energy, ΔL_a is the propagation effect of air absorption, ΔL_t is the propagation effect of the terrain, ΔL_s is the propagation effect of the scattering zones, ΔL_Γ is the propagation effect of obstacle dimensions and surface properties when calculating a contribution from sound reflected by an obstacle [12].

3.1.1.1 Ground effect and type

The shape of the terrain and ground impedance can influence the attenuation of the sound during propagation. The sound pressure level in the receiver point can be predicted based on the vertical terrain cross-section in the distance between the source and receiver point. The distance between the source and receiver point is not flat, as seen in Figure 3.1; the distance is divided into the number of segments, each of which has its roughness σ_r and flow resistivity.
The Fresnel-zones concept is broadly used for the propagation model in Nord2000 while predicting the effect of the ground properties on the reflected sound. When the sound is reflected by a plane surface, the intersection between the surface and Fresnel-ellipsoid generate the elliptically shaped Fresnel zone at which each ground type located at Fresnel zone the ground effect can be calculated, then the resulting overall ground is calculated as a weighted average as seen in Figure 3.2.

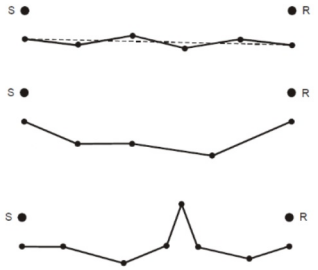

Figure 3.1: The shape of the terrain.

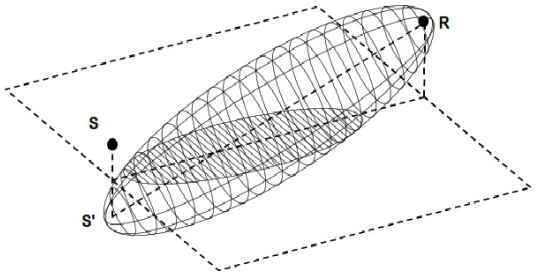

Figure 3.2: The Fresnel-zones.

3.1.1.2 Weather condition

Nord2000 can be applied to various weather conditions which is one of the model's advantages. The yearly average noise level can be obtained in the model by knowing the meteorological data. The model can be used for calculating the following:

- The noise level under specific weather conditions
- The noise level corresponding to actual weather conditions

The propagation is calculated using the concept of sound rays, and the method is to compute the sound pressure for each ray and then add the pressures of all rays to get the total sound pressure. The direction of propagation is namely downward refraction and upward refraction. In downward refraction, the speed of sound increases with height, and the result is downward refraction leading to higher A-weighted noise levels; furthermore, at upward refraction, the speed of sound decreases with altitude, and the upward refraction results to lower A-weighted noise levels.
The speed of sound $c(z)$ play the leading role in weather condition based on the height of ground z, as seen in Equation 3.2:

$$c(z) = Aln\left(\frac{z}{z_0}+1\right)+Bz+C \tag{3.2}$$

Where z_0 is the roughness length, A and B are the logarithmic and linear weather coefficients, and C is the sound speed at the ground, which the above parameters depend on the weather data as wind speed at the 10 m above the ground, wind direction in degree, stability of the atmosphere and air temperature in $c°$.
It can be defined as extra meteorological parameters in Nord2000, namely turbulence strength corresponding to wind C_v^2 and temperature C_T^2, relative humidity RH, stranded deviations of the wind speed σ_w and stranded deviations of fluctuation in the temper-

ature gradient $\sigma_{dt/dz}$. Besides, the air absorption can be predicted using the air temperature and the relative humidity [12] [13].

3.1.1.3 source position

The source model is estimated by calculating the rolling and propulsion sound levels which are defined in terms of three sub-sources at 0.01 m above the road surface for the tire noise, 0.30 m for the passenger cars' propulsion noise and 0.75 m for the heavier vehicles propulsion noise. The majority of the rolling noise (80%) is assumed to be radiating from the source 0.01m above the surface with a minor contribution (20%) associated with 0.30 m and 0.75 m. In the case of propulsion noise, it is assumed that the major contribution (80%) is from the source 0.3 m and 0.75 m for both light and heavy vehicles and a minor contribution (20%) from the source point 0.01 m. The rolling noise is seen in higher frequencies, while the propulsion noise shows up at lower frequencies. The categories of the vehicles at Nord2000 are shown in Table 3.2 [14]:

Table 3.1: The categories of the vehicles at Nord2000

Vehicle category no.	Type	Max. gross weight in kg	Vehicle length in m	explanation
1	Light	3500	< 5.5	Additional input as studded tyres and wet surface
2	Medium	3500-12000	5.6-12.5	2 axles 6 wheels
3	Heavy	>12000	>12.5	3 or more axles

3.1.1.4 Scattering zones

The propagation effect of scattering zones in both urban and vegetation areas can be predicted in Nord2000. Sound propagation in urban regions can be affected by reflections, the building and the ground's diffraction of house corners, and absorption. Reflections, absorption by the trunks, and foliage and scattering significantly impact the sound propagation in the vegetation regions. The effect of vegetation in the calculation can be obtained by adding input parameters like the density of trees, the trunk diameter, and the height of the frost on the ground [15].

3.1.2 RLS-90

The RLS-90 (Richtlinien für den Lärmschutz an Straben) is a German model for predicting traffic noise level L_{mE} at a distance of 25 m from the center of a road lane. L_{mE} is analytically represented in Equation 3.3 that is a function of the number of vehicles per hour Q and the percentage of heavy truck P based on the weight of the truck (weight > 2.8 tons), under idealized conditions i.e., speed of 100 km/h, a road gradient below 5% and a special road surface [16] [17].

$$L_{mE} = 37.3 + 10\log(1 + 0.082p) \tag{3.3}$$

The distinction between actual and idealized conditions is quantifying the different deviations using corrections according to the real speed, the actual road gradient, and the real surface. The mean level L_m in dB(A) is given in Equation 3.4 [17]:

$$L_m = L_{mE} + R_{SL} + R_{RS} + R_{RF} + R_E + R_{DA} + R_{GA} + R_{TB} \tag{3.4}$$

Where R_{SL} is a correction for the speed limit, R_{RS} is a correction for road surfaces, R_{RF} is a correction for rises and falls along the streets, R_E is a correction for the absorption characteristics of building surfaces, R_{DA} is attenuation's coefficient that takes into account the distance from the receiver and air absorption, R_{GA} is attenuation's coefficient due to ground and atmospheric condition and R_{TB} is attenuation's coefficient due to topography and building dimensions.
Furthermore, Lm_E for each lane is defined as Equation 3.5:

$$L_{m_E} = 10\log\left[10^{0.1L}_{m,n} + [10^{0.1L}_{m,f}\right] \tag{3.5}$$

The nearer lane is n and the farther is f [17].

3.1.3 Comparison between Nord2000 and RLS-90

The noise prediction methods Nord2000 and RLS-90 have been explained shortly above. The comparison of the two prediction methods is reviewed in the following Tables 3.2, 3.3, and 3.4; by knowing the pros and cons of the methods, more comprehensive information can be obtained such as application, traffic condition, vehicle type, source characteristics, input data, noise descriptor, gradient effect, ground effect, atmospheric absorption and refraction, and meteorological effects. The Nordic noise prediction method, Nord2000 was introduced by the Danish Environmental Protection Agency for noise mapping, and Nordic countries have used it since 2007. However, RLS-90 played a major role in this study to investigate how noise prediction methods can be affected by the results [18] [19] [20].

Table 3.2: The comparison between Nord2000 and RLS-90

Model	Government users	Application	predict traffic volume	traffic condition	Vehicle type
Nord2000	Scandinavian (Norway, Denmark, Sweden and Finland)	Road and rail traffic	No	Constant speed,grades	Light(< 3500kg) ,medium (3500–12,000 kg) heavy vehicle (> 12,000 kg)
RLS-90	Germany	Highways and car parks	Yes	Motorway,urban motorway,main road, urban road,urban road or feeder road in residential area,residential road	Light and heavy vehicle

Table 3.3: The comparison between Nord2000 and RLS-90

Model	Basic model	Source characteristics	Input data	Noise descriptor
Nord2000	Sound power level derived from pass-by measurement normalized to 10 m and angle of integration of 2.75 rad	Vertically and horizontally spaced point sources that are illustrated for road and railway lines. Vehicle is presented as noise source at height of 0.01 m, 0.03 m and 0.75 m	Traffic intensity and speed, type of the road, road surface , local topology,temperature and humidity	$L_{Aeq}, L_{den}, L_{night}$
RLS-90	Average level L_{mE} at a distance of 25 m from centre of lane which is the function percentage of heavy vehicles and number of vehicles per hour	Single stream noise levels are achieved at a distance of 10 m from the nearest edge of highway as a reference	Traffic type, flow, road data	L_{eq}, L_{mE}

Table 3.4: The comparison between Nord2000 and RLS-90

Model	Gradient effect	Ground effect	Atmospheric absorption and refraction	Meteorological effects
Nord2000	Terrain profile is divided to several segments and is assumed to be completely flat. Segmented terrain and ground roughness handled ground fluctuations.	Using of ray theory, defined the coherence factor for effect of scattering zones, surface roughness, refraction and turbulence	Air absorption obtained according to ISO 9613-1, curve sound rays applied for refraction modelling	Vertical sound speed profile defined by using wind and temperature gradient
RLS-90	Gradient correction: $R_{RS} = 0.6 \mid g \mid -3$ for $g > 5\%$ $R_{RS} = 0$ for $g \leq 5\%$	Level difference caused by ground absorption and free field is affected by meteorological	Attenuation defined caused by distance and air absorption	Attenuation defined due to ground and atmospheric effects

4

Methods

The methodology chapter explains the different methods or techniques used in the project and how the data is collected and analyzed. Generally, measurement locations, measurement procedures and equipment, measurement analysis, and the simulation in SoundPLAN are discussed in this section.

4.1 Noise measurements

The noise measurement plan consisted of measurements at five locations near the highway (E18) at Tønsberg- Sandefjord in Norway. The purposes of the measurements were road traffic noise measurement L_{Aeq} and L_{Fmax} from E18 (long-term) and the sound propagation measurement of the surrounding houses (short-term) for three places.

The traffic noise measurement included continuous noise measurement (24-hour measurement) for five locations in the winter and compared with recorded 17-day continuous noise measurements in summer for a site to know sound level fluctuations due to atmospheric conditions.

The next measurements were limited to noise minoring at three locations with short-term measures (1-hour) for the sound propagation of the surrounding houses in each location.

4.2 Measurement locations and procedures

4.2.1 Measurements sites

All noise measurements were performed near E18 between Tønsberg and Sandefjord in Norway. The areas were selected for noise testing because there have been complaints about high noise levels from the highway, especially with opening windows for ventilation. The measurement sites are shown in Figure 4.1.

Figure 4.1: The measurement sites between Tønsberg and Sandefjord in Norway.

The measurement sites, distance for the highway, and type of measurements performed in each site are summarized in Table 4.1. Winter measurement was done in February 2021, and summer measurement was done in June 2020. The explanations of each site are given below:

- Site 1: Solbergveien 33, is located west side of E18 with a distance of 122 m from the center-line of the traffic lane. Long-term measurement (24-hour) is performed in winter.

- Site 2: Solbergveien 37, two long-term measurements are done at this site; Sigmund Olafsen collected 17 days of continuous sound measurements in summer, and long-term measurement (24-hour) was monitored in winter. In addition, 1-hour measurement was performed for the sound propagation of the surrounding houses. The measurement points were at 128 m in winter and 132 m in summer from the center lane of the traffic line.

- Site 3: Lånheveien 5, long-term sound measurements collected by Sigmund Olafsen in summer (the location and the measurement equipment are shown in Appendix A)

- Site 4: Lånheveien 11, long-term measurement (24-hour) is monitored in winter at 340 m from the highway. 1-hour measurement is performed for the sound propagation of the surrounding houses.

- Site 5: Kodalveien 31, Long-term measurement (24-hour) with a distance of 597 m from the motorway and 1-hour measurement for the sound propagation of the surrounding houses is performed in winter.

Table 4.1: The measurement sites

Sites	Distance from highway	Measurement types	Measurement Season
Solbergveien 33	122 m	long-term	Winter
Solbergveien 37	128 m 132 m (summer)	long-term short-term	Winter Summer
Lånheveien 5	290 m	long-term	Summer
Lånheveien 11	340m	long-term short-term	Winter
Kodalveien 31	597 m	long-term short-term	Winter

4.3 Measurement Equipment and Procedures

The field equipment used for the measurements is described below:

- Continuous noise monitoring for all sites using sound level meter Nor 140, A-weighted, and 1/3 octave band data were collected at 30 min intervals for 24 hours.
- Short-term noise monitoring for three sites, 1-hour noise measurements were performed using SQuadriga-Head Acoustics with four microphone positions for recording sound pressure levels with A frequency weighting at 1.5 m above the floor and 1.5 m far way from the facades. The measurement time was approximately 60 minutes at each point.

The aerial photos of noise measurement sites are shown in the following Figures 4.2-4.6:

(a) The position of equipment. (b) Distance of E18.

Figure 4.2: The aerial photo at Solbergveien 33.

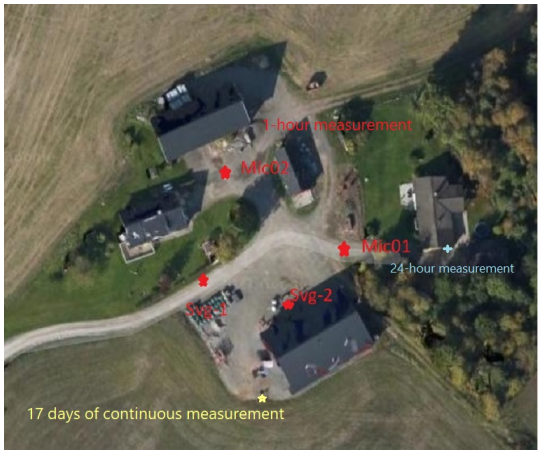

(a) The position of equipment.

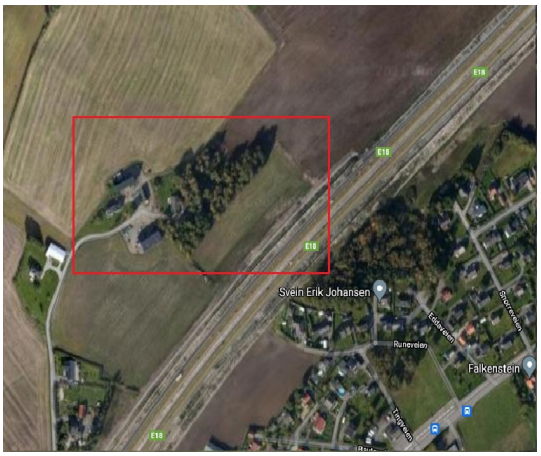

(b) Distance of E18.

Figure 4.3: The aerial photo at Solbergveien 37.

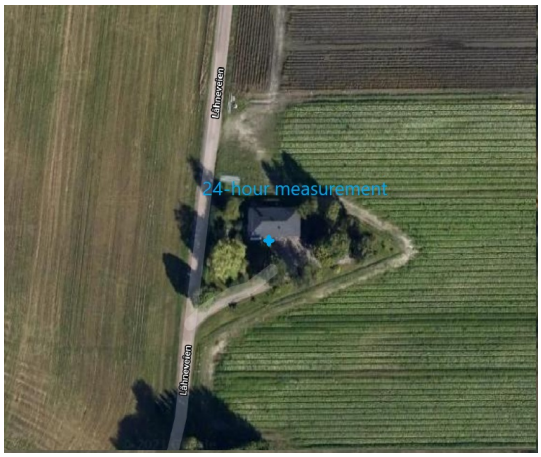

(a) The position of equipment.

(b) Distance of E18.

Figure 4.4: The aerial photo at Lånheveien 5.

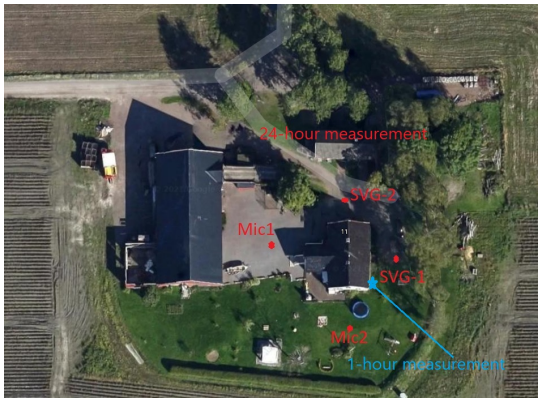

(a) The position of equipment.

(b) Distance of E18.

Figure 4.5: The aerial photo at Lånheveien 11.

(a) The position of equipment.

(b) Distance of E18.

Figure 4.6: The aerial photo at Kodalveien 31.

4.4 Analysis of measurements

4.4.1 Long-term noise measurement

This section describes the overall results of traffic noise measurement; the L_{Aeq} and L_{AFmax} were monitored for 24 hours at each site. Also, the day level L_d, the evening level L_e, the night level L_n and the day-evening-night level L_{den} which is a descriptor of noise level based on energy equivalent noise level (Leq) for a day with a 10 dB(A) adjustment for noise during the night (23.00-7.00) and additional adjustment of 5 dB(A) for evening noise (i.e., 19.00-23.00) [27] [28] [29].

The data for all sites are given graphically in Figures 4.7-4.10 and in Tables 4.2-4.6:

Table 4.2: Solbergveien 33.

Date	Hours (Day-evening-night)	(L_d, L_e, L_n) dB(A)	L_{den} dB(A)	L_{AFmax} dB(A) (Hour)
11 Feb 2021	24 (12-4-8)	(72.13, 64.74, 68.21)	75.03	72.4 (16:30)

Table 4.3: Kodalveien 31.

Date	Hours (Day-evening-night)	(L_d, L_e, L_n) dB(A)	L_{den} dB(A)	L_{AFmax} dB(A) (Hour)
09 Feb 2021	20 (8-4-8)	(66.54, 57.98, 61.46)	68.92	80.5 (09:30)

Table 4.4: Solbergveien 37 for summer and winter measurement. (the data graphically are shown in Appendix A).

Date	Hours (Day-evening-night)	(L_d, L_e, L_n) dB(A)	L_{den} dB(A)	L_{AFmax} dB(A) (hour)
11 February 2021	24 (12-4-8)	(75.57, 63.60, 70.96)	77.84	98.30 (16:30)
9 June 2020	14 (9-4-1)	(66.79, 59.74, 54.70)	68.22	86.50 (10:00)
10 June 2020	24 (12-4-8)	(63.65, 58.37, 59.18)	66.32	75.50 (20:00)
11 June 2020	24 (12-4-8)	(65.81, 59.55, 57.98)	66.51	88.60 (9:00)
12 June 2020	24 (12-4-8)	(70.37,61.67, 59.68)	69.69	76.50 (16:00)
13 June 2020	24 (12-4-8)	(66.03, 58.44, 56.34)	65.81	75.20 (22:00)
14 June 2020	24 (12-4-8)	(63.72, 63.12, 57.60)	66.21	76.70 (11:00)
15 June 2020	24 (12-4-8)	(63.69, 56.96, 60.70)	67.28	74.60 (03:00)
16 June 2020	24 (12-4-8)	(65.90, 60.32, 59.17)	67.22	85.90 (19:00)
17 June 2020	24 (12-4-8)	(66.79, 59.74, 54.70)	66.90	77.40 (12:00)
18 June 2020	24 (12-4-8)	(65.26, 61.03, 58.72)	66.84	69.10 (14:00)
19 June 2020	24 (12-4-8)	(66.69, 61.01, 58.60)	67.34	68.20 (17:00)
20 June 2020	24 (12-4-8)	(63.01, 54.97, 56.14)	64.05	83.00 (24:00)
21 June 2020	24 (12-4-8)	(72.26, 65.12, 56.17)	70.61	94.20 (20:00)
22 June 2020	24 (12-4-8)	(68.65, 56.71, 58.32)	67.91	77.10 (19:00)
23 June 2020	24 (12-4-8)	(67.34, 61.98, 56.85)	67.12	76.20 (10:00)
24 June 2020	24 (12-4-8))	(66.79, 62.03, 59.53)	67.94	75.80 (08:00)
25 June 2020	24 (12-4-8)	(68.48, 62.15, 64.19)	71.18	81.00 (15:00)
26 June 2020	13 (6-0-7)	(62.10, 0.00, 62.63)	67.90	70.80 (04:00)

Table 4.5: Lånheveien 5 for summer measurement

Date	Hours (Day-evening-night)	(L_d, L_e, L_n) dB(A)	L_{den} dB(A)	L_{AFmax} dB(A) (hour)
9 June 2020	12 (7-4-1)	(63.70, 58.78, 48.90)	63.48	75.10 (17:00)
10 June 2020	24 (12-4-8)	(62.01, 57.09, 57.39)	64.61	78.40 (12:00)
11 June 2020	24 (12-4-8)	(65.83, 61.61, 58.70)	67.11	74.00 (15:00)
12 June 2020	24 (12-4-8)	(67.68,62.17, 61.47)	69.65	79.00 (05:00)
13 June 2020	24 (12-4-8)	(65.10, 57.93, 56.84)	65.51	78.50 (17:00)
14 June 2020	24 (12-4-8)	(61.47, 61.49, 58.59)	65.86	70.50 (02:00)
15 June 2020	24 (12-4-8)	(65.85, 58.94, 59.62)	65.85	81.00 (20:00)
16 June 2020	24 (12-4-8)	(64.46, 59.76, 59.27)	66.74	79.50 (18:00)
17 June 2020	14 (7-0-7)	(58.90, 0.00, 57.92)	65.34	74.20 (02:00)

Table 4.6: Lånheveien 11.

Date	Hours (Day-evening-night)	(L_d, L_e, L_n) dB(A)	L_{den} dB(A)	L_{AFmax} dB(A) (Hour)
09 Feb 2021	23 (11-4-8)	(79.44, 65.28, 68.58)	78.39	103.1 (10:30)

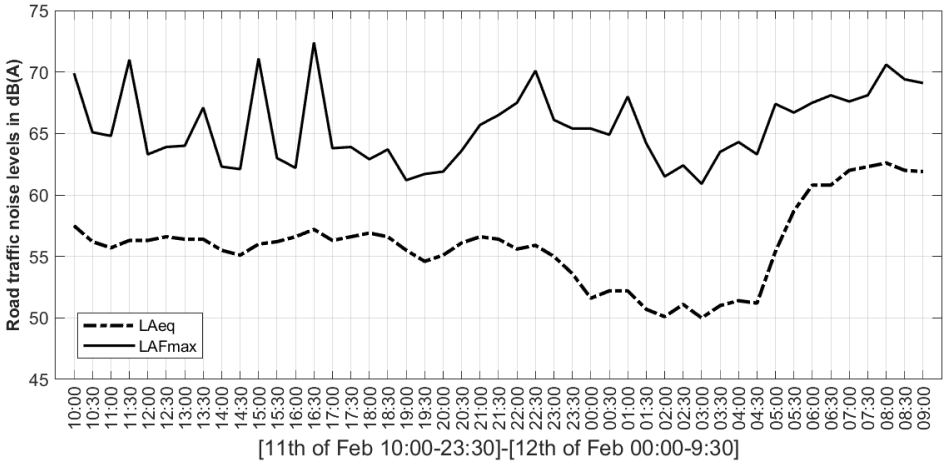

Figure 4.7: $LAeq,24h$ and $LAFmax$ at Solbergveien 33.

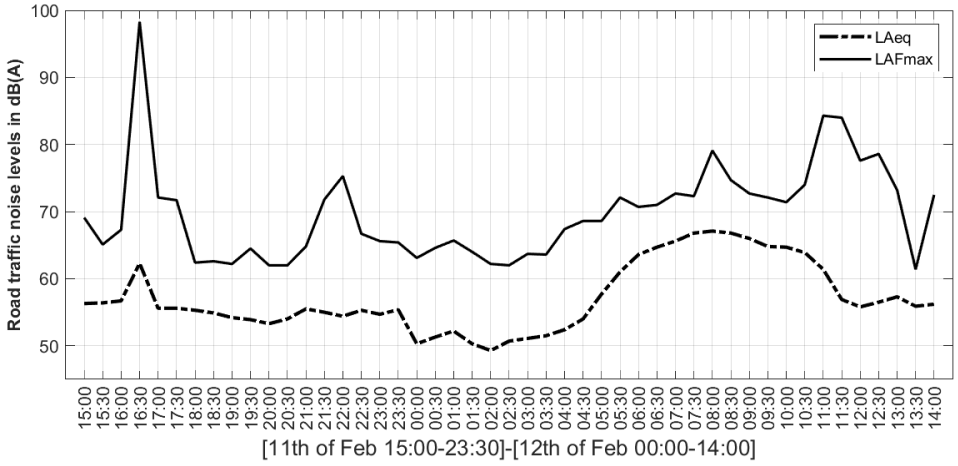

Figure 4.8: $LAeq,24h$ and $LAFmax$ at Solbergveien 37.

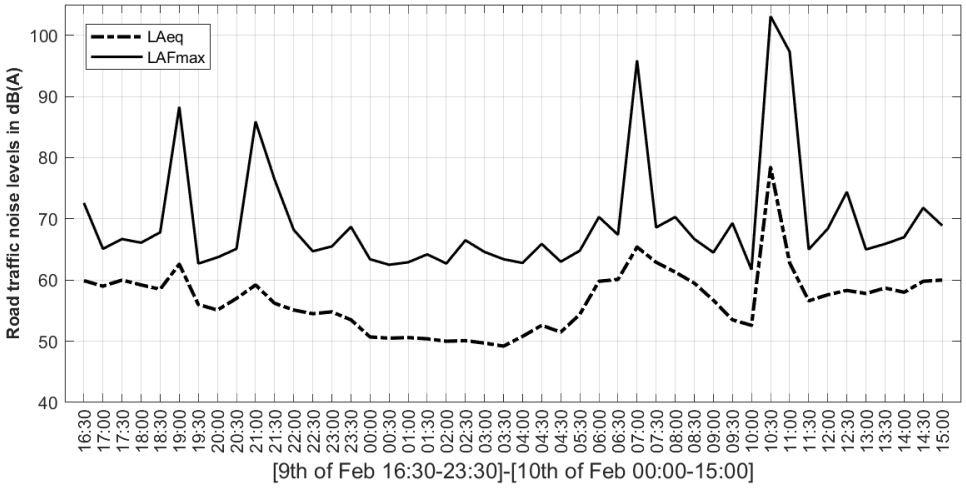

Figure 4.9: $LAeq,24h$ and $LAFmax$ at Lånheveien 11.

Figure 4.10: $LAeq,24h$ and $LAFmax$ at Kodalveien 31.

The important points at the mentioned sites from the measured data are:

- The data at Solbergveien 33, $L_{Aeq,24h}$ and L_{AFmax} are shown during the day, the day level is L_d=72.13 dB(A) where there is a rise at 4:30 and reached to the highest value 62.6 dB(A) at 8:00. The evening level L_e, Night level L_n and L_{den} are 64.74 dB(A), 68.21 dB(A) and 75.03 dB(A) respectively. The deviation within ± 2 dB(A) occurred between 10:00 to 22:30,and L_{AFmax} is 72.4 dB(A) at 16:30.
- The L_{den} are compared in winter and summer measurement at Solbergveien 37, the L_{den} is 77.84 dB(A) in winter and ranged from 65.81 to 71.18 dB(A) in summer which the L_{den} in winter is 6.66 dB(A) higher than the maximum value in summer. Furthermore, L_d is 77.57 dB(A) in winter and the maximum value in summer (17 days continuous measurement) measured in 21st of June with 72.26 dB(A). Also, L_{AFmax} is measured by 98.3 dB(A) at 16:30 in winter (11th of February) with comparison to 94.2 dB(A) on 21st of June at 20:00.
- The summer measurement is done during nine days at Lånheveien 5, and the L_{den} ranged from 63.48 dB(A) (9th of June 2020) to 69.65 dB(A) (12th of June 2020) and the maximum value of the L_{AFmax} is measured by 79.5 dB(A) at 18:00 in 12th of June 2020.
- The noise levels are expressed in terms of L_{day}, L_{evening} and L_{night} at Lånheveien 11 within L_d=79.44 dB(A), L_e=65.28 dB(A), L_n=68.58 dB(A) and the L_{den} is 78.39 dB(A). The results are presented in terms of $L_{Aeq,24h}$ which the day level L_d (7:00-19:00) seen a steep drop at 7:00 from 65.4 dB(A) to 52.6 dB(A) at 10:00, and it is noted a remarkable rise to 78.4 dB(A) at 10:30, and it fell dramatically again to 56.6 dB(A) at 11:30 . Also, 6 dB(A) variation is observed between 11:30-19:00 in the daytime. The evening level L_e (19:00-23:00) fluctuated 8 dB(A) from top-level 62.6 at 19:00 to the reduced level 54.8 dB(A) at 23:00. The night level L_n (23:00-7:00) increased from 49.2 dB(A) at 3:30 to 65.4 dB(A) at 7:00. L_{AFmax} for the day time is 103.1 dB(A) at 10:30, the evening time is 83.3 dB(A) at 19:00 and the night time is 95.9 dB(A) at 7:00.
- The equivalent sound level L_{eq} in 20 hours in terms of L_{day}, L_{evening} and L_{night} at Kodalveien 31 are L_d=66.54 dB(A), L_e=57.98 dB(A), L_n=61.46 dB(A) and L_{den}=68.92. The night sound level (23:00-7:00) went up from 42.4 dB(A) at 4:00 to 55.9 dB(A) at

6:30, and the evening level dropped from 50.9 dB(A) to 46.1 dB(A) at 23:00 within 6 dB(A) reduction during 19:00-23:00. Moreover, the maximum value for L_{Aeq} is 57.6 is measured at 8:00. L_{AFmax} in terms of day, evening, and night time is 80.5 (9:30), 66.8 dB(A) (19:30) and 72.2 dB(A) (3:30) respectively.

In the specific case at Solbergveien 37, the continuous measurement was carried out and compared in summer and winter; the meteorological effects such as temperature, wind, and humidity are considered. The meteorological data were collocated from the Norwegian meteorological institute (seklima.met.no and yr.no), which is the nearest station to Solbergveien 37 named Sandefjord-Mosserød (the elevation 72 m with 1.5 km distance to the measurement location) and E18-Rødbøl (the elevation 70 m) and the elevation of the measurement points are in the range of between 71-74 m. The daily temperature variation in the summer and winter are illustrated in Figure 4.11.

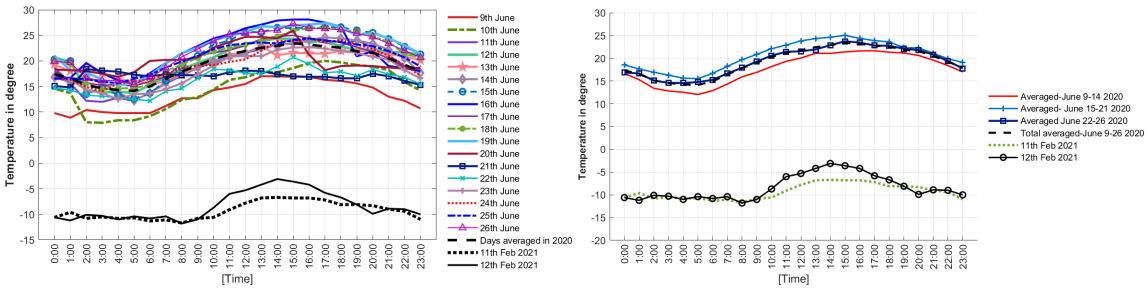

(a) Daily. (b) Weekly.

Figure 4.11: Diurnal Variation of temperature at Solbergveien 37.

The daily temperature variations for Solbergveien 37, the time of sunrise and sunset in winter is at 8:00 and 17:00, and the time of sunrise and sunset in summer is approximately at 4:00 and 22:30 for the period of 9^{th}- 26^{th} of June 2020. In summer, the maximum temperature is 21.4°c in the first week (9^{th}-14^{th} of June), the second week (15^{th}-21^{st} of June) is 25°c, and the maximum temperature is about 23.7°c at the third week (22^{nd}-26^{th} June). The maximum temperature occurred at 15:00 for each averaged week, whereas the minimum temperature values are 12°c, 15.5°c, and 14.7°c for each week, respectively. Additionally, the average minimum temperature in the winter is about -11.8°c at 8:00, with highs of -3.1°c at 14:00 on 12^{th} of February 2021 and -6.7°c at 14:00 on 11^{th} of February 2021.

Atmospheric absorption can be higher under high-temperature and low-humidity conditions. Increasing the air temperature allows the air to hold more water molecules, and relative humidity decreases and vice versa. The temperature is high in the afternoon, and the relative humidity is minimum. Hence the relative humidity is maximum in the morning when there is a noticeable drop in temperature. Also, the relative humidity is higher in times for sunrise in both summer and winter [30]. The relative humidity is plotted in Figure 4.12.

The wind data were collected from the weather station website, illustrated in Figure 4.13; the wind speed is lower in the night and the early morning hours in the winter and the summer; however, the wind speed in the summer is lower than the winter, the wind speed at 12^{th} of February is in the range of 1.5 m/s- 2.5 m/s between 7:00-11:00 which are on a level with the averaged days in the summer time. The highest values in

the winter season are about 5.5 m/s at 14-15 in 11th of February.

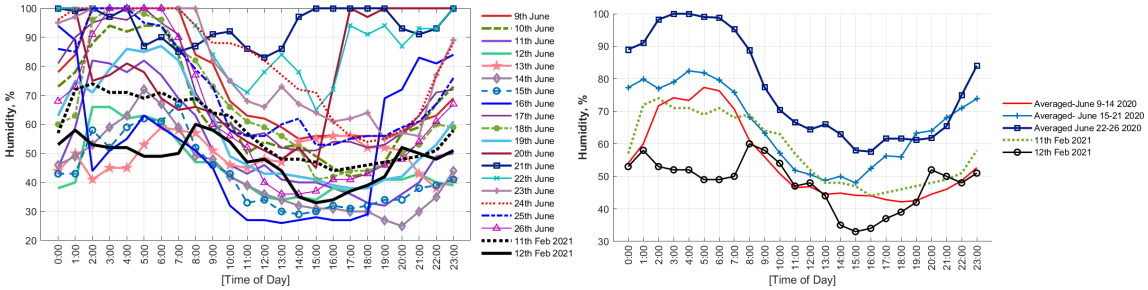

(a) Daily. (b) Weekly.

Figure 4.12: Diurnal Variation of relative humidity at Solbergveien 37.

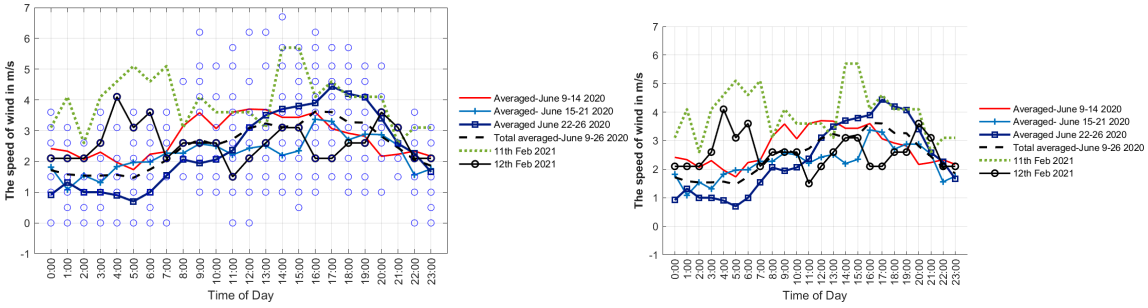

(a) Daily. (b) Weekly.

Figure 4.13: Diurnal Variation of wind at Solbergveien 37.

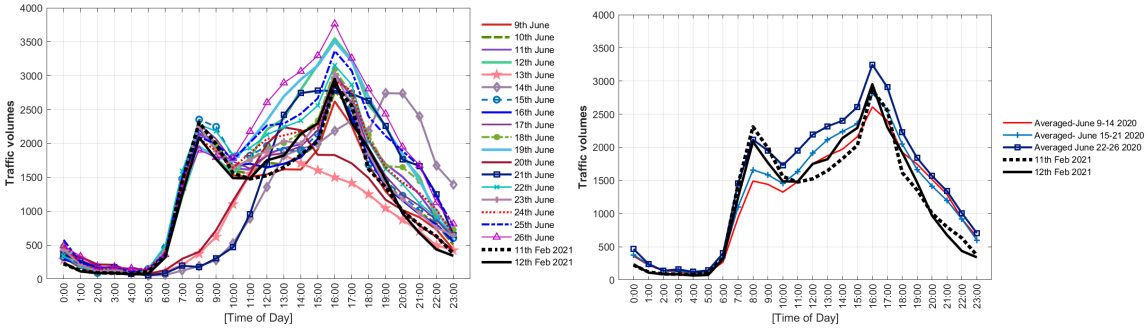

(a) Daily. (b) Weekly.

Figure 4.14: Diurnal Variation of traffic volumes at Solbergveien 37. (The traffic data are given in tables as well in Appendix A).

The traffic volume is collected from vegvesen.no/trafikkdata, the collected data point near Solbergveien 37 called EV18-S33D1-m4732 which the traffic volume per hour for selected days are shown in Figure 4.14 for both traffic lanes with the mentioned three vehicle categories in Nord2000. The number of vehicles in the summer stabilized between 1:00-5:00 at night while it dramatically increased from 150 to approximately 1900-2300 at 8:00. There is a sharp drop to the average of 1500 at 10:00, and it rocketed

to an average of 2880 at 16:00. Meanwhile, the number of vehicles declined sharply to 600 at 23:00. The winter traffic data in Figure 4.14 shows a consistent pattern with the summer traffic data in which the traffic peak is the same as summer at 8:00. Also the traffic peak in the afternoon is at 16:00 in the winter. The first and the second traffic peaks in the winter stood at over 2000 and 2900 vehicles, respectively, and it plummeted to about 500 at 23:00 [30].

4.4.2 Short-term noise measurement

As mentioned earlier, the short-term noise measurement has been recorded by Artemis suite Data Acquisition Module (SQuadriga) connected to four microphones at four different positions shown in the locations mentioned above. Figure 4.15 shows the setup and equipment for short-term measurement.

(a)SQuadriga

(b)Microphone with windscreen

(c)Microphone on stands

(d)BNC cables

Figure 4.15: The setup and equipment for short term measurement.

4.5 Simulation with SoundPLAN 8.2

Noise mapping helps us to quantify the effect of environmental noise in urban areas by estimating the level of noise pollution in specific areas. Noise mapping can be generated by comparing propagation sound measurements in the surrounding houses.

SoundPLAN simulations are performed using RLS-90 and Nord2000 models to predict the noise levels in the surrounding houses for three locations by applying various atmospheric conditions based on the measurement condition in summer and winter.
For this purpose, three selected regions are:

- Kodalveien 31, Sandefjord.
- Solbergveien 37, Sandefjord.
- Låhneveien 11, Tønsberg.

4.5.1 The Computerised Model in SoundPLAN 8.2

The first step consisted of importing the topographic data to SoundPLAN in which the input data must have an adequate level of accuracy for generating the noise mapping. Therefore, terrain data is downloaded from the Norwegian mapping authority's altitude through Høydedata.no with a resolution of 1 meter as point clouds- LAZ format or XYZ format. Using the LAStools software suite, Laz format is converted to ASCII format so that spot height points can be filtered and imported to SoundPLAN. Figure 4.16 shows the topographic map, and spot height for Koldaveien 31 [31].

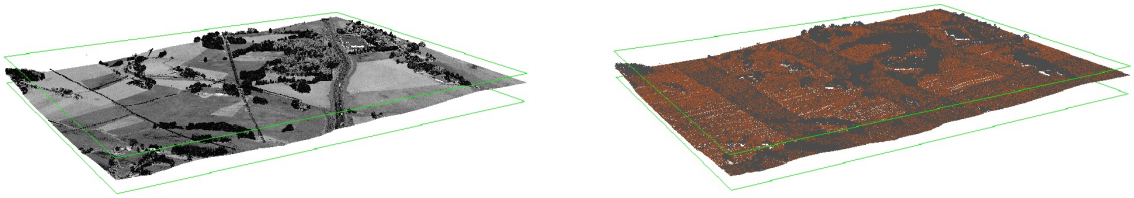

(a) The topographic map. (b) The spot heights.

Figure 4.16: The topographic map at Kodalveien 31.

One way of comparing two noise models (RLS-90 and Nord2000) is to compare the noise contour outputs for both models in each location. To do this, the same input and model setting should be defined [32] [33].
For all cases, noise counter maps are generated for both models, RLS-90 and Nord2000. L_d, L_e, L_n and L_{den} indicators have been used for Nord2000 (L_{den} assessment) with three periods of hours day (07:00-19:00), evening (19:00-23:00) and night (23:00-07:00). The assessment for RLS-90 is L_{eq} $6-22$ | $22-06$ | $00-24$, L_D and L_N are assessment indicators for noise disturbance during the day and the night that these are A-equivalent long-term average sound levels with two periods day (06:00-22:00) and night (22:00-06:00) [34].
Simulation can be performed in SoundPLAN by providing a default set of values as an input for its parameters and setting; for example, each model has its unique parameters as road properties for defining a road source. The road properties are compared for models RLS-90 and Nord2000 for three locations motioned above. In addition, the meteorological conditions need to be added to the simulation to determine the yearly average noise levels in Nord2000. Hence, the comparison between summer and winter is made in meteorological parameters like air temperature, air pressure, air humidity, and wind speed.

To do a simulation with greater accuracy, the hourly meteorological data corresponding to the measurement days for short-term measurement (1 hour) is collected from the Norwegian meteorological institute (yr.no and seklima.met.no) for each location.

4.5.1.1 Solbergveien 37

Parameters and settings used in noise simulation are summarised for the mentioned locations for both models RLS-90 and Nord2000 as below. Table 4.7 shows the difference in the road properties parameters at Solbergveien 37.

Table 4.7: Road properties setting for RLS-90 and Nord2000 at Solbergveien 37.

Road properties E18	RLS-90	Nord 2000
Traffic volumes	ADT (veh/24h) = 24065	ADT (veh/24h) = 24065
Road type	RLS-90 highway	Type A Highway 110-130 km/h
Speed	110 km/h	Cat1: 110 km/h, Cat 2,3: 80 km/h
Road surface	Smooth asphalt/ asphalt concrete	SMA 11
profile	7.50/2.00/7.50 (RQ 20)	7.50/2.00/7.50 (RQ 20)

The actual meteorological parameters can be used for calculating the noise levels in summer and winter, which is further explained in Section 3.1.1.2; the short-term measurement was performed in February, and the meteorological data is imported to SoundPLAN for the exact time of the measurement, those parameters are listed in Table 4.8 [35].

Table 4.8: The meteorological parameters for Nord2000 at Solbergveien 37.

Environmental data	Winter	Summer
Temperature [$^{\circ}C$]	-6.7	23
Humidity %	48	70
Air pressure [mbar]	1012	1013
Wind speed [m/s]	5.7	3

4.5.1.2 Låhneveien 11

Låhneveien 11 is the next simulation location with road properties shown in Tables 4.9, 4.10 and 4.11 while is located on the east side of E18, north side of Ramnesveien and south side of Bispeveien, also the house is near to highway exit ramp and overpass road between E18 and Ramnesveien.

Table 4.9: E18 road properties setting for RLS-90 and Nord2000 models at Låhneveien 11.

E18 road properties	RLS-90	Nord 2000
Traffic volumes	ADT (veh/24h) = 16839	ADT (veh/24h) = 16839
Road type	RLS-90 highway	Type A Highway 110-130 km/h
Speed	110 km/h	Cat1: 110 km/h, Cat 2, 3: 80 km/h
Road surface	Smooth asphalt/ asphalt concrete	SMA 11
profile	7,50/2,00/7,50 (RQ 20)	7,50/2,00/7,50 (RQ 20)

Table 4.10: Bispeveien road properties setting for RLS-90 and Nord2000 at Låhneveien 11.

Bispevein road properties	RLS-90	Nord 2000
Traffic volumes	ADT (veh/24h) = 7323	ADT (veh/24h) = 7323
Road type	Highway urban area	Type D Mainroad in city 60/70 km/h
Speed	60 km/h	Cat 1, 2, 3: 60 km/h
Road surface	Smooth asphalt/ asphalt concrete	SMA 11
profile	3,75/3,75 (RQ 10,5)	3,75/3,75(RQ 10,5)

Table 4.11: Ramnesveien road properties setting for RLS-90 and Nord2000 at Låhneveien 11.

Ramnesveien road properties	RLS-90	Nord 2000
Traffic volumes	ADT (veh/24h) = 3500	ADT (veh/24h) = 3500
Road type	Highway urban area	Type D Mainroad in city 60/70 km/h
Speed	60 km/h	Cat 1, 2, 3: 60 km/h
Road surface	Smooth asphalt/ asphalt concrete	SMA 11
profile	3,25/3,25 (RQ 9,5)	3,25/3,25 (RQ 9,5)

The simulation has been done using the listed meteorological parameters at Table 4.12 for Låhneveien 11:

Table 4.12: The meteorological parameters for Nord2000 at Låhneveien 11.

Environmental data	Winter	Summer
Temperature [$^{\circ}C$]	-9.1	18
Humidity %	80	75
Air pressure [mbar]	1013	1012.1
Wind speed [m/s]	2	3

4.5.1.3 Koldaveien 31

The noise prediction simulation has been carried out for the third location at Koldaveien 31, which is placed adjacent to Koldaveien with 600 m far away from E18, according to the noise prediction method already mentioned, road data and actual meteorological used for the calculated noise level can be found in following Tables 4.13, 4.14 and 4.15:

Table 4.13: Road properties setting for RLS-90 and Nord2000 models at Koldaveien 31.

E18 road properties	RLS-90	Nord 2000
Traffic volumes	ADT (veh/24h) = 25795	ADT (veh/24h) = 25795
Road type	RLS-90 highway	Type A Highway 110-130 km/h
Speed	110 km/h	Cat1: 110 km/h, Cat 2, 3: 80 km/h
Road surface	Smooth asphalt/ asphalt concrete	SMA 11
profile	7,50/2,00/7,50 (RQ 20)	7,50/2,00/7,50 (RQ 20)

Table 4.14: Koldaveien road properties setting for RLS-90 and Nord2000 at Koldaveien 31.

Koldaveien road properties	RLS-90	Nord 2000
Traffic volumes	ADT (veh/24h) = 2190	ADT (veh/24h) = 2190
Road type	Highway urban area	Type D Mainroad in city 60/70 km/h
Speed	60 km/h	Cat 1, 2, 3: 60 km/h
Road surface	Smooth asphalt/ asphalt concrete	SMA 11
profile	3,75/3,75 (RQ 10,5)	3,75/3,75(RQ 10,5)

Table 4.15: The meteorological parameters for Nord2000 at Koldaveien 31.

Environmental data	Winter
Temperature [$^{\circ}C$]	-5
Humidity %	58
Air pressure [mbar]	1013
Wind speed [m/s]	3.1

4.5.2 Uncertainty in the Prediction of Sound Levels in SoundPLAN

With the rapid growth of cities, outdoor noise simulation has been widely used for environmental noise assessment, a methodology for predicting noise levels for road traffic called noise mapping. The Grid Noise Map (GNM) results can be processed into noise contour maps. GNM is based on results from multiple receivers in a grid; knowing the results of grids can be used to interpolate a complete map. The grid of receivers has a significant impact on the final results. With a grid with more receivers, the final results are more accurate, which is a cause for increasing the calculation time. Generally, sources of uncertainty in noise mapping are three factors that can be contributed to uncertainty in noise prediction:

- Input data uncertainty
- Model uncertainty
- Uncertainty in the running of the software

The element of the input data can be classified into two groups the calculation method and the acoustic model that the variables are cited in Tables 4.16 and 4.17 [36] [37].

Table 4.16: The variables of the calculation method.

Group	Variables	Data
Calculation Method	Traffic Flow	Taken from vegvesen.no/trafikkdata
	Average Speed	Taken from the speed limit traffic sign
	Road Surface	Taken from the E18 contractor document
	Road Gradient	Digital Ground Model (DGM) is built it
	Width of the Median	Measured in situ
	Emmision Band	Emission levels are calculated by software

Table 4.17: The variables of the acoustic method.

Group	Variables	Data
Acoustic Model	Digital Ground Model	The spot heights built DGM (Høydedata.no)
	Ground Surface	Taken ground factor 0.5 for soil and vegetation
	Height of the buildings	Taken from the spot heights
	Humidity	Taken from seklima.met.no
	Air pressure	Taken from seklima.met.no
	Temperature	Taken from seklima.met.no
	The receiver distance to facade	Measured in situ

As it is clear that the data is generally collected from different sources for noise mapping, and the accuracy of the input data performs a significant duty in the prediction of the noise. The question is if the input data are not so accurate, how many decibels could be predicted noise levels to vary from the measured noise levels? Also, the geometry of the imported model in SoundPLAN plays a significant role in the sound propagation of the noise from the source to the receiver. Therefore, the accuracy of terrain data is essential for noise mapping since the terrain data is used from the Norwegian mapping authority's altitude with a resolution of 1 meter. The data was simplified before imparting to SoundPLAN because the data's complexity increased the software's running time. Accordingly, simplifying the data can cause uncertainty in the predicted noise level. The model of noise assessment affects the accuracy of the noise map due to the discrepancies between the model algorithms. Two different evaluations, Nord2000 and RLS-90, have been used in this study; by increasing the physical factors used in each algorithm, the uncertainty can be higher in each model; for instance, meteorological factors are the main part of the Nord2000 model caused by the complexity of the calculation in the model. Also, the noise is propagated from source to receiver in the simulation, and the ground effect is a cause of uncertainty; hence the correct ground type needs to be added to the model.
The uncertainty caused by running SoundPLAN can be specified as grid design, grid interpolation, and the height of the buildings. The size of the grid was a crucial factor in the simulation while the grid space and the height of the grid above the ground in meters were modified, so the sound levels for the grid cell at the receiver position were varied, thereby the various sizes of the grid were applied during the simulation as an example at Solbergveien 37 the grid size of 5×5 meters was mapped, and the grid cell in the exact location of the receiver position was fairly close to the measured values. Furthermore, the grid spacing at Lånheveien 11 has been chosen by the size of 10×10 meters for the larger calculation area, and the calculation time was reduced. The predicted values were accurate enough to the measured values in all receiver positions. Interpolation during the grid noise map calculation was another case of uncertainty in which the field size defines the maximum size of the block for the interpolation. The filed size 9×9 was utilized in the simulation, which means that in the blocks of 9×9 receivers, a sup-gird of 81 receivers is calculated. The four corners of the blocks and the middle receiver are always calculated, and the other blocks are interpolated. The next element of uncertainty is the building data, the height of buildings were not measured in situ, and the building heights were read from the spot heights imported to SoundPLAN. The average size of the building based on the roof was used to build the houses. Therefore, the height of the building between the source and the receiver at Koldaveien 31 was a case of uncertainty as well; the sound pressure level in the mic01 receiver position was varied up to 2-3 dB(A) by changing the height of the roof with 0.5 meters. Also, the same scenario was seen at Solbergveien 37 for the receiver position: the building is between the sound source and the receiver position. Single-point simulation is carried out for all cases to validate the obtained values in the grid noise map. In contrast, the noise levels were lower in some receiver positions by 2-3 dB(A) in all locations compared to the Grid Noise Map values due to GNM calculating reflections from all buildings. The levels can be up to 3 dB(A) higher than single point receiver simulation [38].

5
Results

5.1 The comparison of long measurement under summer and winter conditions at Solbergveien 37

Long-term measurements have been carried out during summer (17 days continuous measurement) and winter (for a 24-hour) conditions while measuring the equivalent continuous sound pressure level $L_{Aeq,T}$ and T is the period of observation for a 24-hour. The instrument used for measuring $L_{Aeq,T}$ was an integrating sound level meter mounted on the facade with an A-weighting filter. However, for the uninterrupted 17-day measurement with known traffic load, a microphone mounted in a stand was used at a point with a level very similar to the free field value for the house. In Figure 5.1 L_{Aeq} is compared under summer and winter conditions which 17-day measurement (9^{th}-26^{th} of June 2020) is averaged for each week in summer, and 24-hour measurement was done on the 11^{th} and the 12^{th} of February 2021 in winter time.
It is evident that sound pressure levels early in the morning in winter are higher than normal sound pressure levels in summer conditions, and it is because of atmospheric conditions. As mentioned in Chapter 2, it has been understood that atmospheric effects such as temperature and wind can be caused by refraction (bending) of the sound waves, and the refraction of sound is a result of significantly higher or lower sound pressure levels.
As outlined above, solar radiation heats the earth's surface on a typical sunny day, making the air warmer on the earth's surface; hence, with increasing elevation, the air temperature tends to decrease, known as a temperature lapse. Measurement has been carried out in winter, characterized by short days and low solar radiation. On the measurement day with a clear sky and sunshine, the ground was covered by cold snow and ice, and its white color could be reflected by all heat coming in, although the cooling of the land continued over a more extended period in the winter night. Furthermore, the lack of wind fluctuations prevent air mixing near the ground; this condition is called temperature inversion, which is caused sound waves to bend down, and sound levels can be enhanced and higher than normal; the result is contrary to expectation with the normal air pattern (i.e., warmer air below and cooler air above) then with increasing elevation, the air temperature tends to increase [30].
In Figure 5.1, it is evident that the temperature inversion condition occurred over periods of 5:00-11:00 in the 12^{th} of February 2021 in wintertime, which the maximum sound pressure level happened in sunrise at 8:00 with 67 dB(A) although the averaged sound pressure level for the same time in summer is 53 dB(A), the result of comparison between the sound pressure levels in winter and summer as observed at 8:00 confirm

that the area is prone to high sound levels due to temperature inversion condition that sound pressure level increased by 14 dB(A). Further, the sound pressure level dropped about 5 dB(A) from about 8:00 to 11:00 and reached 62 dB(A), which is about 7 dB(A) more than the average sound pressure (50 dB(A)) in summer at 11:00.
The effects of temperature inversion appeared at 5:00, and the transition from inversion to lapse is taken four hours. The maximum sound pressure level because temperature inversion happened at sunrise at 8:00. It was expected that temperature inversion would occur at sunrise. The temperature inversion was initiated at 5:00, the period before sunrise is known as twilight, in which the atmosphere is partly illuminated by the sun. Twilight is classified into three categories: civil twilight, nautical twilight, and astronomical twilight, which describe how far the sun is below the horizon. The sun's geometric center is 6°, 12°, and 18° below the horizon for civil, nautical, and astronomical twilight, respectively. The effect of traffic volumes on the L_{eqs} is also reviewed under winter and summer conditions (Figure 4.14); the traffic volumes are lowest between 1:00-7:00 on the 11th and the 12th of February 2021 on wintertime and the highest traffic volume in the morning is observed at 8:00 when the sound pressure level is approximately near to the highest level, the traffic volume is reached to 2900 vehicles per hour at 14:00; however, the sound pressure level is not the highest of the day. On the other hand, the neutral atmospheric condition is established in the summertime, which is not influenced by lapse or temperature inversion, and the maximum L_{Aeq} is measured at 16:00 in the summer when the traffic volume is at the highest level with the averaged of 2800 vehicles per hour in two lanes.

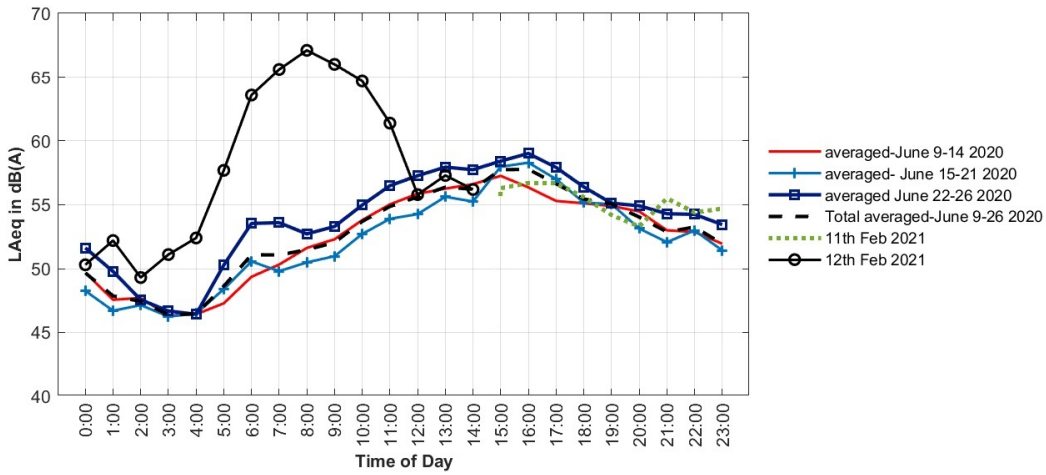

Figure 5.1: The comparison of long measurement under summer and winter conditions at Solbergveien 37.

The exact time for civil, nautical, astronomical twilight, the day and the night for the 12th of February 2021 are found in Table 5.1

Table 5.1: The 12th of February 2021- the sun in Solbergveien 37.

Astronomical twilight	Nautical twilight	Civil twilight	Day	Night
05:43 - 06:30	6:30 - 7:18	07:18 - 08:01	08:01 - 17:06	00:00 - 05:43

5.2 Results achieved with SoundPLAN 8.2

This section summarizes the short-term measurements (1-hour) performed for the three cases Solbergveien 37, Lånheveien 11, and Kodalveien 31 which noise maps will be presented and compared with the site-measured data in both summer and winter conditions according to two models, RLS-90 and Nord2000. As discussed earlier, the short-term measurements have been carried out at different times in a day for each case, as mentioned in Table 5.2:

Table 5.2: Date and time of the short-time measurements.

Locations	Date of measurement	Time of measurement
Solbergveien 37	12^{th} of February 2021	14:00-15:00
Lånheveien 11	11^{th} of February 2021	18:00-19:00
Kodalveien 31	9^{th} of February 2021	16:30-17:30

Additionally, the policy of indoor and outdoor noise criteria in Norway are shown below in Table 5.3, the threshold values for noise in Norway that people should not be exposed to noise levels higher than the threshold values stated below:

Table 5.3: Outdoor and indoor noise criteria in Norway [48].

Outdoor and indoor noise criteria
30 dB(A) equivalent sound pressure level indoors (L_{Aeq},24)
45 dB(A) maximum sound pressure level indoors at night L_{AFmax}
55 dB(A)day–evening–night noise level or L_{den} outdoors (at façade)
70 dB(A) maximum sound pressure level in the yard in connection to the residence L_{AFmax}

5.2.1 Solbergveien 37

To calculate the noise level for four receiver positions, SoundPLAN 8.2 is used according to two models, RLS-90 and Nord2000. The noise monitoring was undertaken at the same positions with 1.5 m above the ground level at Solbergveien 37. One of the aims of noise simulation is to give an overall view of noise propagation in the surrounding houses. In general, two values with the influence of the meteorology data are compared with the measured data in both summer and winter conditions for Nord2000. The predicted noise levels in the surrounding of the houses based on Nord2000 for the following noise indicators L_{den}, L_d, L_e and L_n are illustrated in Figure 5.2 for the winter and the summer conditions.

(a) L_{den}

(b) L_d

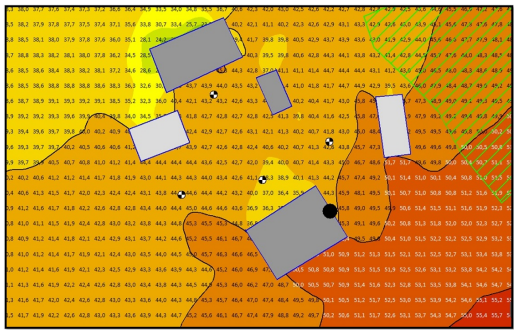

(c) L_e

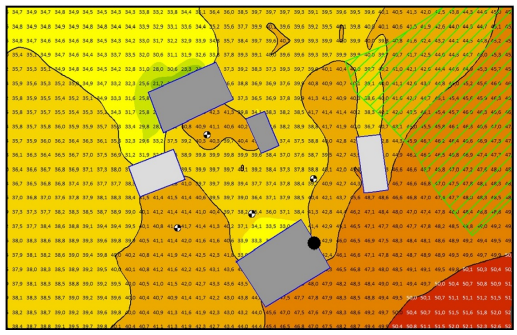

(d) L_n

Figure 5.2: Grid Noise maps (GNM) and the predicted noise levels based on Nord2000 for the noise indicators L_{den}, L_d, L_e and L_n on the winter.

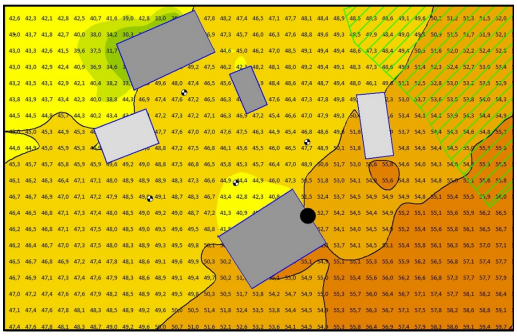

(a) L_{den}

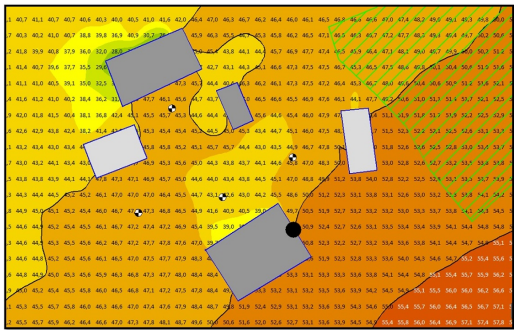

(b) L_d

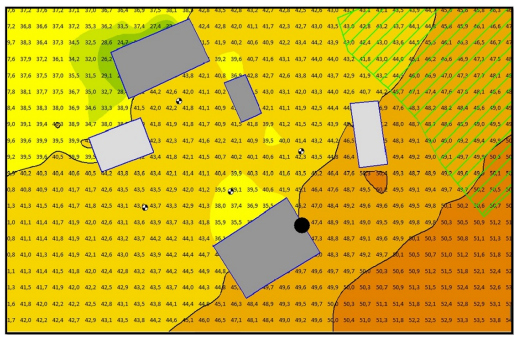

(c) L_e

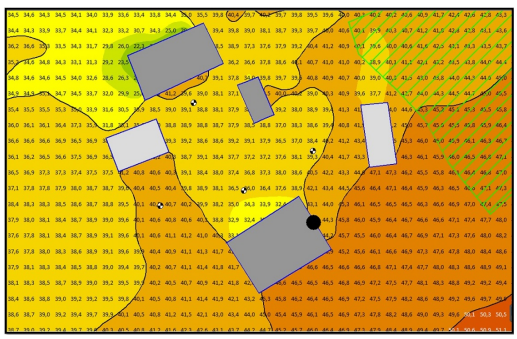

(d) L_n

Figure 5.2: Grid Noise map (GNM) and the predicted noise levels based on Nord2000 for the noise indicators L_{den}, L_d, L_e and L_n on the summer (Enlarged photos are included in Appendix B and the non-zoomed simulation results for all mentioned locations also are included in Appendix C) (continued).

The monitored sound pressure levels were compared with the predicted values in four-receiver positions in the surrounding houses based on the Nord2000 assessment in winter and summer conditions. The simulation's names and measurement microphone positions are illustrated in Section 4.3, where the same positions are selected for the modeling in SoundPLAN. The microphones labeled as Mic01, Mic02, Svg-1, and Svg-2 which the predicted noise level for L_{den} in winter and summer varied from 46.6 dB(A) to 49.2 dB(A) and 44.9 dB(A) to 49.1 dB(A) respectively. The predicted L_{day} are about 2 dB(A) smaller than L_{den}, and also L_{evening} and L_{night} are about 5.5 dB(A) and 6.5 dB(A) smaller than L_{den} in both winter and summer for four receiver positions. The labeled microphone Svg-1 is exposed to highway noise more than other receivers. In contrast, the microphone Svg-2 is positioned in front of a high building, which was a barrier between the receiver and the road (the source). The sound pressure level (SPL) dropped for all noise indicators L_{den}, L_d, L_e, and L_n at that microphone position, and SPL was quite lower as compared with other microphone positions. The measured and the predicted sound pressure levels based on Nord2000 can be found in the following Tables 5.4- 5.7:

Table 5.4: The monitored sound pressure levels compared with the predicted L_{den} in SoundPLAN at Solbergveien 37 based on Nord2000.

Microphone positions	Mic01	Mic02	Svg-1	Svg-2
The measured values in dB(A)	47.2	47.3	47.4	48.3
The predicted L_{den} in dB(A) in winter	48.1	48.6	49.2	46.6
The predicted L_{den} in dB(A) in summer	47.7	47.8	49.1	44.9
The difference in dB(A) (winter)	-0.9	-1.3	-1.8	1.7
The difference in dB(A) (summer)	-0.5	-0.5	-1.7	3.4
The difference ($L_{den(win)}$-$L_{den(sum)}$)in dB(A)	0.4	0.8	0.1	1.7

Table 5.5: The monitored sound pressure levels compared with the predicted L_d in SoundPLAN at Solbergveien 37 based on Nord2000.

Microphone positions	Mic01	Mic02	Svg-1	Svg-2
The measured values in dB(A)	47.2	47.3	47.4	48.3
The predicted L_d in dB(A) in winter	46.1	47.4	47.4	44.5
The predicted L_d in dB(A) in summer	45.8	45.7	47.3	43.1
The difference in dB(A) (winter)	1.1	-0.1	0.0	3.8
The difference in dB(A) (summer)	1.4	1.6	0.1	5.2
The difference ($L_{d(win)}$-$L_{d(sum)}$) in dB(A)	0.3	1.7	0.1	1.4

Table 5.6: The monitored sound pressure levels compared with the predicted $L_{evening}$ in SoundPLAN at Solbergveien 37 based on Nord2000.

Microphone positions	Mic01	Mic02	Svg-1	Svg-2
The measured values in dB(A)	47.2	47.3	47.4	48.3
The predicted L_e in dB(A) in winter	42.8	43.2	44.6	41.1
The predicted L_e in dB(A) in summer	42.3	42.2	43.6	39.5
The difference in dB(A) (winter)	4.4	4.1	2.8	7.2
The difference in dB(A) (summer)	4.9	5.1	3.8	8.8
The difference ($L_{e(win)}$-$L_{e(sum)}$) in dB(A)	0.5	1.0	1.0	1.6

Table 5.7: The monitored sound pressure levels compared with the predicted L_{night} in SoundPLAN at Solbergveien 37 based on Nord2000.

Microphone positions	Mic01	Mic02	Svg-1	Svg-2
The measured values in dB(A)	47.2	47.3	47.4	48.3
The predicted L_n in dB(A) in winter	39.7	40.9	41.7	38.2
The predicted L_n in dB(A) in summer	39.3	39.1	40.5	36.0
The difference in dB(A) (winter)	7.5	6.4	5.7	10.1
The difference in dB(A) (summer)	7.9	8.2	6.9	12.3
The difference ($L_{e(win)}$-$L_{e(sum)}$) in dB(A)	0.4	1.8	1.2	2.2

To represent the magnitude of errors between the measured and the predicted sound pressure levels shown in the tables above, L_{den} and L_d indicators are selected to compare with the measured sound pressure levels. The short-term measurement was done at day 14:00-15:00 in winter, as stated the predicted L_d is less than 2 dB(A) compared with L_{den} for all receiver positions. The predicted L_d in winter were almost the same for the receiver positions the Mic02 and the Svg-1 as in summer, while the Svg-2 receiver position was 3.8 dB(A) and 5.2 dB(A) less than the measured values for winter and summer respectively. It can be seen that from Table 5.5, the Mic02 and Svg-1 receiver positions in winter are close to the measured values. However, the Mic02 is 1.6 dB(A) less than the measured values in summer. The difference between the predicted L_d and the monitored SPL for the Mic01 receiver position is 1.1 dB(A) in winter and 1.4 dB(A) in summer.
Additionally, Table 5.4 shows the differences between the predicted L_{den} and the short-term measurement values since the predicted L_{den} are much closer to the monitored values compared with L_d. It is clear that the measured values for the Svg-2 receiver point are more than the predicted value of 1.7 dB(A) in winter and 3.4 dB(A) in summer, while the Mic01 receiver point is roughly equal to the measured SPL with the difference of 0.8 for the predicted value in winter and 0.4 for the predicted value in summer condition. Also, the increment of the predicted L_{den} for the Svg-1 receiver position was slightly larger than Mic01 and the Mic02 with 1.7 dB(A) in winter and 1.6 dB(A) in summer compared to the monitored values. As mentioned above, the predicted L_e and L_n are about 5.5 dB(A) and 6.5 dB(A) smaller than L_{den} in both winter and summer for four receiver positions.

On the other hand, the RLS-90 model is run to predict sound pressure levels for the aforementioned receiver locations for the comparison with Nord2000 results. The RLS calculation is explained in detail in Section 3.1.2, and the GNM based on the RLS-90 model is indicated in Figure 5.3. It is noticed from Table 5.8 that there are correlations between the predicted L_{den} based on Nord2000 and the predicted L_{rD} based on RLS-90 for the selected microphone positions by having similar predicted values for the Mic02 and the Svg-2. In contrast, L_{rD} is 0.3 dB(A) less than L_{den}. The discrepancy between the predicted L_{den} and L_{rD} for the Mic01 and Svg-1 is 0.4 dB(A) and 1.8 dB(A), respectively. It differed slightly between the measured values, the predicted L_{den} and L_{rD} which the measured values for the Mic01 0.8 dB(A), the Mic02 1.2 dB(A), and the Svg-1 1.7 dB(A) are smaller than the predicted L_{den} as well as for the Mic01 0.4 dB(A) and the Mic02 0.9 dB(A) are less than the predicted L_{rD}, besides, the measured values for the Svg-2 are larger 1.7 dB(A) compared with the predicted L_{den} and 2 dB(A) compared with the predicted L_{rD}.

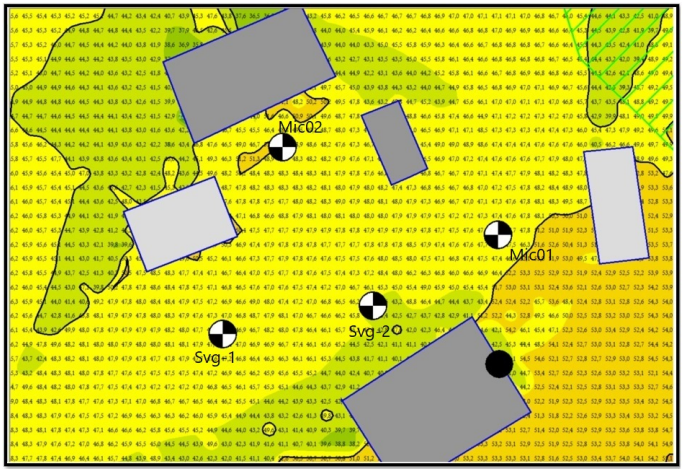

Figure 5.3: Grid Noise maps (GNM) and the predicted noise levels based on RLS-90.

Table 5.8: The monitored sound pressure levels compared with the predicted sound pressure levels in SoundPLAN at Solbergveien 37 based on Nord2000 and RLS-90.

Microphone positions	Mic01	Mic02	Svg-1	Svg-2
The measured values in dB(A)	47.2	47.3	47.4	48.3
The predicted L_{den} in dB(A) based on Nord2000	48.1	48.6	49.2	46.6
The predicted L_{rD} in dB(A) based on RLS-90	47.7	48.3	47.4	46.3
The difference in dB(A) (Nord2000)	-0.8	-1.2	-1.8	1.7
The difference in dB(A) (RLS-90)	-0.4	-0.9	0.0	2.0
The difference (L_{den}-L_{rD}) in dB(A)	0.4	0.3	1.8	0.3

Grid Cross Section Map (GCSM) is also calculated and displayed in the following Figures 5.5, and 5.6 based on RLS-90 for the receiver positions, the schematic of the cross-section map with the position of the receivers are shown in Figure 5.4 that the residence building with other houses is visualized.

The cross-sectional study aimed to evaluate the vertical distribution of the sound pressure levels in the plane passed by the receiver positions with a height of 15 m, Figure 5.5 shows the predicted L_{rD} based on RLS-90 that the sound pressure in the Mic01 near to the residence building is equal 47.7 dB(A). It can be seen in Table 5.8; moreover, a maximum difference of 10 dB(A) arises in the vertical cross-section from the ground to the top of the plane. The noise levels L_{rD} are calculated for the Mic02 and the Svg-2 (the receiver near the E18) which the variation of the predicted sound pressure levels L_{rD} is 18 dB(A) concerning the height of the cross-section plane, and it has been depicted based on the simulation results that the Mic02 is 48 dB(A) and the Svg-2 is 46 dB(A) in Figure 5.6 [49] [50] [51] [52] [53].

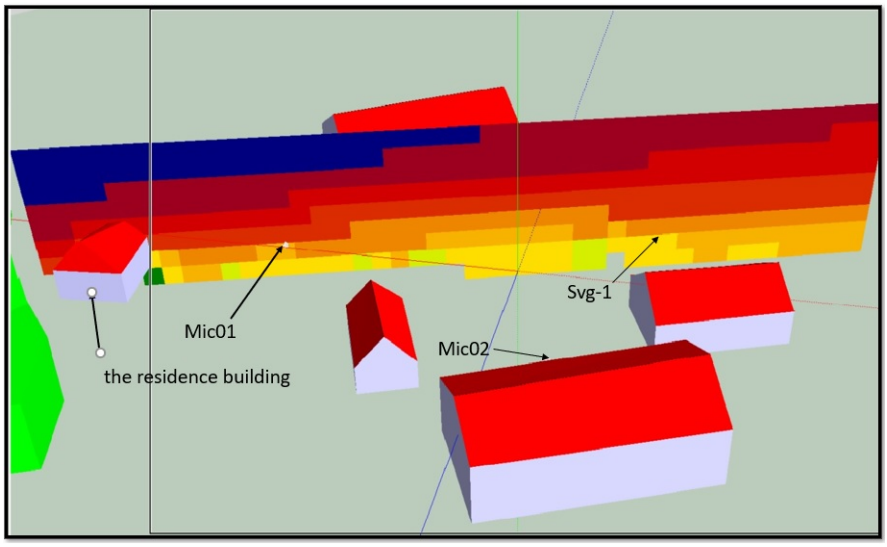

Figure 5.4: Cross Noise Map (CNM) plane passed by the microphone positions Mic01 and Svg-1 based on RLS-90.

Figure 5.5: Cross section map and the predicted noise levels passed by Mic01 based on RLS-90.

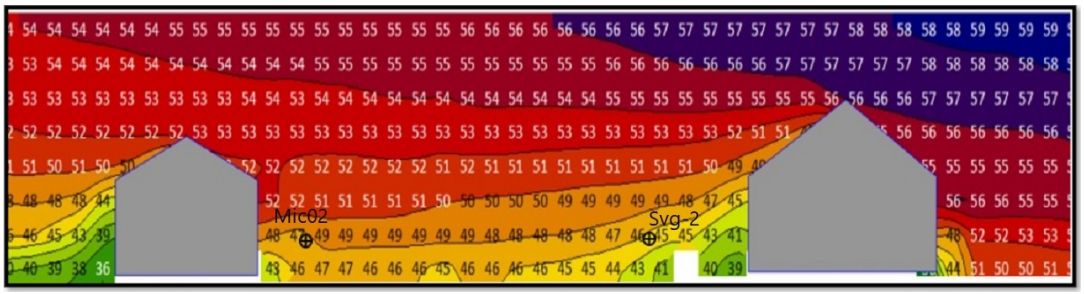

Figure 5.6: Cross section map and the predicted noise levels passed by Mic02 and svg-2 and based on RLS-90.

5.2.1.1 The simulation without the nearest building to the E18 at Solbergveien 37

A new building is built on the parallel side of the highway and used as storage, the acoustic properties of the area surrounding the houses can be changed with and without the house then the predicted data set is obtained by modeling without the house near the E18 and compared with results obtained from the simulation with the house. Figure 5.7 shows GNM and the predicted noise levels based on the noise indicators Nord2000 L_{den}, L_d, L_e and L_n without the house near the E18.

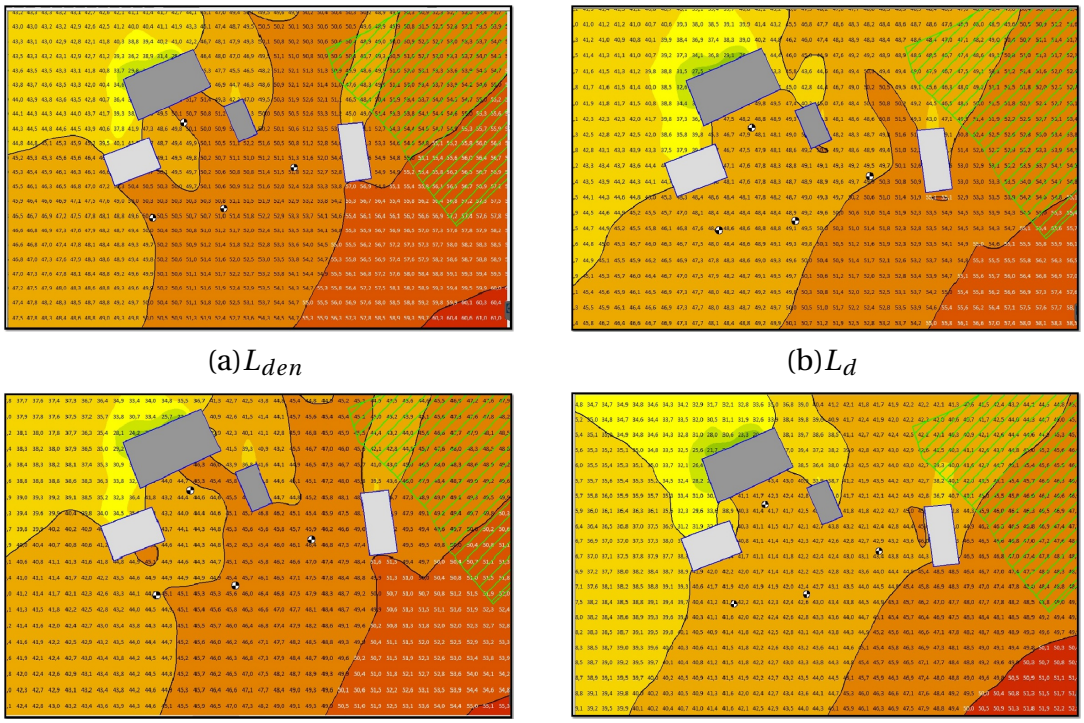

(a) L_{den} (b) L_d

(c) L_e (d) L_n

Figure 5.7: Grid Noise map and the predicted noise levels based on Nord2000 for the noise indicators L_{den}, L_d, L_e and L_n without the building near to E18 (Enlarged photos are included in Appendix B).

By removing the closest building to the E18, the predicted sound pressure levels increased in all receiver positions compared with the condition of the building located

in the front of the E18 in day-evening-night levels, as expected. The house is acted as a noise barrier which is effective in mitigating roadway noise, especially in the Svg-2 receiver position; the difference between the predicted L_{den} with and without the building is readily discernible from Table 5.9, the predicted L_{den} without building for the Mic01 receiver point is 3.7 dB(A) more than the predicted L_{den} with the located building. Besides, the Mic02 receiver position is 1.5 dB(A), the Svg-1 receiver position is 1.3 dB(A), and the Svg-2 receiver position is 4.5 dB(A) higher than the same receiver positions in the situation with the building located near to E18.

Table 5.9: The monitored sound pressure levels compared with the predicted L_{den} in SoundPLAN based on Nord2000 with and without the building at Solbergveien 37.

Microphone positions	Mic01	Mic02	Svg-1	Svg-2
The measured values in dB(A)	47.2	47.3	47.4	48.3
The predicted L_{den} in dB(A) without building	51.8	50.1	50.5	51.1
The predicted L_{den} in dB(A) with building	48.1	48.6	49.2	46.6
The difference in dB(A) (Without building)	-4.6	-2.8	-3.1	-2.8
The difference in dB(A) (With building)	-0.9	-1.2	-1.8	1.7
The difference in dB(A) (both predicted values)	3.7	1.5	1.3	4.5

The predicted L_d is characterized by Table 5.10; it can be observed that the predicted L_d without the building is more than with the located building in all receiver positions. Also, it can be shown the Mic02 and the Svg-1 receiver positions were not affected by the located building, and there is a slight difference of 0.6 dB(A) and 1.2 dB(A) between the predicted values with and without the building for the same points. In addition, the disparity between the predicted L_d for the Mic01 and the Svg-2 is 3.4 dB(A) and 4.6 dB(A), respectively.

Table 5.10: The monitored sound pressure levels compared with the predicted L_d in SoundPLAN based on Nord2000 with and without the building at Solbergveien 37.

Microphone positions	Mic01	Mic02	Svg-1	Svg-2
The measured values in dB(A)	47.2	47.3	47.4	48.4
The predicted L_d in dB(A) without building	49.5	48.0	48.6	49.1
The predicted L_d in dB(A) with building	46.1	47.4	47.4	44.5
The difference in dB(A) (Without building)	-2.3	-0.7	-1.2	-0.7
The difference in dB(A) (With building)	1.1	-0.1	0.0	3.9
The difference in dB(A) (both predicted values)	3.4	0.6	1.2	4.6

It is also helpful to consider the predicted sound pressure levels in the night L_e compared with the measured data, which is indicated in Table 5.11; it is seen that the measured data reported bigger values in comparison with the predicted values with and without the building. Moreover, the same patterns are repeated for the predicted L_e compared to the predicted L_{den} and L_d that the Mic01 and Svg-2 receiver positions are more affected by the located building.

Table 5.11: The monitored sound pressure levels compared with the predicted L_e in SoundPLAN based on Nord2000 with and without the building at Solbergveien 37.

Microphone positions	Mic01	Mic02	Svg-1	Svg-2
The measured values in dB(A)	47.2	47.3	47.4	48.3
The predicted L_e in dB(A) without building	46.4	44.5	45.0	45.6
The predicted L_e in dB(A) with building	42.8	43.2	44.6	41.1
The difference in dB(A) (Without building)	0.8	2.8	2.4	2.7
The difference in dB(A) (With building)	4.4	4.1	2.8	7.2
The difference in dB(A) (both predicted values)	3.6	1.3	0.5	4.5

The predicted sound pressure level L_n is then considered for the latest review in Table 5.12; it is seemingly the variation between the predicted L_n with and without the building is close enough to the pattern of the predicted levels above L_{den}, L_d and L_e with the highest values for the Mic01 receiver position (3.7 dB(A)) and the Svg-2 receiver position (4.4 dB(A)). Additionally, there are easily noticeable differences between the monitored values and the predicted L_n with and without the building.

Table 5.12: The monitored sound pressure levels compared with the predicted L_n in SoundPLAN based on Nord2000 with and without the building at Solbergveien 37.

Microphone positions	Mic01	Mic02	Svg-1	Svg-2
The measured values in dB(A)	47.2	47.3	47.4	48.3
The predicted L_n in dB(A) without building	43.4	41.7	41.9	42.6
The predicted L_n in dB(A) with building	39.7	40.9	41.7	38.2
The difference in dB(A) (Without building)	3.8	5.6	5.5	5.7
The difference in dB(A) (With building)	7.5	6.4	5.7	10.1
The difference in dB(A) (both predicted values)	3.7	0.8	0.2	4.4

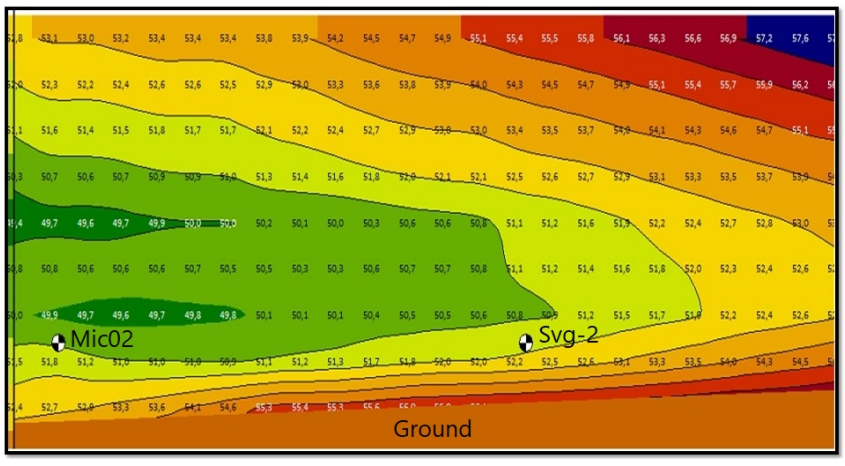

Figure 5.8: Cross Section Map (CSM) and the predicted noise levels based on Nord2000 without the located house.

The cross-section map is shown in Figure 5.8, which visualizes the prediction of sound pressure levels on a vertical grid for the noise from the E18. The receiver positions

pass the cross-section plane titled the Mic02 and the Svg-2 with the height of 20 m. A maximum difference of 4 dB(A) is raised on the cross-section map for the predicted L_{den}. Referred to Table 5.9, the values for the Mic02 and the Svg-2 correspond to those displayed in Figure 5.8 for the two mentioned receiver positions.

5.2.1.2 The calculation performed by SWECO without the nearby house to E18

SWECO also performed a calculation of outdoor noise level for E18, the outdoor sound levels are shown as the A-weighted average sound levels L_{den} for the day, evening, and night, where the values for evening and night are given an additional penalty of 5 dB(A) for the evening and 10 dB(A) for the night. Figure 5.9 and 5.10 are indicated the calculated values processed at CadnaA for the assessment and the prediction of the noise from E18.

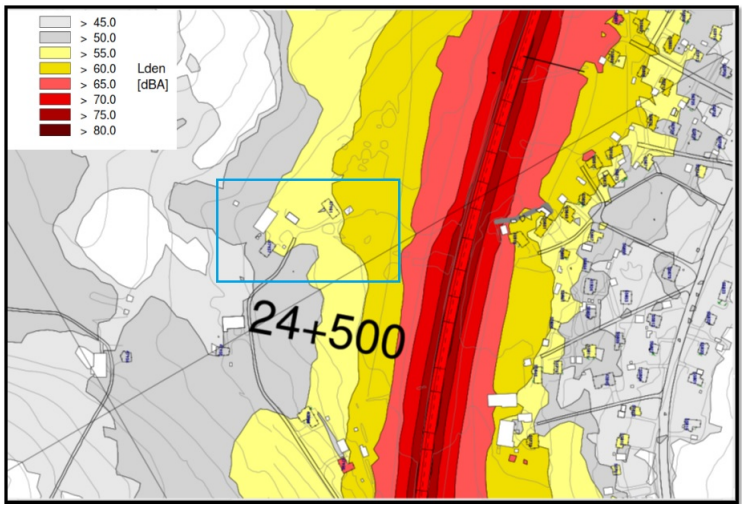

Figure 5.9: The predicted noise levels based on the Nordic method performed by SWECO at Solbergveien 37, shown in the blue frame [54].

To compare the predicted values obtained by SWECO in CadnaA with the predicted values in SoundPLAN, the noise maps and the areas affected by noise levels are indicated in Figure 5.10, and 5.11, which the receiver positions are also added for both situations stated above. The L_{den} noise map calculated by SWECO with the receiver locations is shown in Figure 5.10 that the areas affected by noise are divided into two parts based on the receiver positions, one part where the noise levels were not exceeded the limit value of 55 dB(A) with the located receiver positions Mic01, Mic02 and Svg-2 in this area showing by light lemon color, the next area was exposed to the noise is less than 50 dB(A) which Svg-1 was positioned in the area showing by gray color. The predicted L_{den} determined in SoundPLAN without the located house nearby to E18 is the same as the simulated model in CadnaA; they compared with the predicted L_{den} based on the area of the located receiver positions and it is seen that the areas affected by noise levels are correlated. In other words, the Mic01, the Mic02, and Svg-2 are placed in the area affected by noise levels between 50-55 dB(A), and the Svg-1 is situated in the area

affected by noise levels between 45-50 dB(A). The predicted L_{den} values in SoundPLAN for both simulated models with and without the located house is found in Table 5.13.

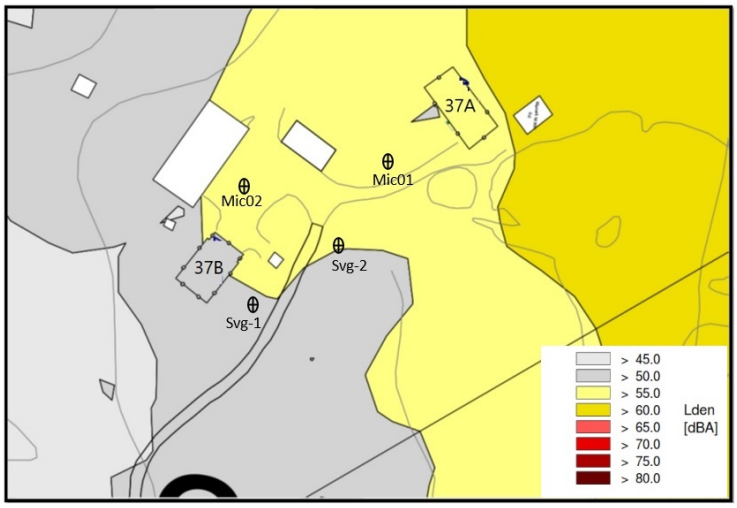

Figure 5.10: The predicted noise levels based on the Nordic method performed by SWECO at Solbergveien 37 (The blue frame is zoomed with the receiver positions) [54].

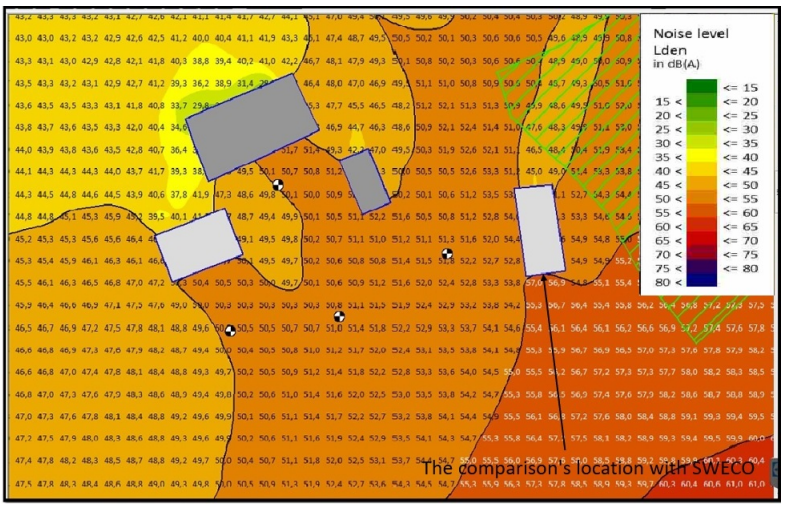

Figure 5.11: The comparison's location in the facade and the predicted values compared with SWECO (The zoomed pic is shown in B.9).

Table 5.13: The predicted L_{den} in SoundPLAN based on Nord2000 with and without the house at Solbergveien 37.

Microphone positions	Mic01	Mic02	Svg-1	Svg-2
The predicted L_{den} in dB(A) without house	51.8	50.1	50.5	51.1
The predicted L_{den} in dB(A) with house	48.1	48.6	49.2	46.6

The residence buildings 37A and 37B are shown in Figure 5.10, and the noise map is achieved in CadnaA, calculation points on all facades assigned to the residential build-

ings. However, the point on the facade nearby E18 is selected for the evaluation of the variation of the predicted L_{den} which is marked in Figure 5.11.

Table 5.14: The evaluation of the predicted value variation L_{den} on the facade in SoundPLAN and CadnaA at Solbergveien 37A.

The simulated model	SoundPLAN	CadnaA
The predicted L_{den} in dB(A)	57	56

The comparison between the simulation predicted values in SoundPLAN and CadnaA (SWECO) is seen in Table 5.14; it can be observed that the predicted values are almost the same with a 1 dB(A) increment for the simulated model in SoundPLAN with the value of 57 dB(A) and the value of 56 dB(A) in CadnaA.

5.2.2 Kodalveien 31

As noted, the comparison is made between the outlined methods RLS-90 and Nord2000. The layout of the houses and the roadways at Kodalveien 31 is shown in Figure 5.12.

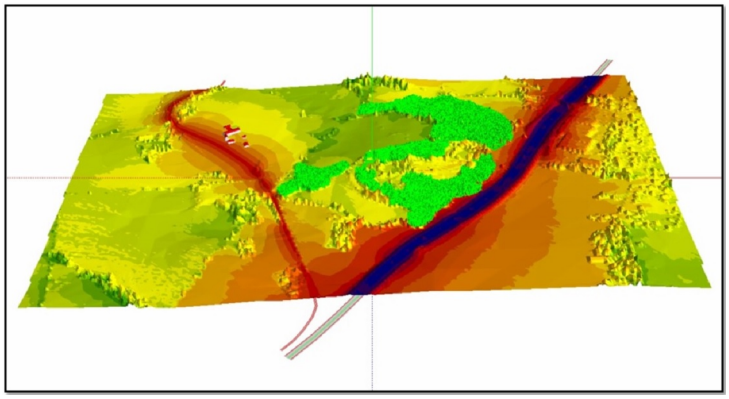

Figure 5.12: The layout at Kodalveien 31.

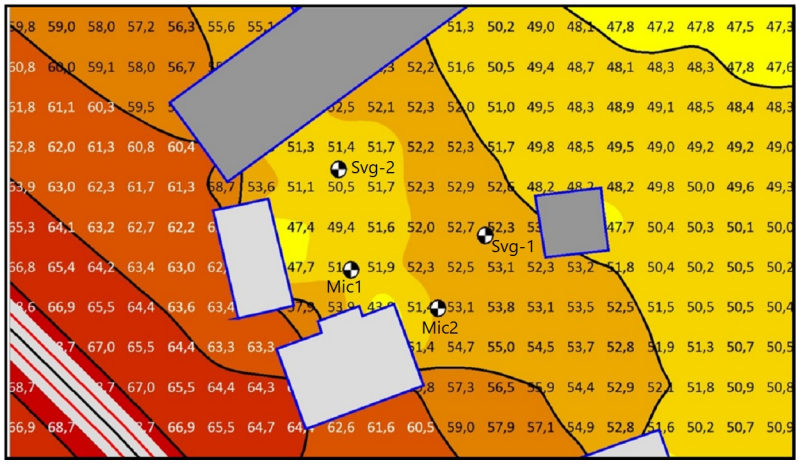

Figure 5.13: GNM and the predicted noise levels based on RLS-90 for the noise indicators L_{rD} at Kodalveien 31.

The receiver points at Kodalveien 31 have the longest distance from the E18 compared to the other measurement sites shown in Table 4.1. The same calculation for RLS-90 as mentioned in Section 4.5 was also performed at Kodalveien 31; the predicted noise levels L_{rD} is indicated above in Figure 5.13 for the surrounding houses.

In the second case, four receiver positions were chosen for monitoring the noise levels with 1.5 m height from the ground. The same calculations compared the predicted noise levels with the measured data. The Cross-Section Map and the predicted sound pressure levels in the surrounding of the houses for four receiver positions can be seen in Figure 5.14 and 5.15 [55].

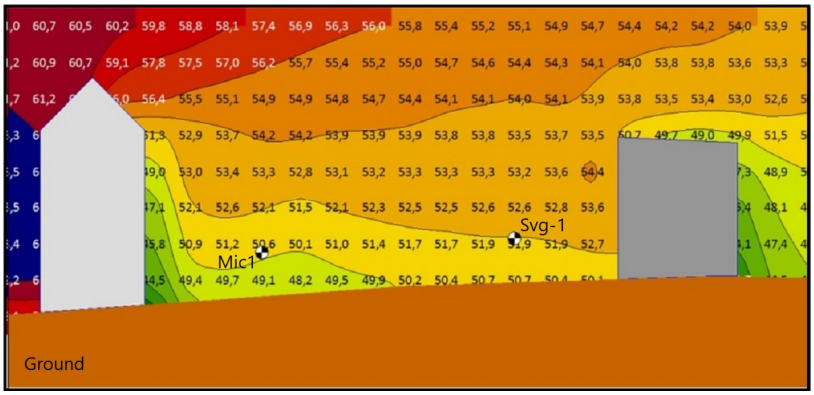

Figure 5.14: Cross Section Map and the predicted noise levels L_{rD} based on RLS-90 for the Mic1 and the Svg-1 receiver position.

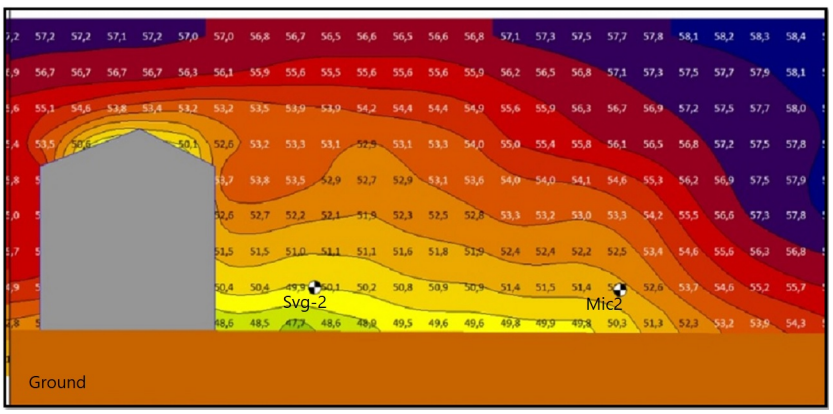

Figure 5.15: Cross Section Map and the predicted noise levels L_{rD} based on RLS-90 for the mic2 and the svg-2 receiver position.

As shown in Figure 5.12, the receiver position area is located among the E18 and Kodalveien, and the noise was audible from the E18 in the nearby building to Kodalveien. The monitored sound pressure levels for the receiver positions are compared with the predicted noise levels L_{rD} in Table 5.15.

Table 5.15: The monitored sound pressure levels compared with the predicted L_{rD} in SoundPLAN based on RLS-90 at Kodalveien 31.

Microphone positions	Mic01	Mic02	Svg-1	Svg-2
The measured values in dB(A)	52.5	50.9	51.3	49.9
The predicted L_{rD} in dB(A)	50.6	51.3	51.9	50.0
The difference in dB(A)	1.9	-0.4	-0.6	-0.1

The measurement results from Table 5.15 concluded that the variation of the measured values is 2.6 dB(A), with the maximum value for the Mic01 52.5 dB(A) and the minimum value for the Svg-2 receiver position with 49.9 dB(A). The reason is that the Mic01 is in the nearby Kodalveien, and the Svg-2 is far from E18 and Kodalveien. Moreover, the sound pressure level for Svg-1 is 51.3 dB(A), ranked second in the monitored values and it is nearby E18. Likewise, the predicted L_{rD} for the Mic01 is not nearly as close to the measured value with 1.9 dB(A) less than it, the other deviation values between the measured data and the predicted values L_{rD} for the Mic02, the Svg-1, and the Svg-2 are 0.4 dB(A), 0.6 dB(A) and 0.1 dB(A) which those are higher than the measured data respectively. Figure 5.16 and 5.17 are shown noise mapping for the noise indicators L_{den} and L_d based on Nord2000.

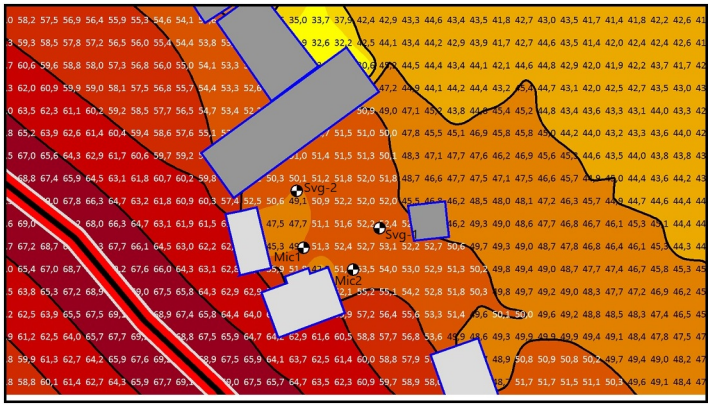

Figure 5.16: GNM and the predicted noise levels based on Nord2000 for the noise indicator L_{den} at Kodalveien 31.

Table 5.16: The monitored sound pressure levels compared with the predicted L_{rD} based on RLS-90 and L_{den}, L_d based on Nord2000 at Kodalveien 31.

Microphone positions	Mic01	Mic02	Svg-1	Svg-2
The measured values in dB(A)	52.5	50.9	51.3	49.9
The predicted L_{den} in dB(A) (Nord2000)	49.9	51.3	52.2	50.1
The predicted L_d in dB(A) (Nord2000)	48.5	50.5	50.8	48.5
The predicted L_{rD} in dB(A) (RLS-90)	50.6	51.3	51.9	50.0
The difference (the measured- L_{den}) in dB(A)	2.6	-0.4	-0.9	-0.2
The difference (the measured- L_d) in dB(A)	4.0	0.4	0.5	1.4
The difference (the measured- L_{rD}) in dB(A)	1.9	-0.4	-0.6	-0.1
The difference L_{den}-L_{rD} in dB(A)	-0.7	0.0	0.3	0.1

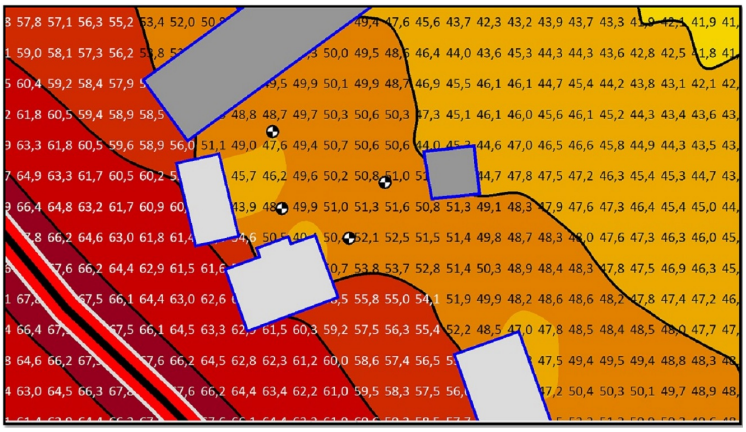

Figure 5.17: GNM and the predicted noise levels based on Nord2000 for the noise indicator L_d at Kodalveien 31.

The purpose of this part is to closely compare the measured data with the simulated values based on Nord2000 with the noise indicators L_{den} and L_d and RLS-90 with noise indicator L_{rD}. The data is collected in Table 5.16, the maximum variation between the receiver positions occurred in the Mic01and the Svg-1, which based on Nord2000 for L_{den} is 2.6-(-0.9)=3.5 dB(A) and for L_{rD} based on RLS-90 is 1.9-(-0.6)=2.5 dB(A) compared with the measured values in the Mic01 and the Svg-2 by 52.2-49.9=2.6 dB(A). Besides, the difference between L_{den} and the measured values for the Mic01 is 2.6 dB(A), the Mic02 is -0.4 dB(A), the Svg-1 is -0.9 dB(A), and the Svg-2 is -0.2 dB(A), in the case of L_{rD} the dissimilarity with the measured data for the Mic01 is 1.9 dB(A), the Mic02 is -0.4 dB(A), the Svg-1 is -0.6 dB(A), and the Svg-2 is -0.1 dB(A). Also, there is a striking resemblance between the predicted values L_{den} and L_{rD} which the dissimilarity for the Mic01 is -0.7 dB(A), the Svg-1 is 0.3 dB(A), and the Svg-2 is 0.1 dB(A), however, L_{den} for the Mic02 is utterly equal to L_{rD} with the value of 51.3 dB(A). Eventually, L_{rD} are much closer to the measured values in all receiver positions than L_{den}. In the daytime, based on Nord2000, the predicted L_d has been varied from 48.5 dB(A) to 50.8 dB(A), which remained less than the monitored values for the Mic01 4 dB(A), the Mic02 0.5 dB(A), the Svg-1 0.5 dB(A) and the Svg-2 1.4 dB(A).

5.2.3 Lånheveien 11

To estimate the predicted sound pressure levels of the surrounding houses at Lånheveien 11, the calculations based on RLS90 and Nord2000 have been performed. The location of houses and the roads are indicated in Figure 5.18.

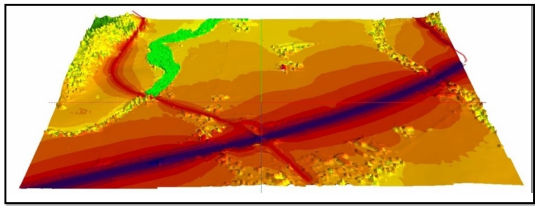

Figure 5.18: The layout for Lånheveien 11.

The calculated sound pressure levels, L_{rD}, at the receiver points based on RLS-90 are shown in Figure 5.19, the direct distance of the main building to E18 is 340 m where the receiver positions are distributed around it, it is shown with the light gray color in Figure 5.19.

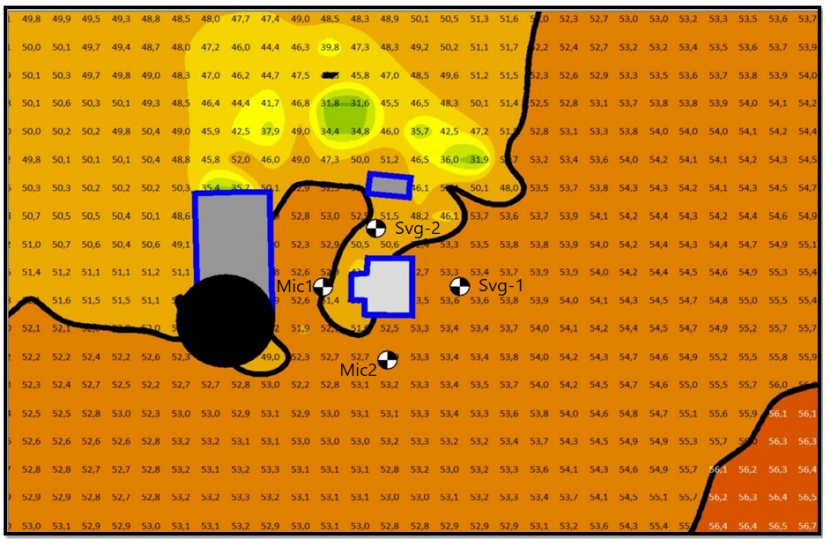

Figure 5.19: GNM and the predicted noise levels based on RLS-90 for the noise indicator L_{rD} at Lånheveien 11.

The predicted L_{rD} levels are in Table 5.17 compared to the measured values.

Table 5.17: The monitored sound pressure levels compared with the predicted L_{rD} in SoundPLAN based on RLS-90 at Lånheveien 11.

Microphone positions	Mic01	Mic02	Svg-1	Svg-2
The measured values in dB(A)	49.9	51.4	54.4	52.9
The predicted L_{rD} in dB(A)	51.4	52.5	53.6	51.5
The difference in dB(A)	-1.5	-1.1	0.8	1.4

Two noise sources in the model are E18 and Lånheveien. The receivers are directly affected by the emission of E18; all receiver positions are not free of the reflections between the houses and the ground reflections. The predicted sound levels L_{rD} at receiver positions for the Mic01 and the Svg-2 are not close to the measured values compared to the Svg-1 with a difference of 0.8 dB(A) with the measured value; additionally, the predicted L_{rD} for the Svg-2 is 1.4 dB(A) smaller than the measured value, not only that the Mic01 and the Mic02 are exceeded 1.5 dB(A) and 1.1 dB(A) from the measured values respectively. The highest measured sound pressure level is on the receiver position of the Svg-1 with 54.4 dB(A), and the lowest measured sound pressure level is on the receiver position of the Mic01 with 49.9 dB(A). The maximum predicted value is for the Svg-1 with 53.6 dB(A), and the minimum predicted value is 51.4 dB(A) for the Mic01 receiver position. It is essential to remember that ground attenuation is mainly the result of sound reflected by the ground surface; when sound is propagated over the ground, attenuation also occurs because of energy losses on reflection, and the losses

depend on the material of the ground surface. The ground attenuation automatically can be set between 0-1 in SoundPLAN, of which the given number in the simulation model is 0.5 for the soil without vegetation. Moreover, there is no sound barrier in the sound propagation path for the actual situation and the simulation model.
The models were set up for Nord2000 in both summer and winter to know more about the meteorological effects on sound propagation. The modeling of the meteorology in summer and winter was performed by the mentioned parameters in Table 4.12 for noise mapping based on Nord2000, considering the situations in summer and winter for noise indicator L_{den} shown in Figure 5.20 and 5.21.

Figure 5.20: GNM and the predicted noise levels based on Nord2000 for the noise indicator L_{den} in the summer at Lånheveien 11.

Figure 5.21: GNM and the predicted noise levels based on Nord2000 for the noise indicator L_{den} in the winter at Lånheveien 11.

It has been noticed from the comparison of grid noise maps between the summer and the winter condition based on Nord2000 in Figure 5.20 and 5.21 that the predicted L_{den}

larger than the measured values are common expect to the Svg-1 and Svg-2 receiver positions in the winter situation. Also, the predicted sound pressure level in the Mic02 has become the largest value in which the L_{den} 2.3 dB(A) and 3.6 dB(A) is larger than the measured values in the winter and the summer, respectively. The L_{den} in the summer is almost 1 dB(A) larger than the L_{den} in the winter. The reason that the predicted L_{den} in the Mic02 receiver position is larger than the measured value is SoundPLAN computed free field values, but the reflected sound from the facade is recorded for the monitored value, and also shrubs obstruct the sound, and it is not included in the simulation models. Table 5.18 shows the L_{den} in the winter and the summer simulation compared to the measured values. The measured sound pressure levels have almost differed by 1 dB(A) for the receiver positions the Svg-1 and the Svg-2; however, the Mic01 in the summer situation 2.8 dB(A) and in the winter situation 1.1 dB(A) is higher than the measured values and the Mic02 in summer 2.3 dB(A) and in winter 3.6 dB(A) higher than the measured ones [56].

Table 5.18: The monitored sound pressure levels compared with the predicted L_{den} both summer and winter at Lånheveien 11 based on Nord2000.

Microphone positions	Mic01	Mic02	Svg-1	Svg-2
The measured values in dB(A)	49.9	51.4	54.4	52.9
The predicted L_{den} in dB(A) in winter	51.0	53.7	53.9	52.1
The predicted L_{den} in dB(A) in summer	52.7	55.0	55.3	53.1
The difference in dB(A) (winter)	-1.1	-2.3	0.5	0.8
The difference in dB(A) (summer)	-2.8	-3.6	-0.9	-0.2

To consider the similarity of RLS-90 and Nord2000 assessment for Lånheveien 11 as regraded in Table 5.19, the measured data is compared to the predicted L_{den} and the predicted L_{rD} for the exact measurement locations. The correlations of the measured results with the predicted values are shown in Table 5.19. They are derived from being relatively the same for all receiver positions, except the Mic02 for Nor2000 in a difference of 1.2 dB(A) with RLS-90 compared with the measured result.

As noted, the procedure based on Nord2000 determined the noise levels for other noise indicators as L_d, L_e, and L_n are shown in Figure 5.22.

Table 5.19: The monitored sound pressure levels compared with the predicted L_{den} based on Nord2000 and L_{rD} based on RLS-90 at Lånheveien 11.

Microphone positions	Mic01	Mic02	Svg-1	Svg-2
The measured values in dB(A)	49.9	51.4	54.4	52.9
The predicted L_{den} in dB(A) (Nord2000)	51.0	53.7	53.9	52.1
The predicted L_{rD} in dB(A) (RLS-90)	51.4	52.5	53.6	51.5
The difference in dB(A) (Nord2000)	-1.1	-2.3	0.5	0.8
The difference in dB(A) (RLS-90)	-1.5	-1.1	0.8	1.4
The difference (L_{den}-L_{rD})in dB(A)	-0.4	1.2	0.3	0.6

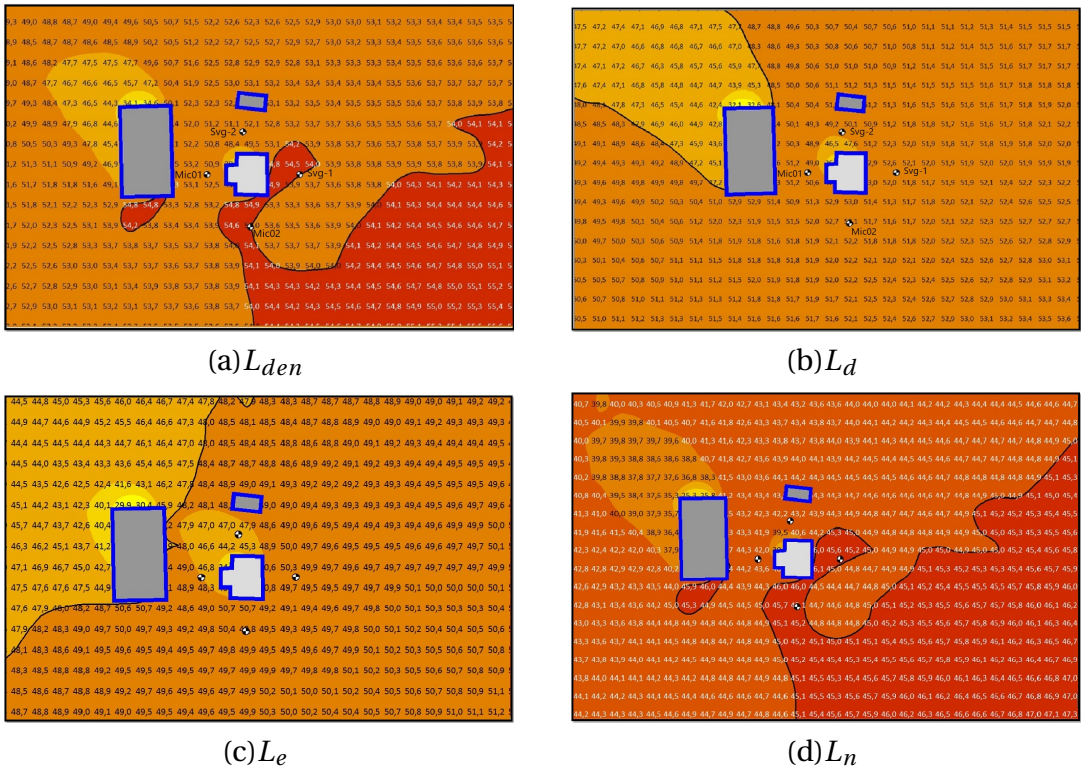

(a) L_{den} (b) L_d

(c) L_e (d) L_n

Figure 5.22: Grid Noise map (GNM) and the predicted noise levels based on the noise indicators Nord2000 L_{den}, L_d, L_e and L_n at Lånheveien 11.

Table 5.20: The monitored sound pressure levels compared with the predicted L_{den}, L_d, L_e and L_n at Lånheveien 11 based on Nord2000.

Microphone positions	Mic01	Mic02	Svg-1	Svg-2
The measured values in dB(A)	49.9	51.4	54.4	52.9
The predicted L_{den} in dB(A)	51.0	53.7	53.9	52.1
The predicted L_d in dB(A)	50.1	52.1	52.0	49.3
The predicted L_e in dB(A)	48.2	49.4	49.7	46.8
The predicted L_n in dB(A)	43.4	44.7	44.9	43.3
The difference (the measured-L_{den})in dB(A)	-1.1	-2.3	0.5	0.8
The difference (the measured-L_d) in dB(A)	-0.2	-0.7	2.4	3.6
The difference (the measured-L_e) in dB(A)	1.7	2.0	4.7	6.1
The difference (the measured-L_n) in dB(A)	6.5	6.7	9.5	9.6

5.3 The predicted and the measured road traffic noise spectra

Spectral analysis has been performed for one-hour measurements to understand better the recorded signals content for the mentioned locations above. Considering the time-domain and frequency-domain based on the spectrum analysis is significant.

5.3.1 Solbergveien 37

As can be seen from Figure 5.23, the measured sound pressure levels with A-weighting applied versus time are indicated as a time-domain signal for one-hour measurement, which is included three peaks for four receiver positions, the first and third peaks of the time-domain signal occurred at 16 minutes (960 s) and 48 minutes (2880 s) for approaching a car and the second peak appeared at 35 minutes (2100 s) due to passing an airplane in the measurement location.

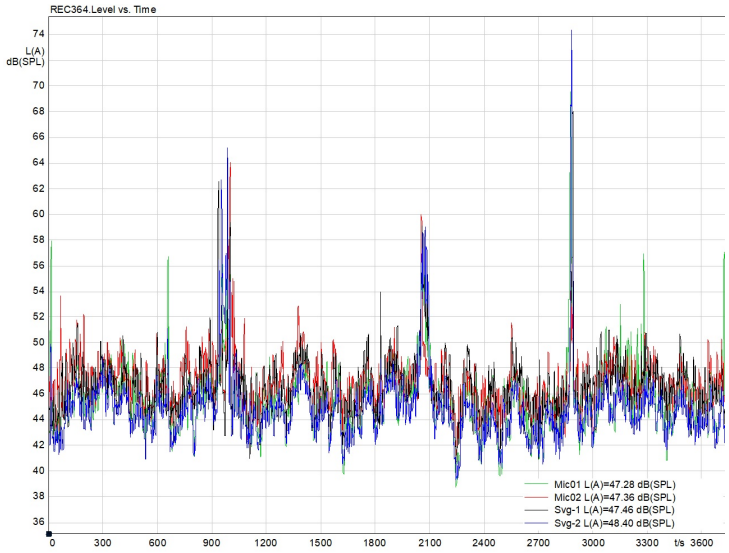

Figure 5.23: Sound pressure levels versus time with A-weighting applied at Solbergveien 37.

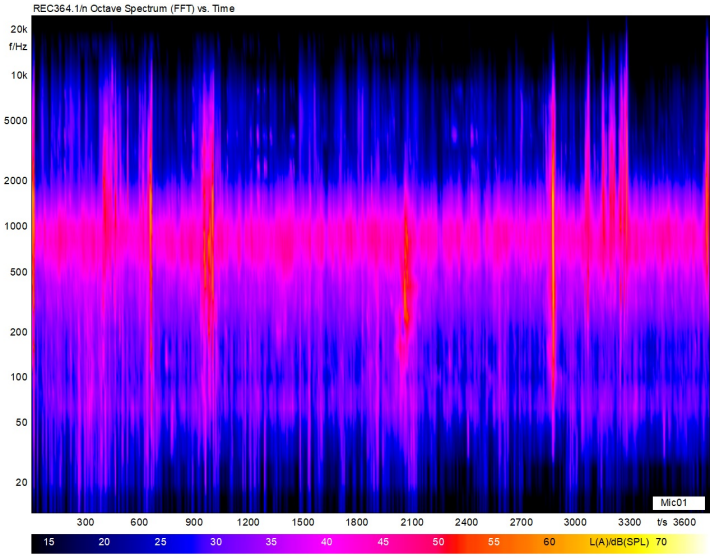

Figure 5.24: FFT vs. time plot for the measurement noise at Solbergveien 37.

The spectrogram shows the spectral data in Hertz and temporal data for the measurement time in seconds concerning magnitude. FFT vs. Time is displayed in Figure 5.24

in 20 Hz to 20 kHz range which the maximum sound pressure level has been detected at frequency 900 Hz for the rolling noise, concerning temporal data that it has an increased SPL in the motioned time 960 s, 2100 s and 2880 s [57] [58].
The spectrum of road traffic noise and its magnitude depends on various factors such as the speed of the vehicle, the road surface, the traffic flow, and the rate of vehicle categories with the proportion of heavy vehicles to cars. Also, the weather conditions can affect the spectrum and the magnitude of road traffic noise [59].
Figure 5.25 shows the measured and the predicted road traffic noise spectra at Solbergveien 37; it can be seen that the predicated spectrum has two peaks; one is at 63 Hz for the propulsion noise, and it causes the outdoor noise spectrum from traffic to have almost a tonal component at low frequencies and the next peak is at 1 kHz for the rolling noise. Also, a study has been carried out by Brekke & Strand Akustikk on more than 2100 outdoor traffic noise spectrums, including the passage of more than 3.5 million vehicles; it is shown that the traffic noise is always included a peak at the low-frequency range of 50-100 Hz [60].
However, the measured spectrum is shown three peaks at 80 Hz, 160 Hz, and 800 Hz in which the peak at 160 Hz is not dominated at the Mic01, the Svg-1, and the Svg-2 receiver positions, and the resonance at 160 Hz at the Mic02 receiver position is likely to be due to the reflection from the facade. It is also linked with the same repetition pattern with the peak at 80 Hz. Furthermore, the peak at 80 Hz is for propulsion noise, and the peak at 800 Hz is for the rolling noise. The predicted traffic noise road spectrum is also plotted using SoundPLAN. In contrast with the measured spectrum, detecting those resonance peaks in the SoundPLAN modeling is impossible.

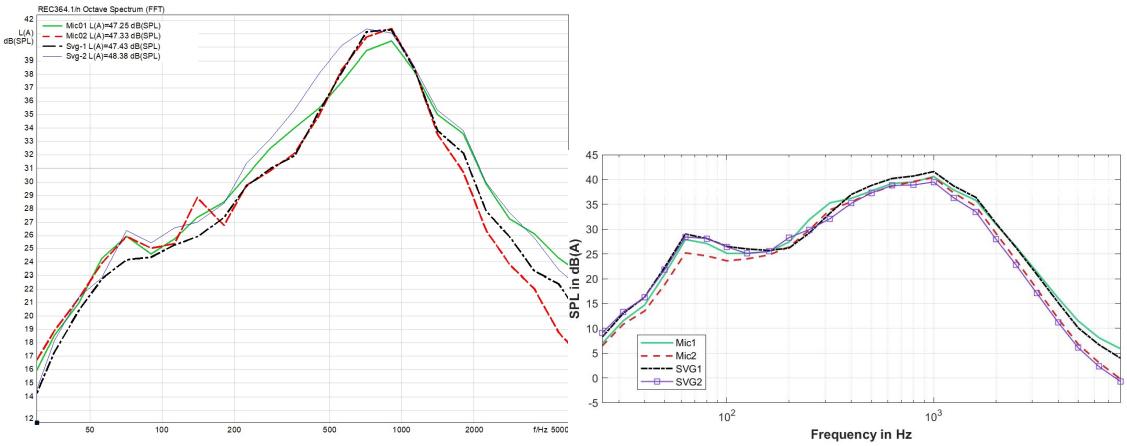

(a) (b)

Figure 5.25: The road traffic noise spectra at Solbergveien 37 (a)the measured spectra (b) the predicted spectra in SoundPLAN.

5.3.2 Lånheveien 11

Using the same procedure technique for the field measurement with four receiver positions in the surrounding of the house, the time-domain noise measurement at Lånheveien 11 is indicated in Figure 5.26, an overview of the noise signals is shown the magnitude of the signals is almost remained constant between 42 dB(A) to 62 dB(A)

during one-hour measurement. There are no background noises as a pulse in the recorded signals, for example, noise from approaching a car and an airplane or animals like the barking of a dog.

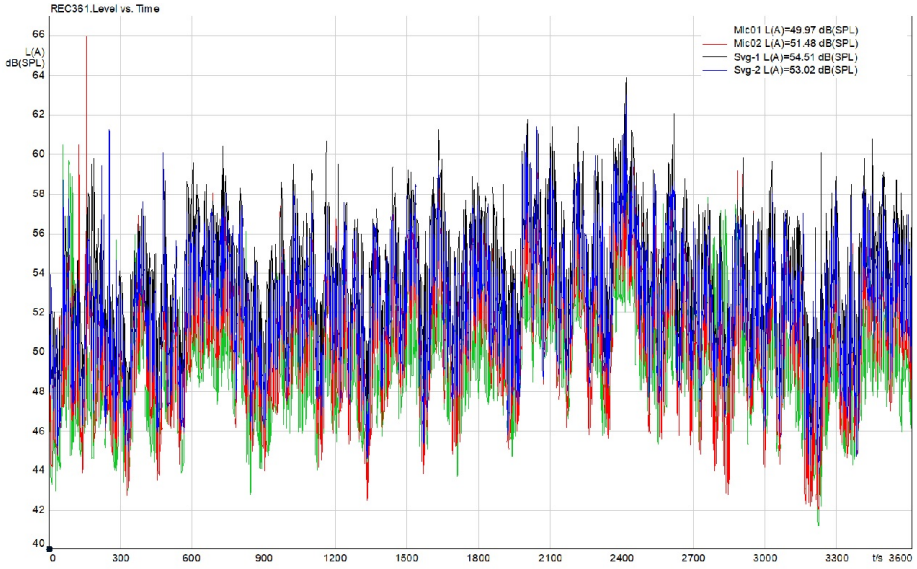

Figure 5.26: Sound pressure levels versus time with A-weighting applied at Lånheveien 11.

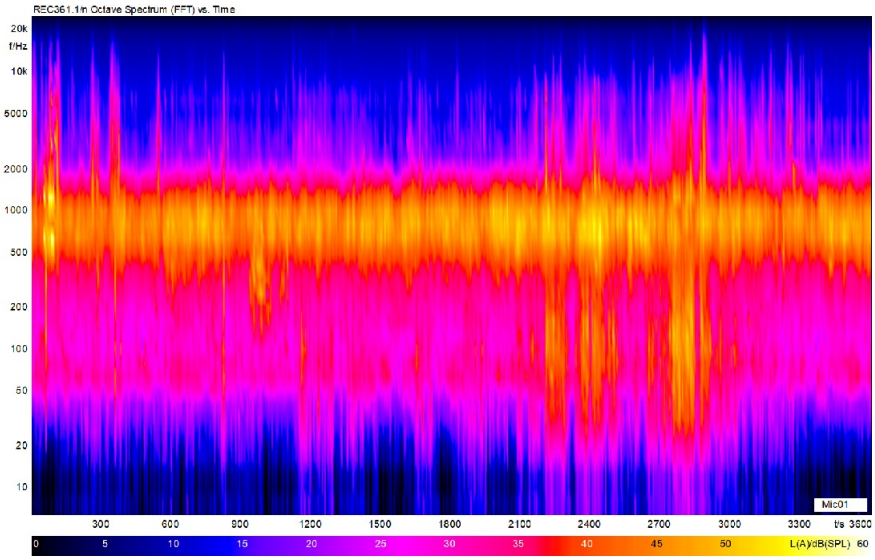

Figure 5.27: FFT vs. Time for the measurement noise at Lånheveien 11.

As stated above, the spectrogram can give deeper consideration to the noise signals, so FFT vs.Time is displayed in a spectrogram in Figure 5.27; as it is motioned earlier, there is a peak in the noise traffic spectrum for the rolling noise at 1 kHz, however, in the study by Sandberg [61] given that most frequency spectra of exterior tires or road noise display a prominent peak in the range of 700-1300 Hz. The rolling noise peak is indicated around 800 Hz at Lånheveien 11, which is the asphalt surface type, the speed,

and the type of the vehicle, as cars or trucks can shift the peak to higher or lower than 1 kHz.

The measured and the predicted traffic noise spectra at Lånheveien 11 are seen in Figure 5.28; the predicted spectrum is obtained for further analysis and is compared with the measured spectrum. Two peaks are dominated in the prediction of noise spectrum in SoundPLAN by frequencies around 63 Hz for the propulsion noise and 1 kHz for the rolling noise.

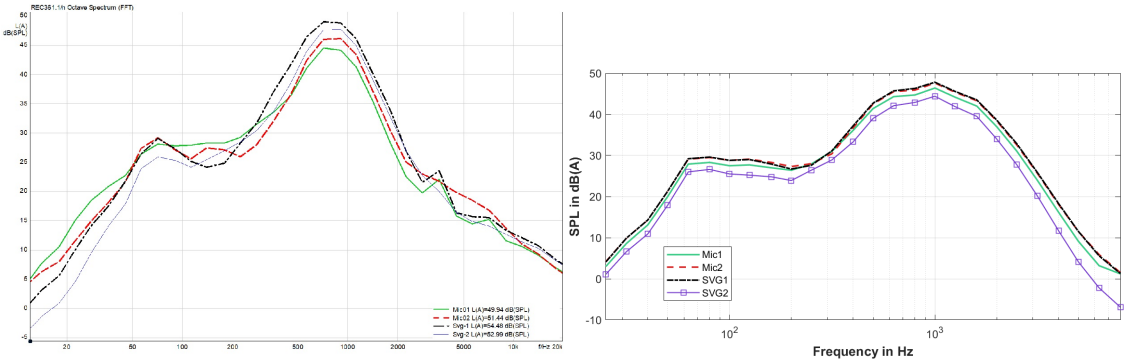

(a) (b)

Figure 5.28: The road traffic noise spectra at Lånheveien 11 (a) the measured spectra (b) the predicted spectra in SoundPLAN.

The measured spectrum is obtained to compare with the predicted spectrum in which two peaks are dominated at low frequencies. Two distinct peaks appeared at higher frequencies. The peaks at lower frequencies are at 80 Hz for all the receiver positions, and it is the typical peak caused by the propulsion noise; the second peak at the lower frequencies is not the same for all the receiver positions, the second peak is not appeared at the spectrum for the Mic01 receiver position, since the second prominent peaks for the Mic02, the Svg-1, and the Svg-2 are at 160 Hz, 200 Hz and 125 Hz respectively. The measured spectrum's third and fourth resonance peaks are dominated at 4000 Hz and 8000 Hz for the Mic01 and the Svg-1 receiver positions.

5.3.3 Kodalveien 31

The time-domain noise measurements at Kodalveien 31 were obtained according to the similar method noted in the last part in which the noise was recorded in four microphones positions; the measurement results in the time-domain are plotted in Figure 5.29. The measurement results consisted of constant fluctuation patterns during one-hour measurement without representing peaks in the noise measurement signals.

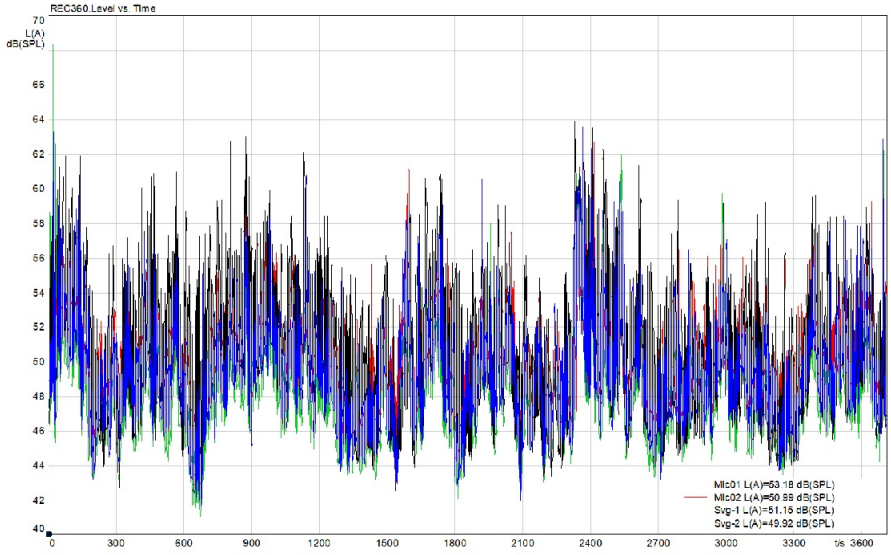

Figure 5.29: Sound pressure levels versus time with A-weighting applied at Kodalveien 31.

As mentioned before, a spectrogram can be visualized the spectrum of frequencies on a signal as it varies with time and the pressure levels of the signal. FFT vs.Time is illustrated in Figure 5.30.

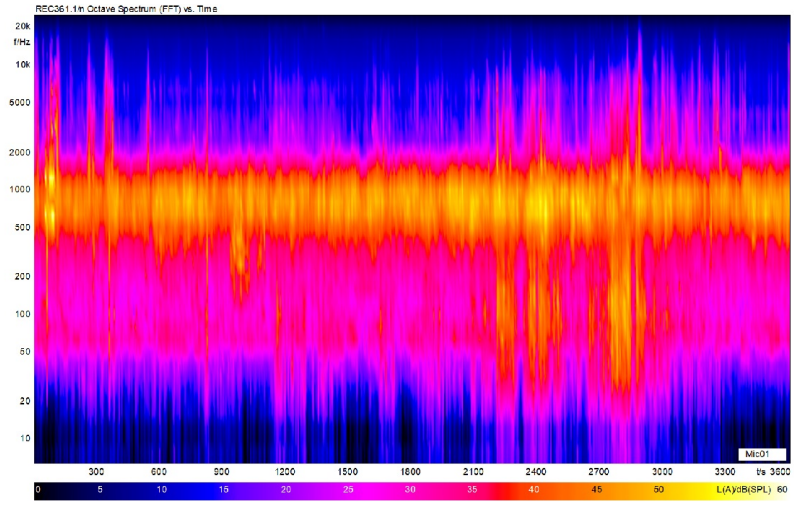

Figure 5.30: FFT vs. Time for the measurement noise at Kodalveien 31.

The measured spectrum was calculated by Artemis SUITE as cited above, and it is shown in Figure 5.31; in this case, more peaks are captured in low frequencies that are common at all receiver positions in 80 Hz, 160 Hz, and 250 Hz and also a prominent peak is displaced at 800 Hz for the rolling noise at all the receiver positions mentioned above. There are more peaks in higher frequencies for the Mic01 microphone poisons at 1600 Hz, 3150 Hz, 8000 Hz, and 12500 Hz. Moreover, the sound pressure levels are higher at the higher frequencies than at the lower ones at the Mic01 receiver position compared with other receiver positions. The location of the receiver poisons is illustrated in Figure 4.6 since the Mic02 and the Svg-2 microphone positions are located in

the middle of the yard, which is far away from the 18 and Kodalveien. In contrast with the Mic01 (nearby Kodalveien) and the Svg-1 (nearby E18), the sound pressure levels are higher at the lower frequencies than the higher ones. The prominent peak at 80 Hz is comparable with other measured locations in which the peak appears in all microphone positions in all measured locations; thereby, the prominent peak at 80 Hz is captured in all measured spectrum, and it is due to the propulsion noise.

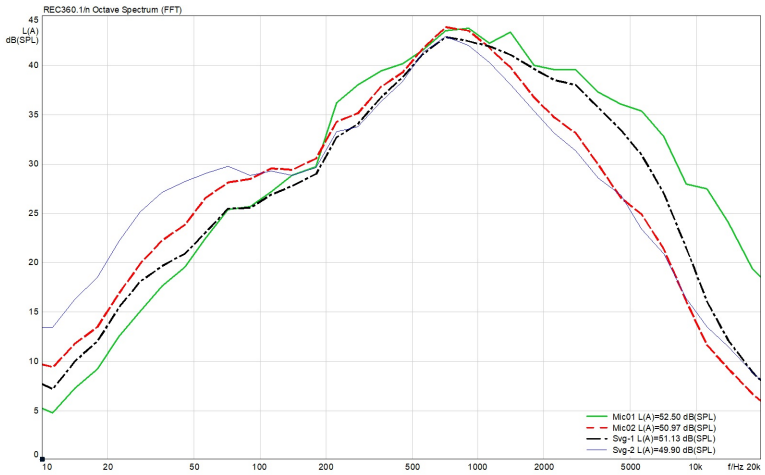

Figure 5.31: The measured road traffic noise spectra at Kodalveien 31.

5.4 The consideration of the factors that can be affected on the measured spectrum

The consideration has been done to determine the effects of traffic density, distance, and microphone height on the measured spectrum at Solbergveien 37 and Lånheveien 11, compared to the measured spectrum from 110 zones for the motorways of E6 and E18 which are measured by Brekke & Strand Akustikk. The measured spectrum is plotted referring to the number of vehicles and distance from the center of the road in two internal code zones R115 and R120, for each spectrum with A-weighting applied in 1/3 octave band in one hour recorded time. This part aims to consider how the spectrum is formed in different statuses based on the number of vehicles, distance from the center of the road, the microphone's height, and the vehicle's speed. Table 5.21 indicates detailed information about the plotted spectrum for the motioned zones. Also, the spectrums of zone R120 are plotted in Figure 5.32 [62] [63].

Table 5.21: The detailed information for the plotted spectrum for the motorways of E6 and E18.

Internal code	Distance of center (m)	Height of Mic. (m)	speed limit (km/h)	The dominant frequency peaks (Hz)
R120	132	2	110	80, 1000, 4000, 5000
R115	180	2	110	80, 800, 4000
R115	190	4	110	80, 800, 4000, 6300
R115	95	4	110	100, 1000
Lånheveien 11	340	2	110	63, 125, 160, 800, 6300, 8000
Solbergveien 37	128	2	110	63, 125, 160, 800, 4000, 6300, 8000

The dominated peaks are shown in the plotted spectrum in the zone R120 with the distance of 132 m and the height of 2 m which the peaks are at 80 Hz, 1 KHz, 4 KHz and 5 kHz. The comparison of the spectrum should be made between R120 and R115 zones to observe how variables interact with each other to change the spectrum. The plotted spectrum in the zone of R115 with the distance of 180 m and the height of 2 m are shown in Figure 5.33, the dominated peaks are observed at 80 Hz, 800 Hz and 4 kHz. Moreover, the spectrum in the zone of R115 with the distance of 190 m and the height of 4 m showed peaks at 80 Hz, 800 Hz, 4000 Hz and 6300 Hz that Figure 5.33 displays the motioned peaks in the spectrum. In addition, the microphone position was mounted on the facade at Lånheveien 11 and Solbergveien 37 with the height of 2 m and the first dominant is on 63 Hz caused by the propulsion noise in both cases, however, in one-hour measurement by having the microphone in the stand in surrounding of houses, the first dominant is on 80 Hz in each of the cases.

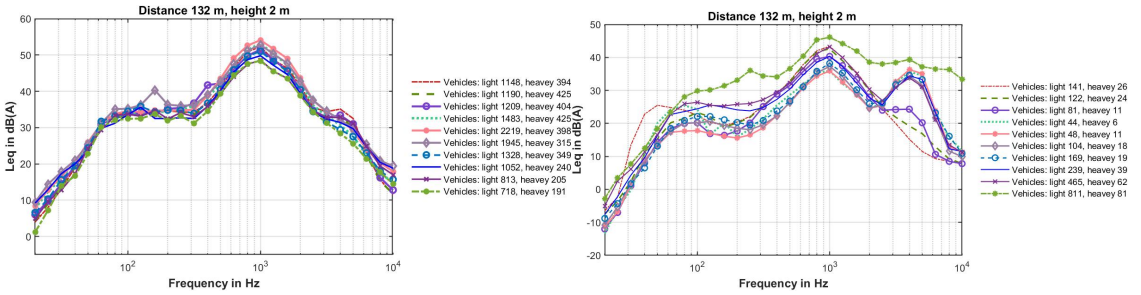

(a)

(b)

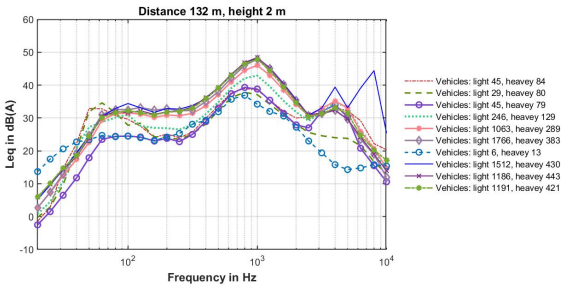

(c)

Figure 5.32: The measured spectrum L_{Aeq} in 1/3 octave for the zone R120 with distance of 132 m and the microphone height above the ground of 2 m during one hour measurement period (continued).

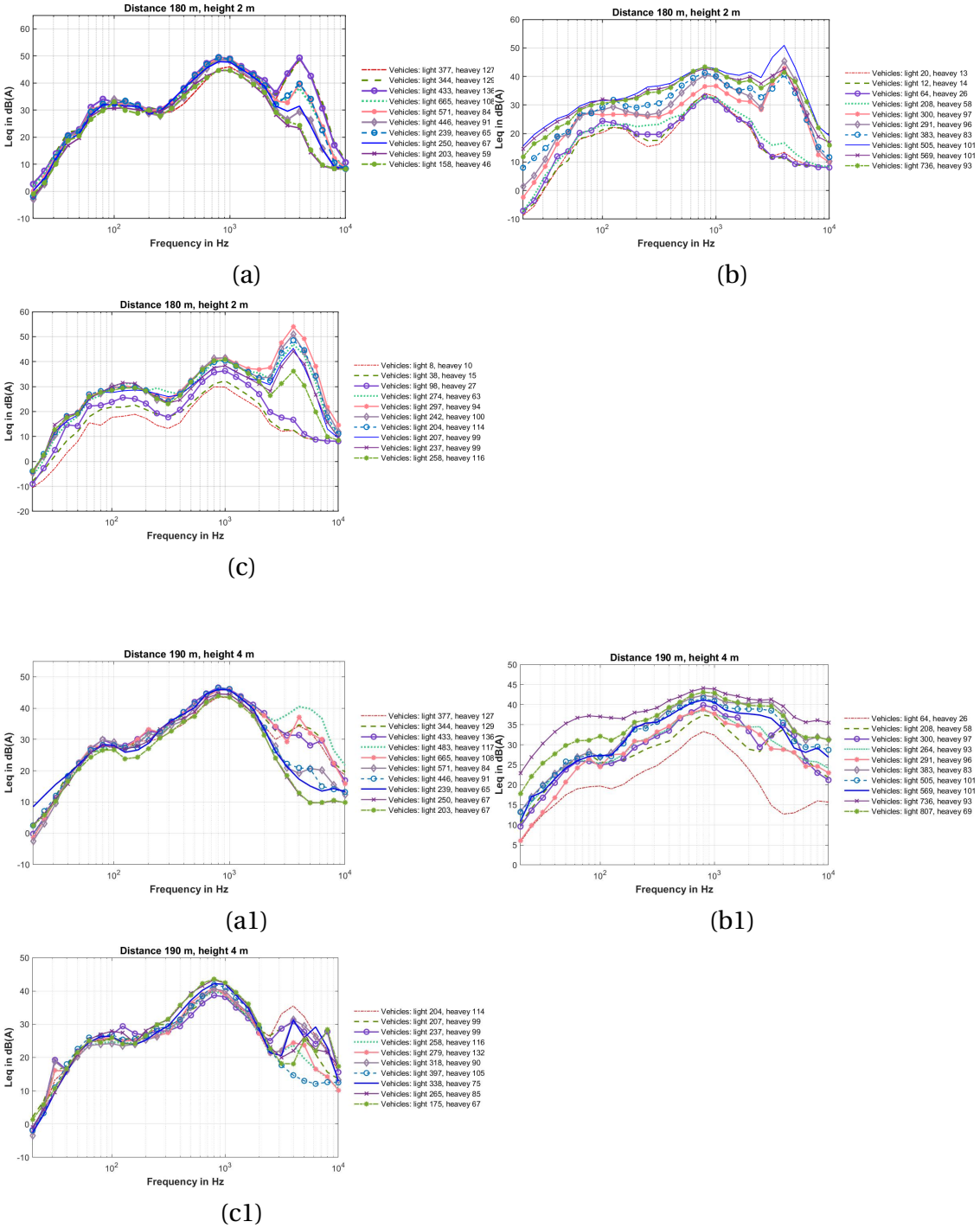

Figure 5.33: The measured spectrum L_{Aeq} in 1/3 octave for the zone R115 with distance of 180 m & 190 m and the height of 2 m & 4 m during one hour measurement period.

In the case of R115 with the distance of 95 m and the height of 4 m, the spectrum is formed with two peaks at 100 Hz and 1 kHz. As can be seen from Figure 5.34 spectrum reached the first peak at 100 Hz which those are flattened out until 160 Hz and the spectrum have been shown to increase to the second peak at 1 kHz, moreover, the spectrum is fallen sharply after 1 kHz without any peaks in the frequency spectra over 1 kHz. The form of the spectrums has been changed with respect to the height of the microphone and the distance to the source or the highway. As explained above, there are two dominant peaks in the spectrum, the first dominant caused by the propulsion is at 100 Hz, and the rolling noise is at 1 kHz.

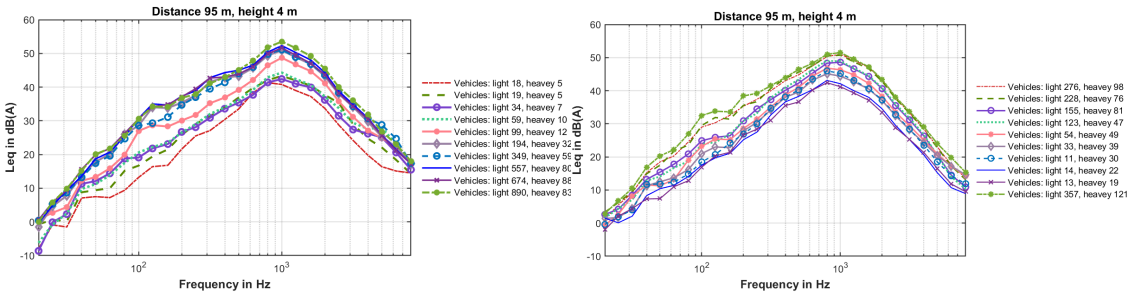

(a) (b)

Figure 5.34: The measured spectrum L_{eq} in 1/3 octave for the zone R115 with distance of 95 m and the height of 4 m during one hour measurement period.

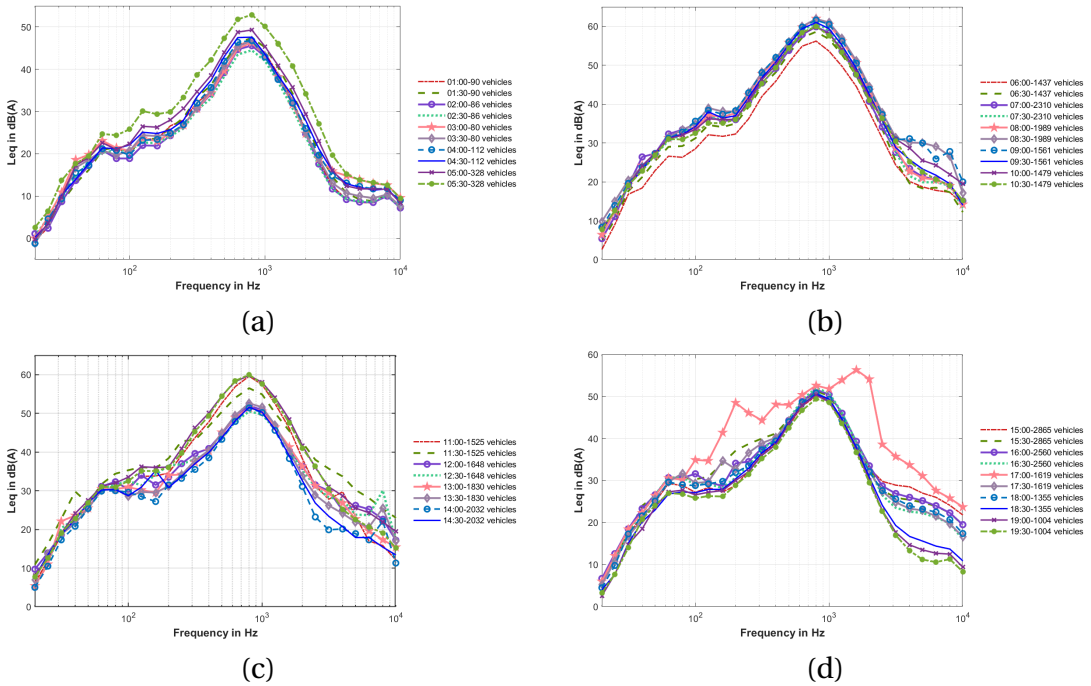

(a) (b)

(c) (d)

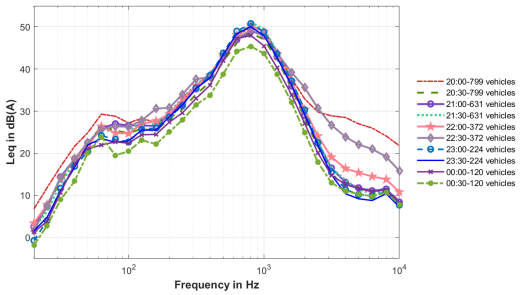

(e)

Figure 5.35: The measured spectrum with A weighing applied L_{Aeq} based on 1/3 octave bands in 24-hour at Solbergveien 37, the hourly spectra are in the Appendix D.

The measured spectrum with A-weighing applied L_{Aeq} based on 1/3 octave bands in 24-hour at Solbergveien 37 are shown in Figure 5.35 for each 30-minute intervals, which are recorded with a mounting microphone in the facade. The peaks in spectra are appeared on 63 Hz caused by the propulsion, 125 Hz, 160 Hz, 800 Hz for the rolling noise, 4000 Hz, 6300 Hz and 8000 Hz. The peaks have not appeared in all intervals spectrum; for instance, the peaks at 6300 Hz are seen from 11:00 to 14:00 during the day.

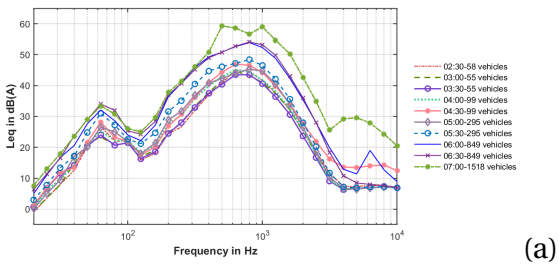

(a)

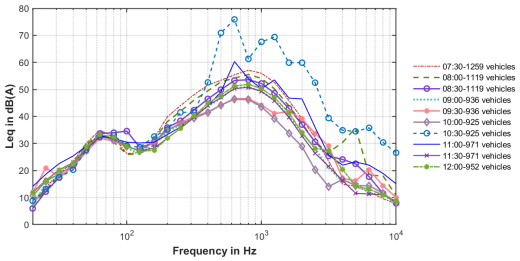

(b)

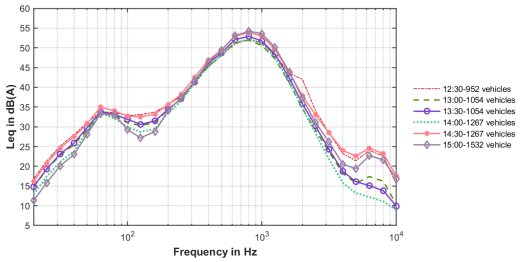

(c)

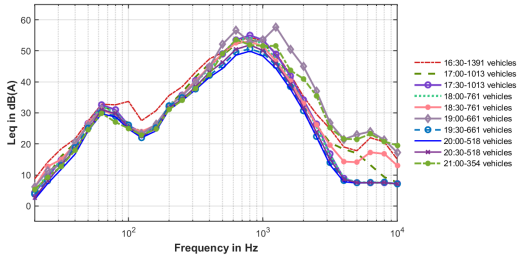

(d)

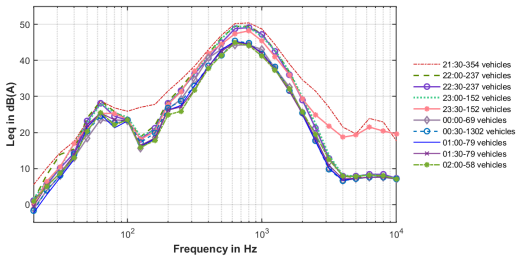

(e)

Figure 5.36: The measured spectrum with A weighing applied L_{Aeq} based on 1/3 octave bands in 24-hour at Lånheveien 11 (continued).

Figure 5.36 shows the measured spectrum L_{Aeq} in 1/3 octave for 24-hour at Lånheveien 11; the spectrum indicated four dominant peaks at 63 Hz, 800 Hz, 6300 Hz and 8000 Hz that most frequency spectra over a 24-hour with 30-minute intervals were shown the mentioned peaks. However, the peaks at 6300 Hz and 8000 Hz are not seen in the plotted spectrum in the night between 24:00-07:00, with an exception at 6:00 with the peak at 6300 Hz. As mentioned earlier, the spectrum can be formed based on the number of vehicles, distance from the center of the road, the height of the microphone, and the speed of the cars; in the present case, only the number of vehicles has a potential for altering the spectrum at 6300 Hz at 6:00 which the number of cars is three times more compared with 5:00 in the morning with the value of 295. Also, a dip occurred in all spectrums at 125 Hz with the lowest values in the dip for L_{Aeq} at night.

5.5 The perceived noise from E18 by residents

Road traffic noise is often accompanied by irritation, nuisance, and other negative associations, and there is a connection between traffic noise and disease; the relationship can affect the quality of life for people exposed to the noise from road traffic. A parallel study has been done by Eli Mari Øverdahl [64] (a master's student in public health science at the Norwegian University of Life Sciences-NMBU) to gain more insight into how road traffic noise is experienced and how it affects the lives of those exposed to the noise. Therefore, the qualitative data collection method by interviews with residents was used. This part investigates the correlation of the perceived noise from E18 by residents obtained in the interviews with the measured or simulated data. Generally, noise pollution affects residents' quality of life near E18 and is perceived as annoying. However, the inhabitants explained the perceived noise in different ways. The common is that the sound is such a constant hissing noise during the day, and the noise is never stopped. Some inhabitants experienced that there is sometimes less noise during the day, usually very early in the morning.

Also, interviewees were asked to discuss their feelings about indoor and outdoor noise during the interview.

The road traffic noise did not affect the inhabitant's indoor environment. The road traffic noise was audible in the rooms if it was hushed inside and if they carefully listened to the traffic noise. It was where the traffic noise disturbed the resident in the bedroom, and it could not always be possible to open the window, especially in the summertime because the traffic noise could interfere with sleep; the owner desired to be able to open the window for ventilation. The indoor environment is affected by noise by opening windows in all measured locations. Although during the interviews, the inhabitants notified that they did not experience sleep disorders, it could happen that they took an afternoon nap or relaxed later in the day, and relaxing during the day could also be disruptive. The residents did not expect it to be hushed but that the situation could improve.

The outdoor noise in the surrounding houses is more annoying when the residents are outside, especially in the summertime for outdoor activities. Everyone experienced that the outdoor environment was reduced due to road traffic noise. Participants were asked to describe the road traffic noise, and the outdoor noise was experienced the worst. Also, participants confirmed that the road traffic noise could be heard all day from morning to evening, except some Sundays and mornings when the traffic noise could be experienced as less intense. By looking at Figure 4.14, which is a diurnal variation of traffic volumes at Solbergveien 37, it can be proved that the perceived traffic noise on Saturdays and Sundays is aligned with the experienced noise on Saturdays, which is less intense due to the traffic volume has only a peak at 13:00. However, there were two peaks in the traffic diurnal variation in regular days, the morning peaks were at 8:00 in summer and winter time and the evening peaks were at 16:00 in summer and wintertime. Moreover, the evening could also be experienced as noisier by residents; they believed there could be something with the air and the temperature. One stated that the noise nuisance varies slightly from day to day with different weather types; it is much worst when it goes towards the evening then there is such a reflection of the sound through the various screens with varying temperatures of air, which makes some of the noise will go up. It will go down again because of reflection in different layers with the temperature in the air. Before it can link up to the noisier evening to weather conditions, it is clear from Figure 4.14 that the traffic volume in the evening is higher than in the morning, especially in the period of 12:00 to 19:00 with more than of the morning peak with 2000 number of vehicles per hour. Additionally, the residents admit that the wind in the summer can make the traffic noise more intense and unpleasant though wind directions generally were reported to vary according to where the inhabitants lived; besides, the traffic noise was perceived as higher if it was raining. The simulation was carried out with actual meteorological data for Nord2000, and the wind was one of the influential factors. The predicted values varied when the different wind speeds entered SoundPLAN. SoundPLAN can input the characteristics of the wind such as direction (down-wind or up-wind) and the speed of the wind, then based on Tables 4.8 (Solbergveien 37) and 4.12 (Låhneveien 11) the different meteorological parameters have been used in the simulation which is particularly temperature, humidity, air pressure, and wind. Therefore, the speed of the wind was set at 5.7 m/s in winter and 3 m/s in summer at Solbergveien 37 and 2 m/s in winter and 3 m/s in summer at Låhneveien 11. The predicted L_{den} for Solbergveien 37 and Låhneveien 11 were found in Tables 5.4 and 5.18, respectively. The predicted L_{den} in winter is lower than the predicted L_{den} in summer at Solbergveien 37, where the speed of the wind in the winter is 2.7 m/s higher than in the summertime. In another comparison at Låhneveien 11, the predicted L_{den} in summer is higher than the predicted L_{den} in winter in all receiver positions. In contrast, the wind speed in summer is 1 m/s more than in winter. Consequently, the speed of the wind in the summertime is equal in both locations with a value of 3 m/s, but the speed of the wind in winter at Solbergveien 37 is 5.7 m/s and at Låhneveien 11 is 2 m/s, in the case with the higher speed of the wind the predicted L_{den} in summer is lower than the predicted L_{den} in winter and vice versa. It should be noted that not only the speed of the wind but also variables such as temperature, humidity, and air pressure can be impacted by the predicted L_{den}. An accurate simulation in SoundPLAN can be performed by measuring various wind parameters

such as wind speed, direction, and altitude.

5.6 The future work

The effect of weather conditions on highway noise propagation from E18 in summer and winter was discussed in this study. The meteorological data was taken from the Norwegian meteorological institute from the station at the same elevation as the measurement position. Further study can be done by measuring the weather characteristics such as humidity, air temperature, pressure, wind speed, and direction in situ; for instance, the vertical temperature profile can be measured by a meteorological tower with anemometers and temperature sensors with the height of 15 meters and repeated the short-term measurement using the same receiver positions in both winter and summer condition [30].

6
Conclusion

The study aimed to investigate the impact of meteorological and atmospheric factors in the measurements and simulations, so for the special case at Solbergveien 37, long-term measurements were carried out during summer (17 days of continuous measurement) and winter conditions (for 24 hours) which the atmospheric effects such as temperate was caused of refraction (bending) of the sound waves and the refraction of sound was a result of significantly higher sound pressure levels. To understand a temperature inversion was occurred, it could be looked at meteorological data such as temperature readings at different altitudes, as well as wind direction and speed while sound pressure level measurements alone may not be sufficient to confirm the occurrence of a temperature inversion. A method could be considered the temperature inversion is to measure the vertical temperature profile by a meteorological tower with anemometers and temperature sensors which is tall enough to capture the relevant atmospheric conditions. The result of the comparison between the sound pressure levels based on L_{Aeq} in winter and in summer, as observed at the time between 8:00-11:00, confirmed that the area was prone to high sound levels concluded to be due to temperature inversion conditions that sound pressure level increased by more than 10 dB(A) at 8:00 on winter time.

Also, one main part of the study dealt with the short-term measurements (1 hour) performed for the three cases, Solbergveien 37, Lånheveien 11, and Kodalveien 31, with the compared simulated results between two prediction models, RLS-90 and Nord2000. At Solbergveien 37, the monitored sound pressure levels were compared with the predicted values in four-receiver positions in the surrounding houses based on the Nord2000 assessment in winter and summer conditions which it was derived that the measured data had a difference of 1 dB(A) with predicted data except in one of the receiver position entitled Svg-2, the Svg-2 receiver positioned in the front of the high building which was such a barrier between the receiver and the source. The discrepancy between the predicted L_{den} and L_{rD} based on RLS-90 was near for three receiver positions except in the Svg-1 receiver position, the predicted L_{den} was 2 dB(A) higher than the predicted value L_{rD} for the reason of the sound propagation model was not the same, and it could be affected by noise propagation coefficients in the models. Moreover, a new building was built on the parallel side of the highway, and the predicted values were obtained by modeling without the house near E18; the predicted L_{den} without the building were higher than the situation with the building located near to E18 due to the new construction was similar to a barrier between the source and receivers and the attenuation happened by the building.

Additionally, SWECO also performed a calculation of the outdoor noise level for E18 before the new house was built in this location, the predicted L_{den} obtained by SWECO

in CadnaA using Nord2000 compared with the predicted values in the SoundPLAN model and the variation of the predicted L_{den} on the facade in SoundPLAN and CadnaA model are almost the same with the difference of 1 dB(A) for the simulated model in SoundPLAN. It was also a validation for the SoundPLAN model.
The same comparison applied between the outlined methods RLS-90 and Nord2000 at Lånheveien 11 and Kodalveien 31, the predicted L_{rD} based on RLS-90 was on a period of hours 06:00-22:00 during the day, and the predicted L_{den} was the average of sound levels L_d, L_e and L_n in receiver positions. In the case of Kodalveien 31, the difference of the predicted values L_{den}- L_{rD} were less than 1 dB(A) and the L_{rD} were much closer to the measured values in all receiver positions. Besides, in the case of Lånheveien 11, the difference of the predicted values L_{den}- L_{rD} were lower than 1 dB(A) in three-receiver positions expect in receiver position Mic02 based on Nord2000. Additionally, the spectrum of road traffic noise and its magnitude formed based on various factors such as the speed of the vehicle, the road surface, the traffic flow, and the rate of vehicle categories with the proportion of heavy vehicles to cars, the spectrum appeared with two peaks; one always included a peak at the low-frequency range 50-100 Hz for the propulsion noise, and the next prominent peak was in the range of 700-1300 Hz for the exterior tires or rolling noise. Finally, the acoustic properties of the environment can also affect the traffic spectrum such as shape and size of the surrounding buildings and the distance between the buildings. Acoustic reflections also can be caused of the peaks in traffic spectrum. Sound waves can reflect off of nearby buildings and the reflections can interfere with the original sound waves. A certain frequencies may be amplified or attenuated by the reflections depending on the geometry of the environment then the reflective surfaces at Solbergveien 37 amplified frequencies in the 160 Hz, the 4 kHz and the 8 kHz and the reflection could contribute to peaks in the traffic spectrum at those frequencies.

Bibliography

[1] Amundsen A., Klæboe R: Long-term effects of noise reduction measures on noise annoyance and sleep disturbance: The Norwegian facade insulation study.

[2] Rossing T. (2007): Handbook of Acoustics. Springer

[3] Embleton T. (1996): Tutorial on sound propagation outdoors, the Journal of the Acoustical Society of America, No.100.

[4] Hannah L. (2006): Ground, Terrain and Structure Effects on Sound Propagation, New Zealand Acoustics, Vol. 20, No.3, pp. 22-29.

[5] Hannah L. (2006): Wind and Temperature Effects on Sound Propagation. New Zealand Acoustics, Vol. 20, No.2, pp. 22-29.

[6] Forssén J. (2017) Building acoustics and community noise (BAC), Chalmers university of technology.

[7] Karpraios B., Jenkin M., Milios E. (2008): Sonel Mapping: A Probabilistic Acoustical Modeling Method.

[8] Ismail M., Oldham D. (2008): Sonel Mapping: A scale model investigation of sound reflection from building facades.

[9] Muller G., Moser M. (2013): Handbook of Engineering Acoustics.

[10] Halmrast T., Moser M. (2015): Why do flutter echoes always end up around 1-2 KHz, Institute of Acoustics, Vol37, Pt.3.

[11] Halmrast T., Moser M. (2019): A very simple way to simulate the timbre of flutter echoes in spatial audio, EAA Spatial Audio Signal Processing Symposium, Paris, France. pp.115-119.

[12] Kragh J. (2011): Traffic Noise Prediction with Nord2000 - An Update.

[13] Delta (2006): NORD2000 for road traffic noise prediction.

[14] Kargh J.(2006): User's Guide Nord2000 Road.

[15] Delta (2003): Nord2000, Comprehensive outdoor sound propagation.

[16] Garg N., Maji S.(2014): A critical review of principal traffic noise models.Environmental Impact Assessment Review,Vol. 46, March 2014, pp. 68-81.

[17] Quartieri J., Mastorakis N.(2009): A critical review of principal traffi c noise models.

[18] Delta (2014): Proposal for Nordtest Method: Nord2000 – Prediction of Outdoor Sound Propagation,Danmark.

[19] Alam P., Ahmad K. (2020): Validation of the Road Traffic Noise Prediction Model RLS-90 in an Urban Area.

[20] Khan J., Ketzel M. (2020): Comparison of Road Traffic Noise prediction models: CNOSSOS-EU, Nord2000 and TRANEX. ASCE Journal of Environmental Pollution.

[21] Keränen J., Hakala J (2019): The sound insulation of facades at frequencies 5–5000 Hz. Building and environmental, Elsevier, 156, pp.12-20.

[22] ISO 16283-3 (2014): Acoustics- Field measurement of sound insulation in buildings and of building elements Part 3: Facade sound insulation.

[23] Homb A. (2018): Assessment of sound insulation of sealing solutions, window slits and openings, SINTEF Building and Infrastructure, Norway.

[24] Urban D., Roozen N.B (2002): Assessment of sound insulation of naturally ventilated double skin facades, AZ Acoustics, 84102, Bratislava, Slovakia.

[25] Buratti C. (2002): Indoor noise reduction index with open window, Applied Acoustics, Elsevier, 63, pp.431-451.

[26] ISO 16283-3 (2014): Acoustics — Rating of sound insulation in buildings and of building elements — Part 1: Airborne sound insulation.

[27] NordTest. (2002): Road Traffic, Measurement of Noise Emission Engineering Method.

[28] Brink M.,Schäffer B. (2018): Conversion between noise exposure indicators L_{eq24h}, L_{Day}, $L_{Evening}$, L_{Night}, L_{dn} and L_{den}: Principles and practical guidance, International Journal of Hygiene and Environmental Health, 221, pp.54-63.

[29] Tandeu A., Mateus D (2001): Sound transmission through single, double and triple glazing. Experimental evaluation, Elsevier, Data in brief, 29.

[30] Saurenman H., Chambers J., Forschner H. (2005): Atmospheric effects associated with highway noise propagation.

[31] Farcas F., Sivertum Å. (2005): Road Traffic Noise - GIS Tools For Noise Mapping and A Case For Skåne Region, Linköping University, Sweden.

[32] Liptai P., Badida M., Lukáčová K.(2015): Influence of Atmospheric Conditions on Sound Propagation - Mathematical Modeling.

[33] Karantonis P., Gowen T.(2010):Further Comparison of Traffic Noise Predictions Using the CadnaA and SoundPLAN Noise Prediction Models. ICA 2010.

[34] Hadzi-Nikolova M., Mirakovski D.(2012): modeling and mapping of urban noise pollution with SoundPLAN software, Trans MOTAUTO 12 , P.P. 182-185.

[35] SoundPLAN GmbH (2019):SoundPLAN User's manual.

[36] Gomez D., Rodriguez V (2015): Assessment of the RLS 90 calculation method for predicting road traffic noise in Colombian conditions, University of Antioquia, P.P. 175-188.

[37] Berndt A. (2004): Uncertainties in environmental noise modelling, SoundPLAN LLC, Shelton, Washington, USA.

[38] Kurra S. (2021): Environmental Noise and Management, chapter 6, Noise mapping.

[39] Lamancusa J. (2000): Noise Control, Transmission of sound through structures.

[40] Narang P.P (1991): A Theoretical Study of Sound Transmission Through Aerogel Glazing Systems, Applied Acoustics, 34, pp.249-259.

[41] Quirt J.D (1982): Sound transmission through windows I. Single and double glazing, Applied Acoustics, 72.

[42] Kim Y., Kim H., Jung S (2002):Dependence of coincidence frequency in double-glazed window on glass thickness and interpane cavity, Applied Acoustics, 63, pp.927–936.

[43] Lorenzen P (2019): Noise control through open windows A solution model, ÅF Buildings, Denmark.

[44] søndergaard L., Egedal R., Hansen M. (2019): Open windows with good sound insulation windows, DELTA, Danish Environmental Protection Agency.
[45] Soubrier D. (1988): Sound Transmission Loss of Glass and Windows in Laboratories with Different Room Design, Belgian Building Research Institute, Brussels, Belgium
[46] Du L., Lau S., Lee s. (2002): Experimental study on sound transmission loss of plenum windows, the Journal of the Acoustical Society of America, 146, EL489.
[47] Buratti C., Moretti E. (2010): Traffic Noise Pollution: Spectra Characteristics and Windows Sound Insulation in Laboratory and Field Measurements, Journal of Environmental Science and Engineering, Volume 4, No.12.
[48] Mattisson K. (2011): Modelling noise exposure from roads – A case study in Burlöv municipality, Department of Earth and Ecosystem Sciences, Lund University, Sweden.
[49] SoundPLAN Report (2016): Supplementary Noise Impact Report SoundPLAN, client – Barratt West Midlands.
[50] Larsson k.(2016): Updated road traffic noise emission models in Sweden, SP Technical Research Institute of Sweden, Sweden.
[51] Asensio C., Recuero M.(2010): Self-adaptive grids for noise mapping.
[52] Liu Y., Oiamo T., Rainham D. (2021): Integrating random forests and propagation models for high-resolution noise mapping, Environmental Research, 195.
[53] Jeong J., Din N., Otsuru T. (2010): An application of a noise maps for construction and road traffic noise in Korea, International Journal of the Physical Sciences Vol. 5(7), pp. 1063-1073.
[54] SWECO (2007): Detail Plan of E18 as a four-lane motorway, Gulli – Langåker, Noise report.
[55] Kargh J. (2015): ON-AIR Assessment of traffic noise in complex situations, Danish Road Directorate.
[56] Begou P., Kassomenos P (2020): Dataset on the road traffic noise measurements in the municipality of Thessaloniki, Greece, Elsevier.
[57] Buratti C., Moretti E., Vergoni M. (2009): Windows sound insulation: experimental evaluation of different traffic noise spectra, Department of Industrial Engineering, University of Perugia, Italy.
[58] Bienert J.(2016): The comparison and analysis of standard production electric vehicle drive-train noise, Technische Hochschule Ingolstadt, Germany.
[59] Mahn J. (2011): Road Traffic and Aircraft Noise Spectrums.
[60] Killengreen T, Olafsen S.(2007): The spectrum shape of outdoor and indoor road traffic noise.
[61] Sandberg U.(2003): The multi-coincidence peak around 1000 Hz in tyre/road noise spectra.
[62] Yang W., Cai M., Luo P.(2020):The calculation of road traffic noise spectrum based on the noise spectral characteristics of single vehicle, Elsevier, Applied Acoustics.
[63] Andriejauskas T., Vaitkus A., Čygas D.(2018): Tyre/Road Noise Spectrum Analysis of Ageing Low Noise Pavements.
[64] Øverdahl E.M. (2021): A qualitative study of subjective experience of traffic noise from E18 Tønsberg - Sandefjord, Norwegian University of Life Sciences, NMBU, Norway.

A

Appendix-Methods

A.1 Long-term noise measurement

A.1.1 The number of vehicles at Solbergveien 37 and at Lånheveien 11.

Table A.1: The number of vehicles in both direction of E18 on 11th of February 2021 at Solbergveien 37.

Time of day	Total	Light < 5.5 (m)	Medium 5.6 -12.5 (m)	Heavy >12.5 (m)	Percentage of heavy vehicle < 5.5 (m)
00-01	120	69	22	29	42%
01-02	90	53	8	29	41%
02-03	86	29	17	40	66%
03-04	80	32	14	34	60%
04-05	112	61	22	29	45%
05-06	328	235	40	53	28%
06-07	1437	1212	104	120	15%
07-08	2310	1985	177	148	14%
08-09	1989	1580	213	195	20%
09-10	1561	1162	192	205	25%
10-11	1476	1094	171	207	25%
11-12	1525	1168	179	178	23%
12-13	1648	1262	197	189	23%
13-14	1830	1426	216	186	21%
14-15	2032	1619	209	203	20%
15-16	2865	2469	203	187	13%
16-17	2560	2232	153	175	12%
17-18	1619	1351	118	149	16%
18-19	1355	1158	85	112	14%
19-20	1004	830	64	108	17%
20-21	799	663	51	85	17%
21-22	631	533	37	61	15%
22-23	372	287	39	46	22%
23-24	224	161	11	52	28%

Table A.2: The number of vehicles in both direction of E18 on 12th of February 2021 at Solbergveien 37.

Time of day	Total	Light < 5.5 (m)	Medium 5.6 -12.5 (m)	Heavy >12.5 (m)	Percentage of heavy vehicle < 5.5 (m)
00-01	111	70	7	34	36 %
01-02	86	45	20	21	47%
02-03	85	37	14	34	56%
03-04	67	28	18	21	58%
04-05	75	30	18	27	60%
05-06	318	221	36	61	30%
06-07	1243	1041	93	108	16%
07-08	2085	1786	160	139	14%
08-09	1768	1428	184	156	19%
09-10	1488	1123	193	172	24%
10-11	1483	1134	185	164	23%
11-12	1750	1406	166	177	19%
12-13	1821	1482	199	138	18%
13-14	2141	1808	194	136	15%
14-15	2294	1983	174	135	13%
15-16	2953	2635	183	134	10%
16-17	2304	2086	110	107	9%
17-18	1920	1735	104	80	9%
18-19	1471	1323	71	77	10%
19-20	969	878	46	45	9%
20-21	678	581	50	47	14%
21-22	436	365	32	39	16%
22-23	341	281	24	36	17%
23-24	237	204	15	17	13%

Table A.3: The number of vehicles in both direction of E18 on 9th of February 2021 at Lånheveien 11.

Time of day	Total	Light < 5.5 (m)	Medium 5.6 -12.5 (m)	Heavy >12.5 (m)	Percentage of heavy vehicle < 5.5 (m)
00-01	77	36	12	34	59 %
01-02	63	18	20	21	65%
02-03	72	19	20	34	75%
03-04	66	18	11	21	48%
04-05	107	51	19	27	42%
05-06	313	213	41	61	32%
06-07	860	637	96	108	23%
07-08	1343	1077	137	139	20%
08-09	1194	808	185	156	28%
09-10	906	588	135	172	33%
10-11	907	565	152	164	34%
11-12	989	626	175	177	35%
12-13	1020	681	147	138	27%
13-14	1074	688	164	136	27%
14-15	1222	865	155	135	23%
15-16	1539	1226	135	134	17%
16-17	1391	1106	130	107	17%
17-18	1013	749	89	80	17%
18-19	761	578	57	77	17%
19-20	661	495	39	45	12%
20-21	518	377	47	47	18%
21-22	354	243	34	39	12%
22-23	237	170	17	36	22%
23-24	152	82	13	17	19%

Table A.4: The number of vehicles in both direction of E18 on 10th of February 2021 at Lånheveien 11.

Time of day	Total	Light < 5.5 (m)	Medium 5.6 -12.5 (m)	Heavy >12.5 (m)	Percentage of heavy vehicle < 5.5 (m)
00-01	69	26	13	30	62%
01-02	79	24	20	35	69%
02-03	58	8	12	38	86%
03-04	55	16	9	30	70%
04-05	99	34	21	44	65%
05-06	295	205	40	50	30%
06-07	849	636	98	112	24%
07-08	1259	993	139	126	21%
08-09	1119	782	149	187	30%
09-10	936	579	174	182	38%
10-11	925	587	138	200	36%
11-12	971	646	140	184	33%
12-13	952	617	155	179	35%
13-14	1054	694	164	196	34%
14-15	1267	897	163	206	29%
15-16	1532	1213	150	166	20%
16-17	1500	1201	130	168	19%
17-18	1041	788	99	152	24%
18-19	858	655	62	141	23%
19-20	682	500	45	137	26%
20-21	517	383	46	88	25%
21-22	373	258	38	77	30%
22-23	262	196	20	46	25%
23-24	138	83	12	43	39%

A.1.2 Long term noise measurement in summer time at Solbergveien 37

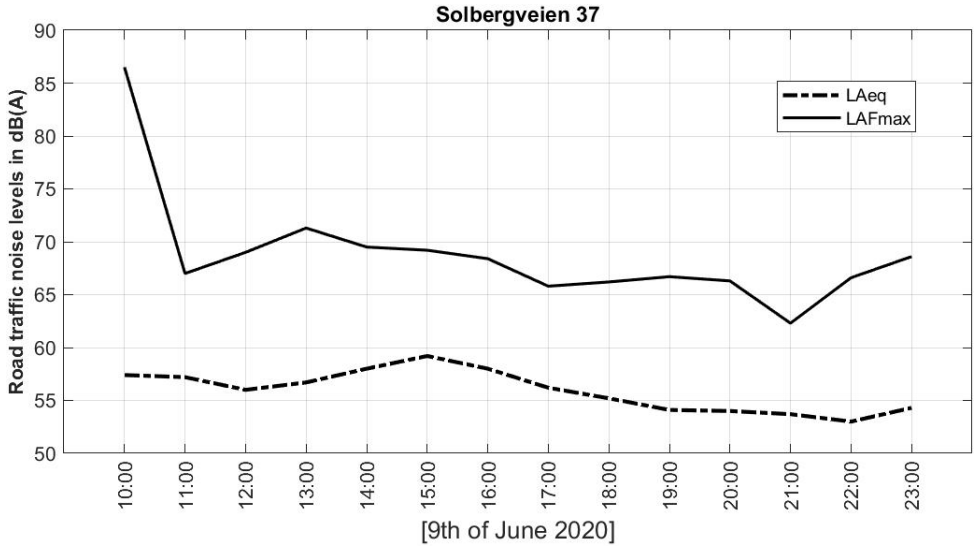

Figure A.1: 9th of June 2020.

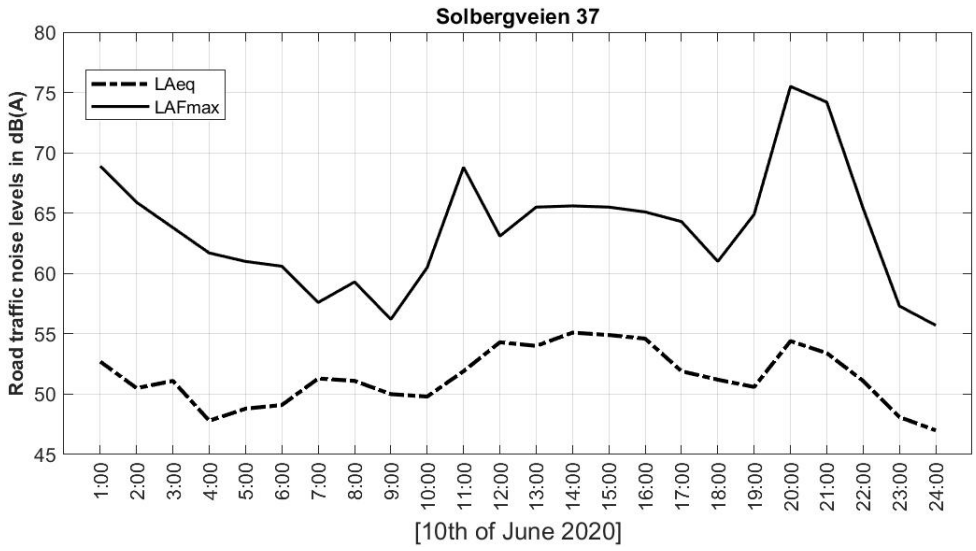

Figure A.2: 10th of June 2020.

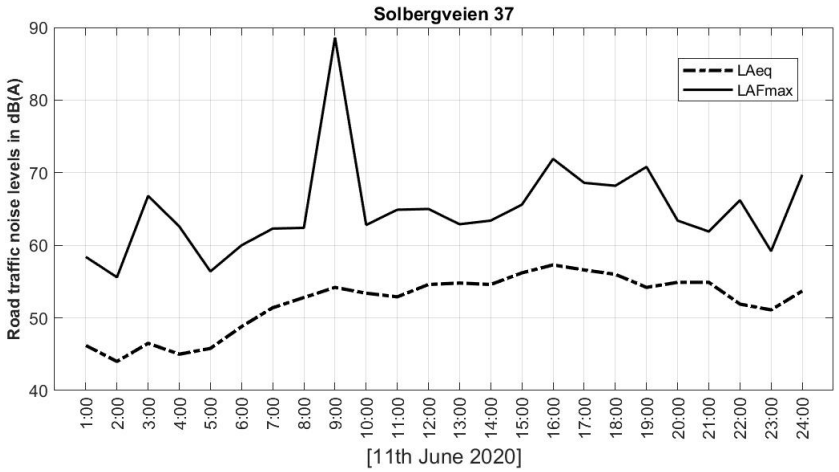

Figure A.3: 11th of June 2020.

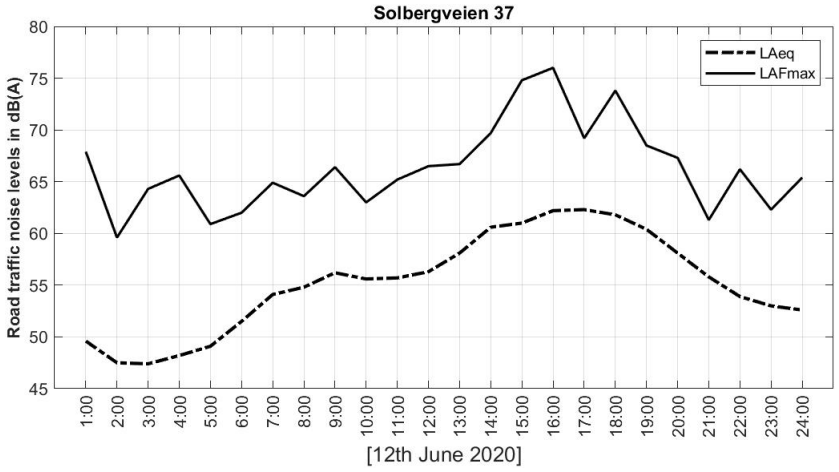

Figure A.4: 12th of June 2020.

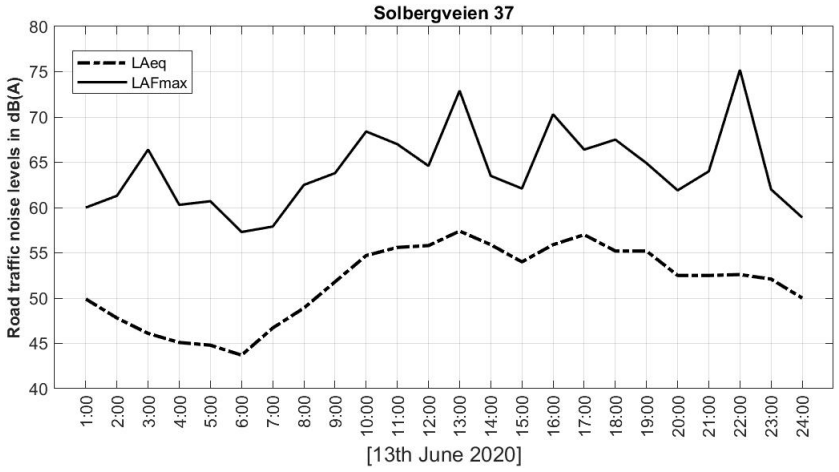

Figure A.5: 13th of June 2020.

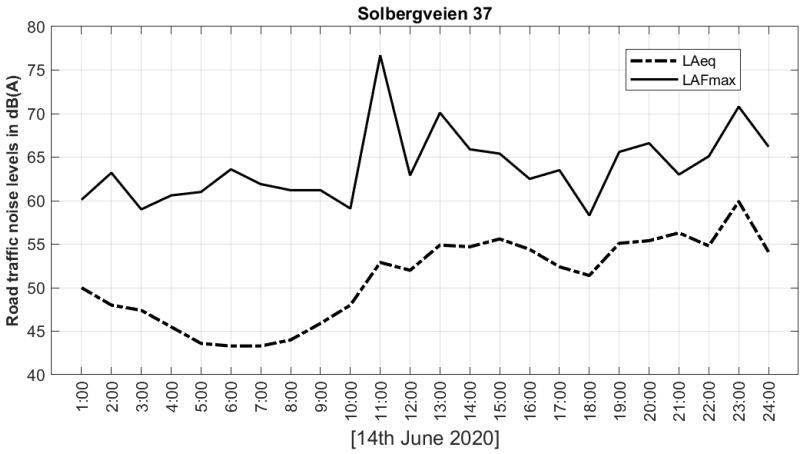

Figure A.6: 14th of June 2020.

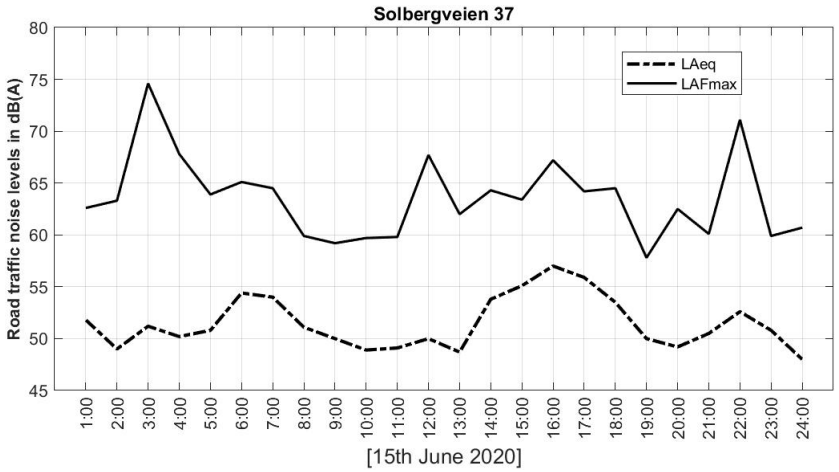

Figure A.7: 15th of June 2020.

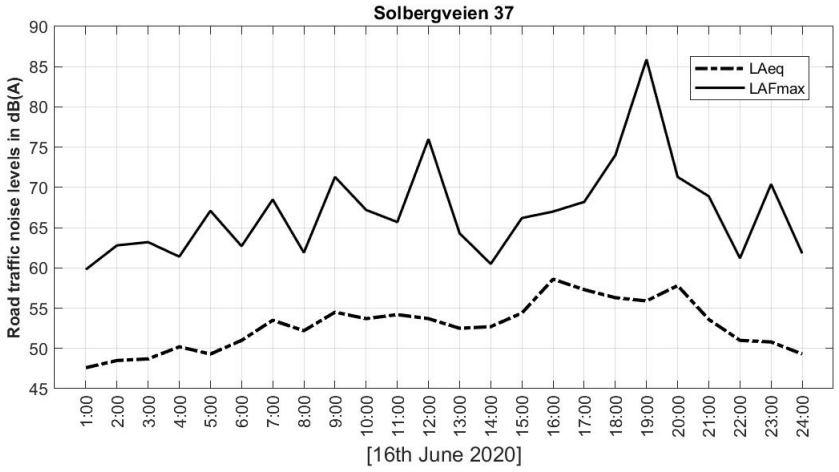

Figure A.8: 16th of June 2020.

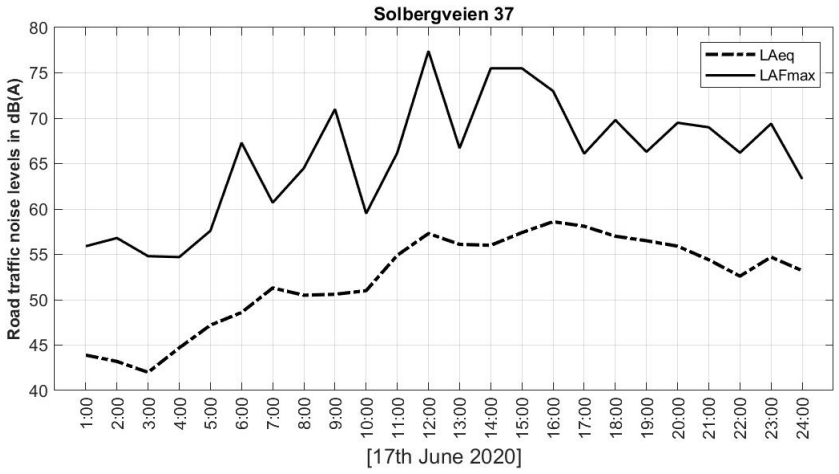

Figure A.9: 17th of June 2020.

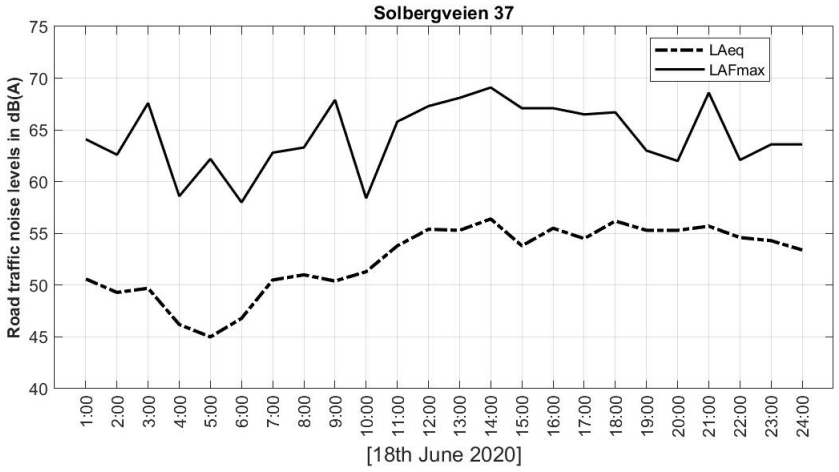

Figure A.10: 18th of June 2020.

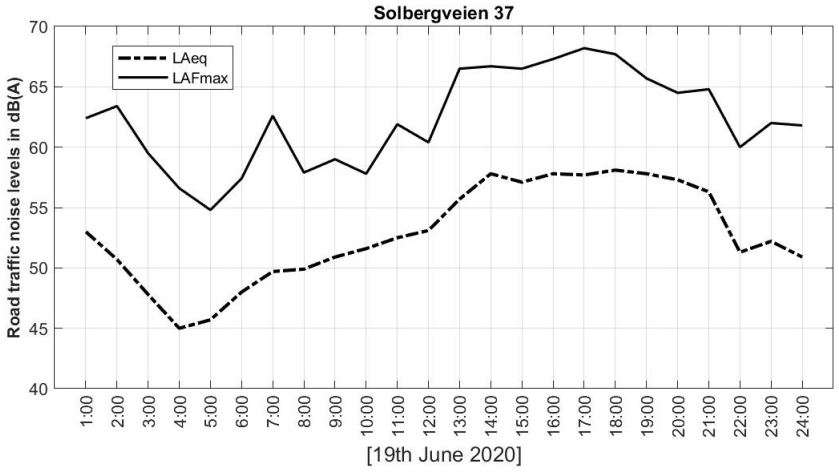

Figure A.11: 19th of June 2020.

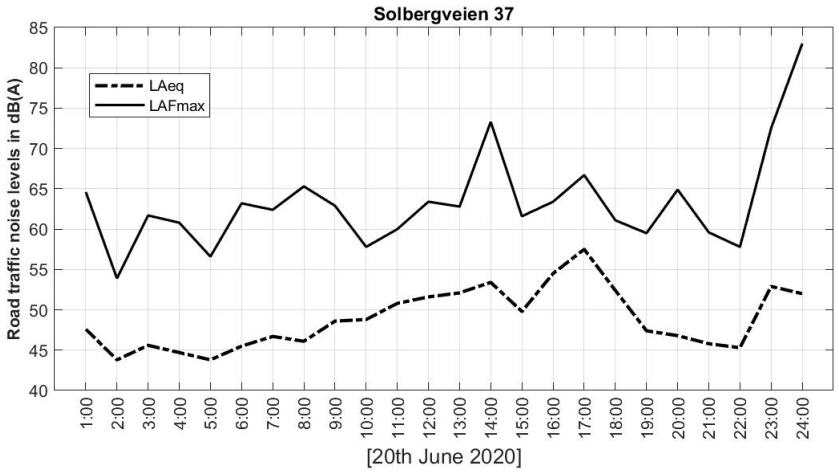

Figure A.12: 20th of June 2020.

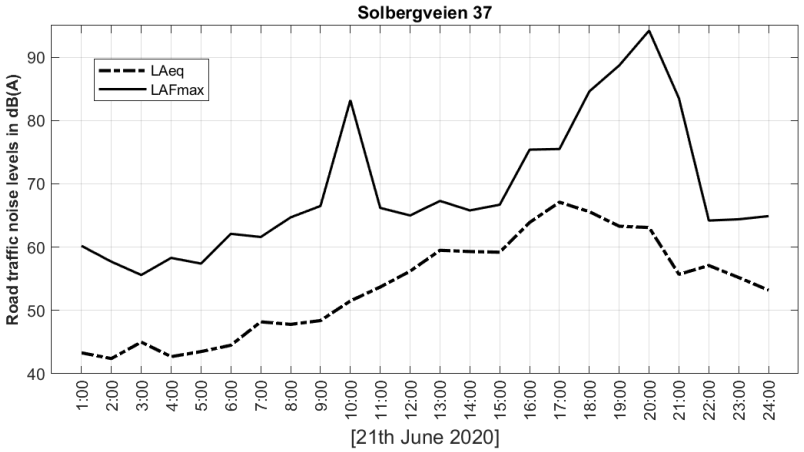

Figure A.13: 21st of June 2020.

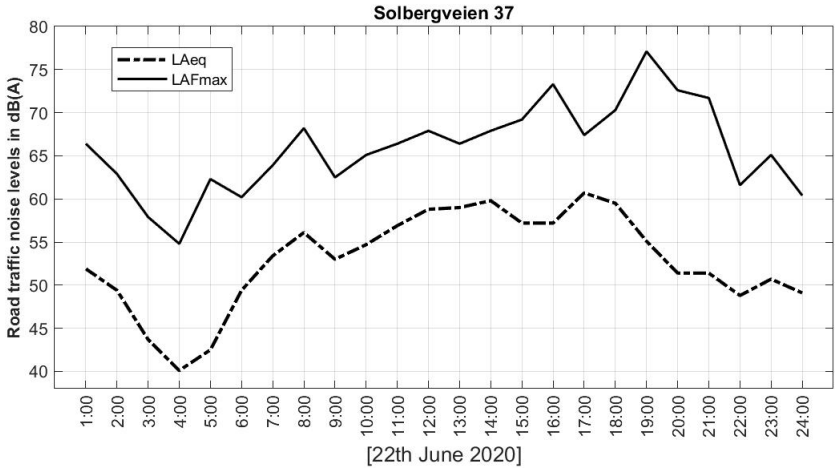

Figure A.14: 22nd of June 2020.

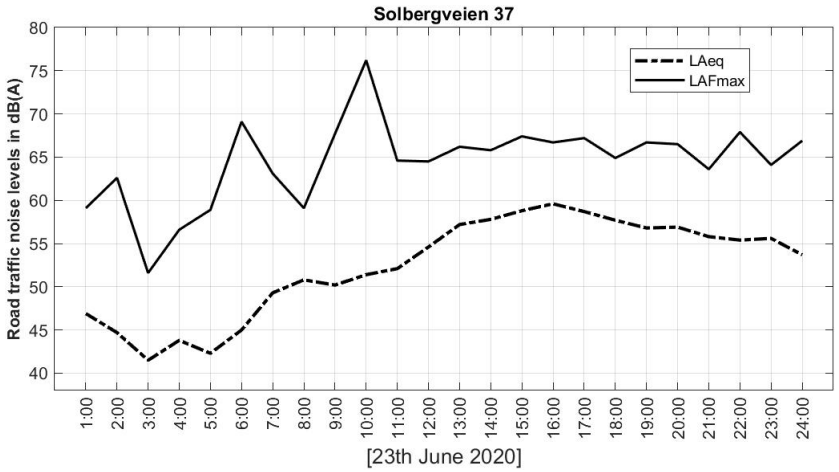

Figure A.15: 23rd of June 2020.

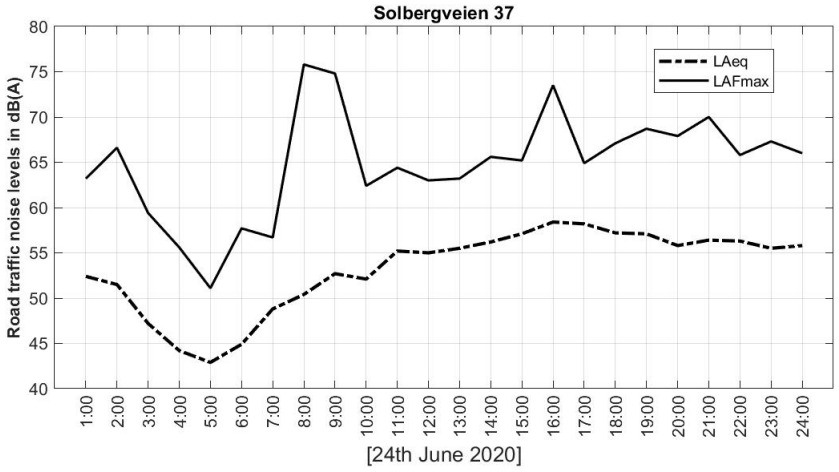

Figure A.16: 24th of June 2020.

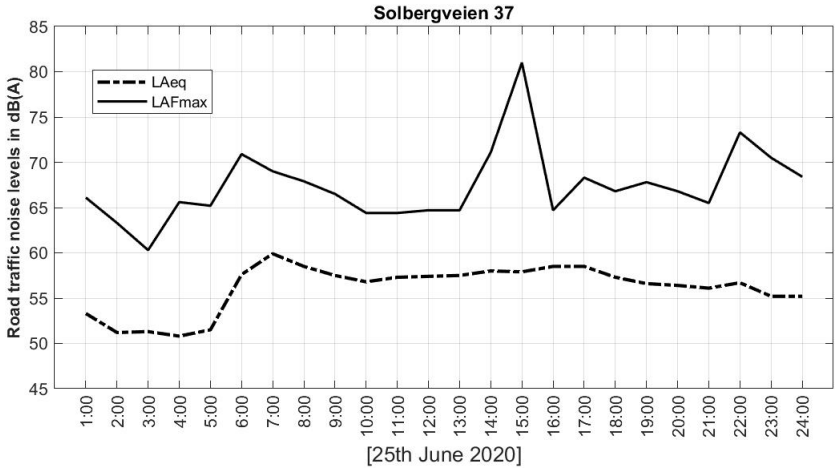

Figure A.17: 25th of June 2020.

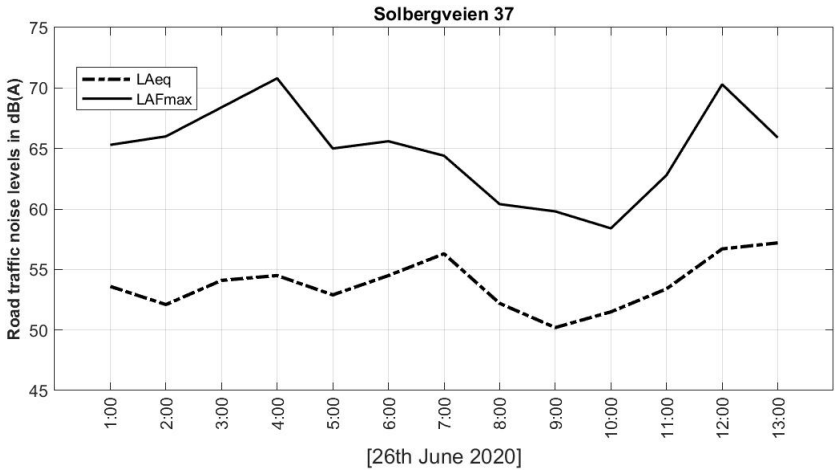

Figure A.18: 26th of June 2020.

A.1.3 Long term noise measurement in summer time at Lånheveien 5

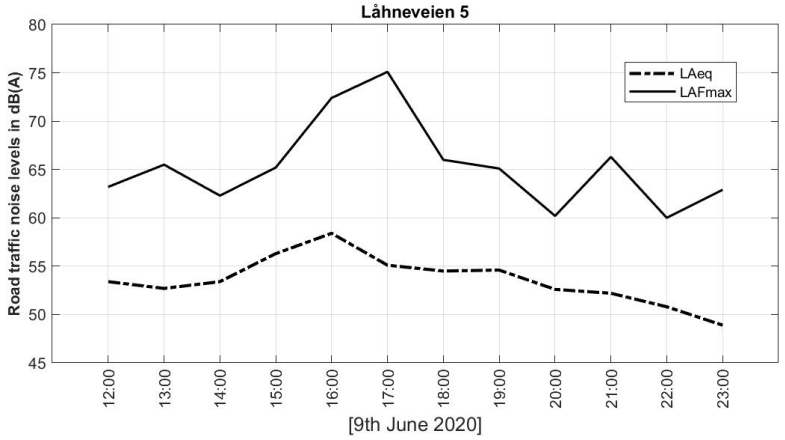

Figure A.19: 9th of June 2020.

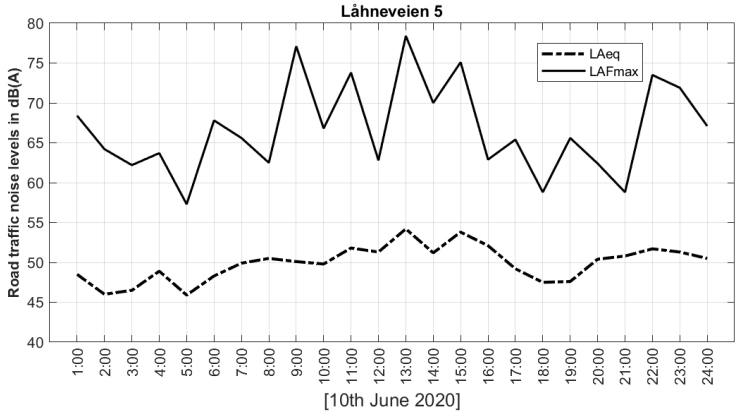

Figure A.20: 10th of June 2020.

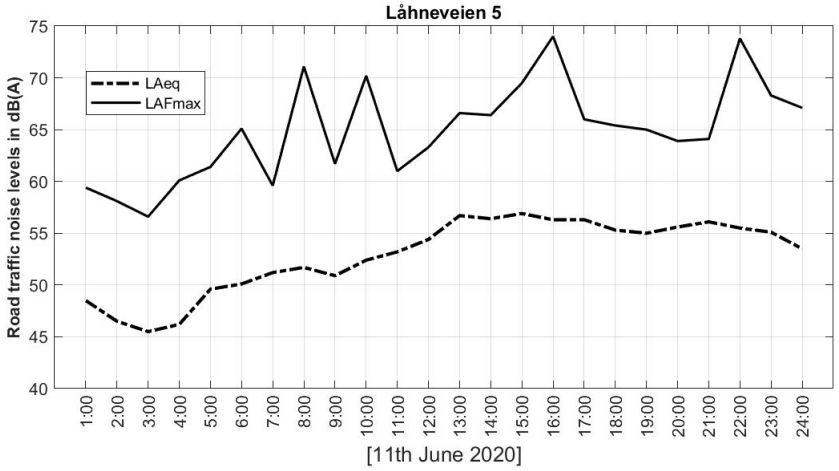

Figure A.21: 11th of June 2020.

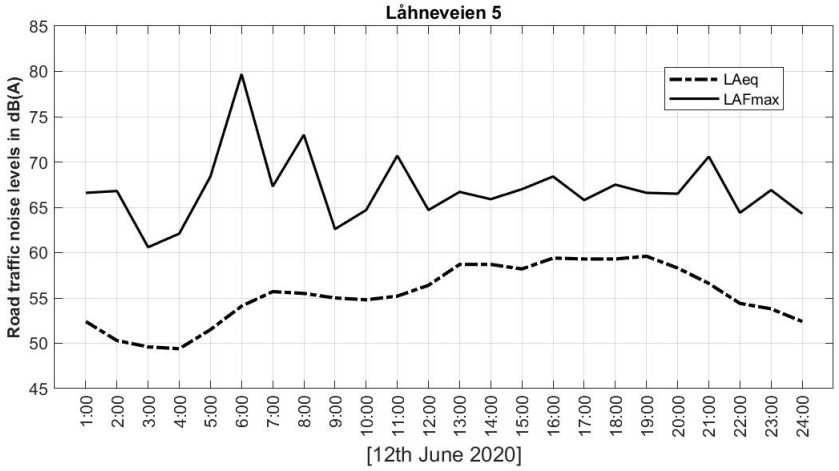

Figure A.22: 12th of June 2020.

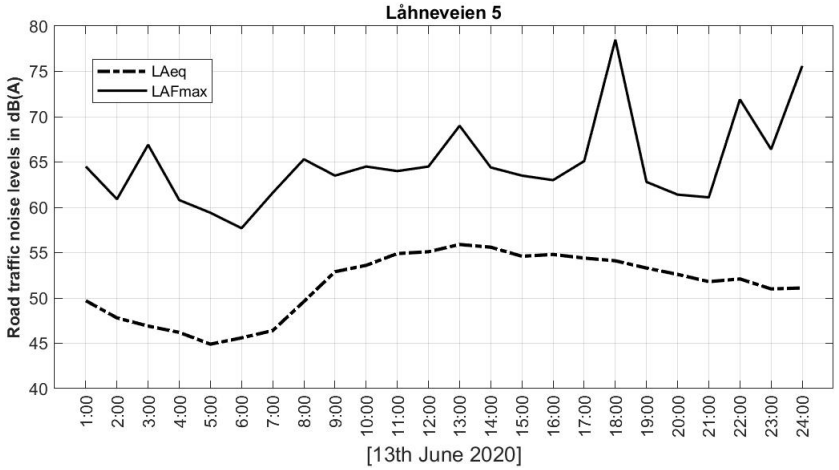

Figure A.23: 13th of June 2020.

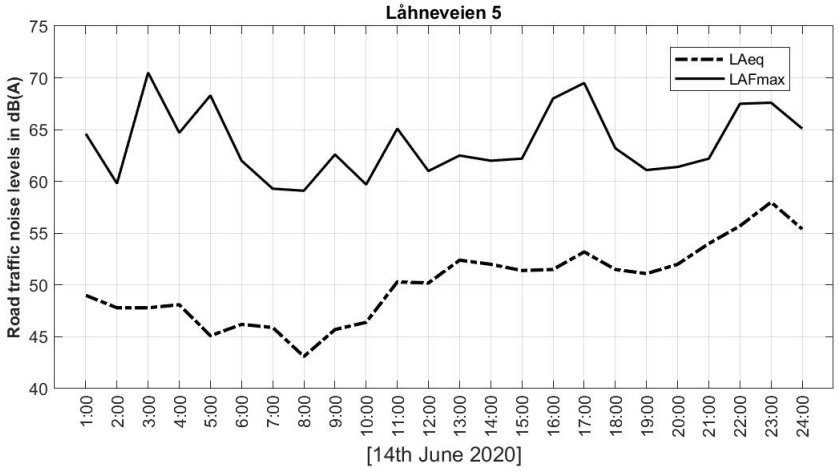

Figure A.24: 14th of June 2020.

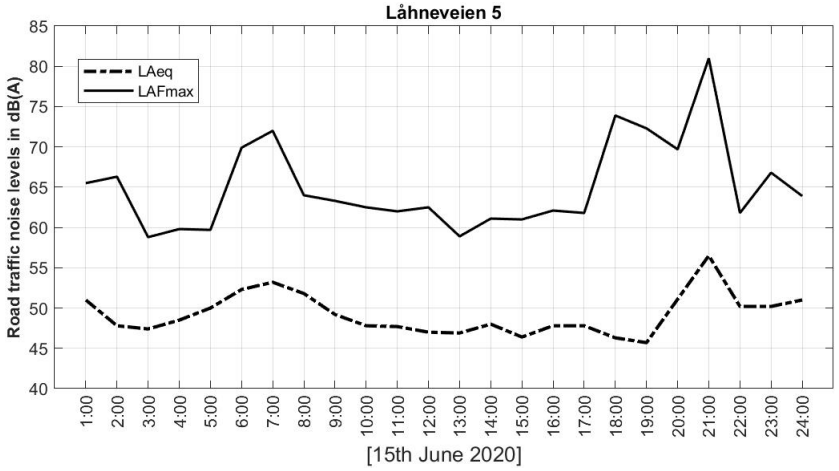

Figure A.25: 15th of June 2020.

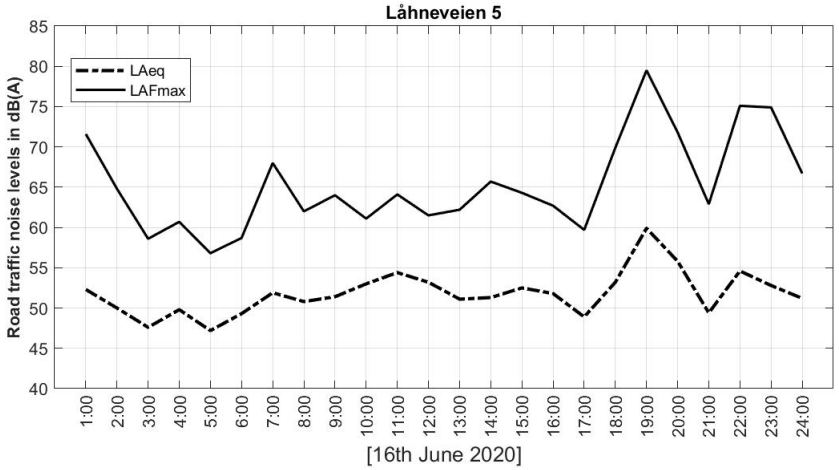

Figure A.26: 16th of June 2020.

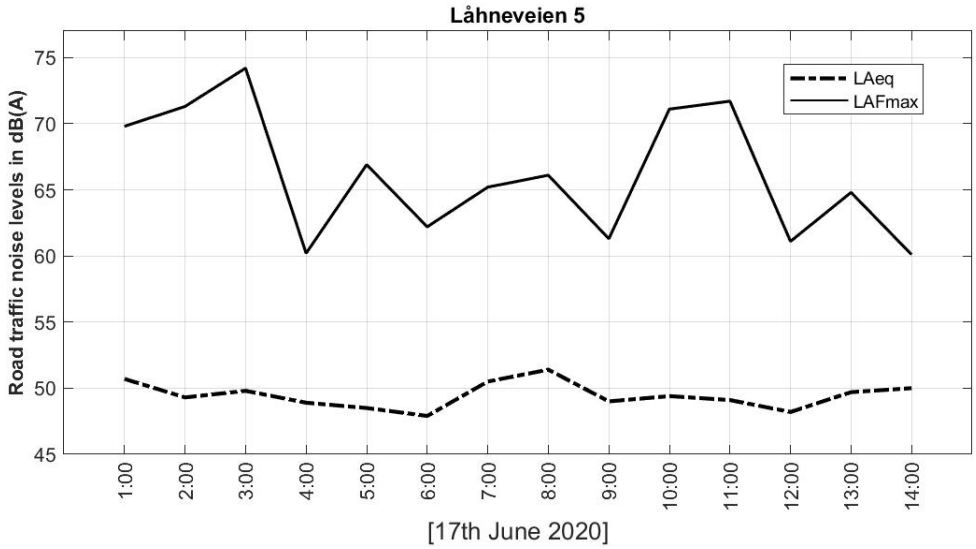

Figure A.27: 17th of June 2020.

A.1.4 The measurements equipment in summer time at Solbergveien 37

Figure A.28: The measurements equipment at summer time at Solbergveien 37 (The photo was taken by Sigmund Olafsen).

(a)The aerial photo (b)The location of measurement

Figure A.29: The measurement location in summer time at Solbergveien 37.

A.1.5 The measurements equipment in summer time at Lånheveien 5

(a)The aerial photo (b)The location of measurement

Figure A.30: The measurement location in summer time at Solbergveien 37.

B

Appendix-Results

B.1 Results achieved with SoundPLAN 8.2

B.1.1 The zoomed view of the receiver positions

B.1.1.1 Grid Noise Map based on Nord2000 in winter at Solbergveien 37

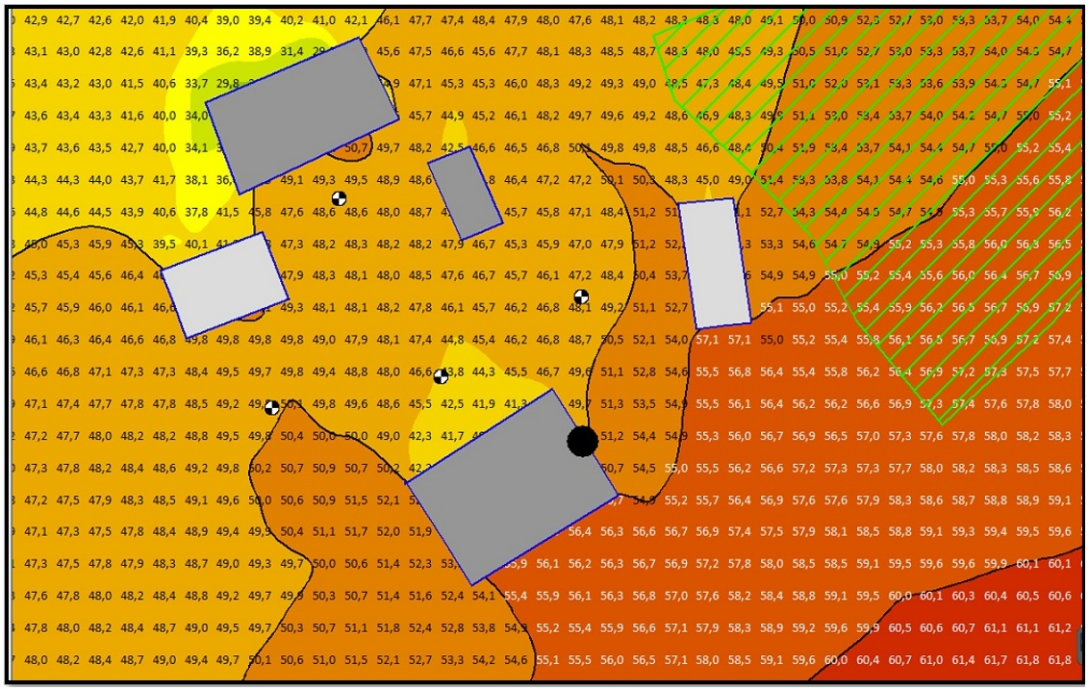

Figure B.1: Grid Noise Map based on Nord2000 for the noise indicator L_{den} at Solbergveien 37 in the winter.

Figure B.2: Grid Noise Map based on Nord2000 for the noise indicator L_d at Solbergveien 37 in the winter.

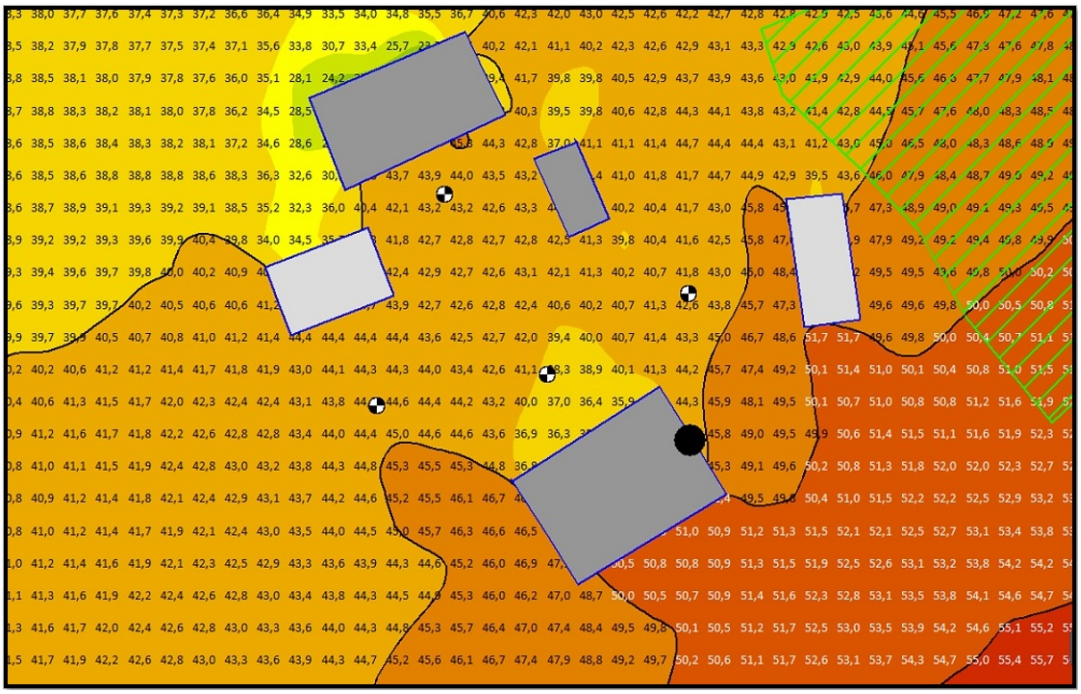

Figure B.3: Grid Noise Map based on Nord2000 for the noise indicator L_e at Solbergveien 37 in the winter.

Figure B.4: Grid Noise Map based on Nord2000 for the noise indicator L_n at Solbergveien 37 in the winter.

B.1.1.2 Grid Noise Map based on Nord2000 in summer at Solbergveien 37

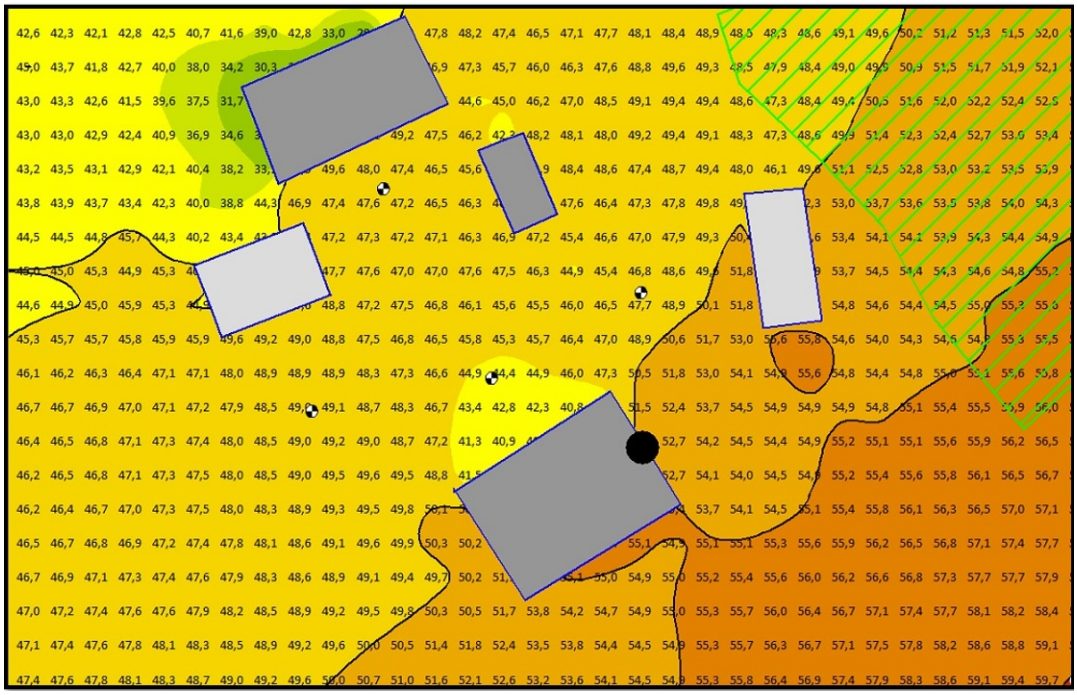

Figure B.5: Grid Noise Map based on Nord2000 for the noise indicator L_{den} at Solbergveien 37 in the summer.

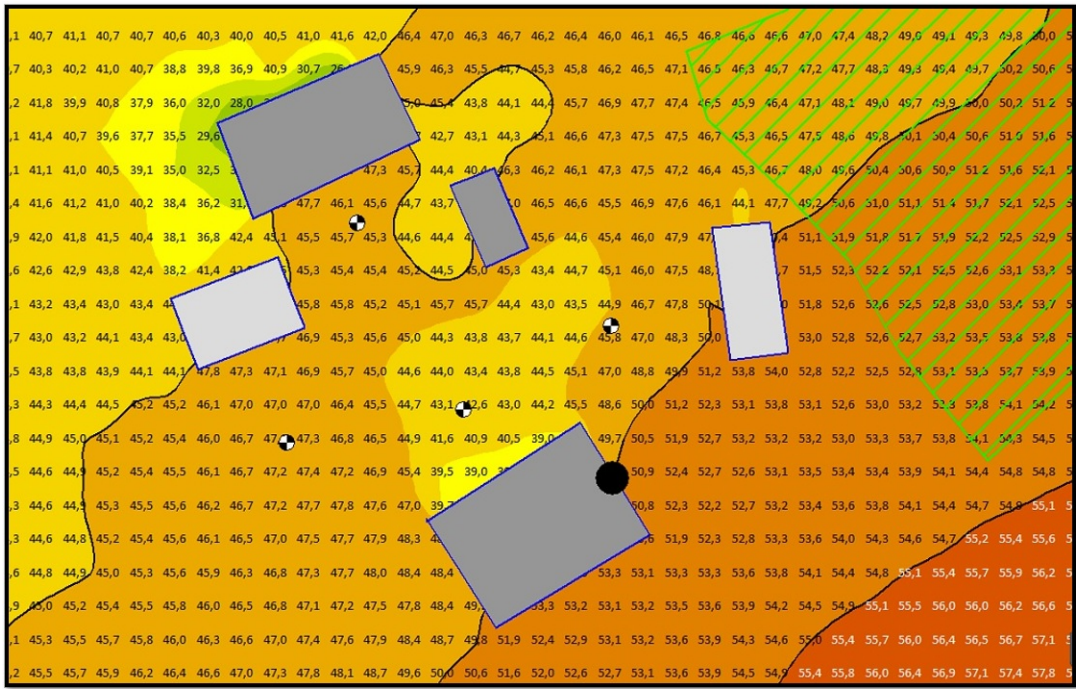

Figure B.6: Grid Noise Map based on Nord2000 for the noise indicator L_d at Solbergveien 37 in the summer.

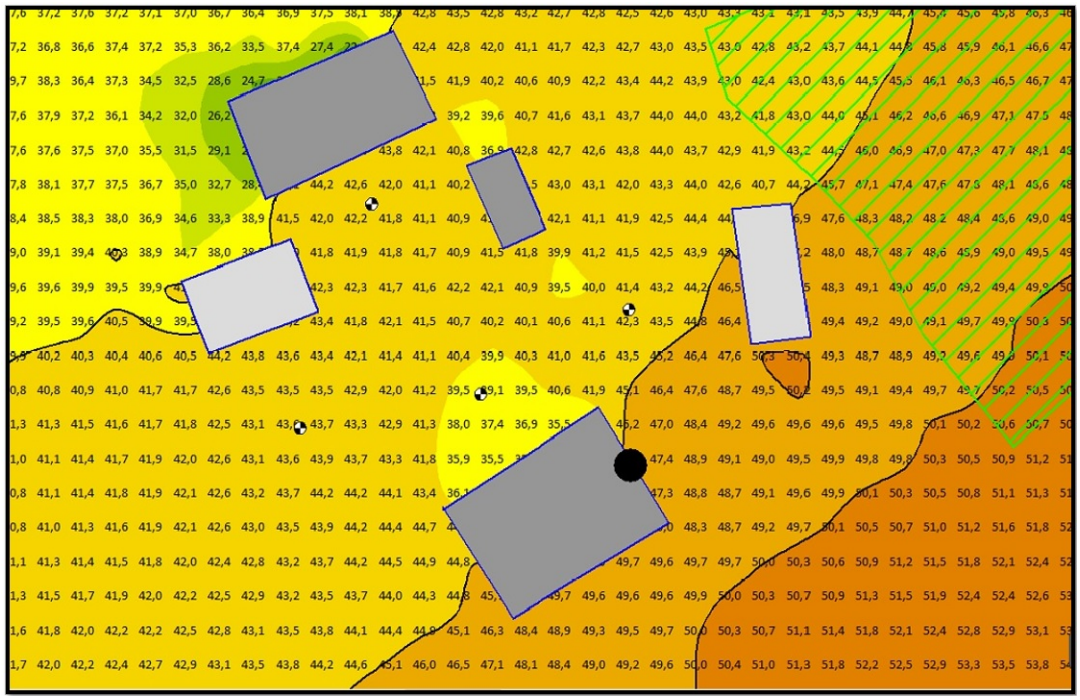

Figure B.7: Grid Noise Map based on Nord2000 for the noise indicator L_e at Solbergveien 37 in the summer.

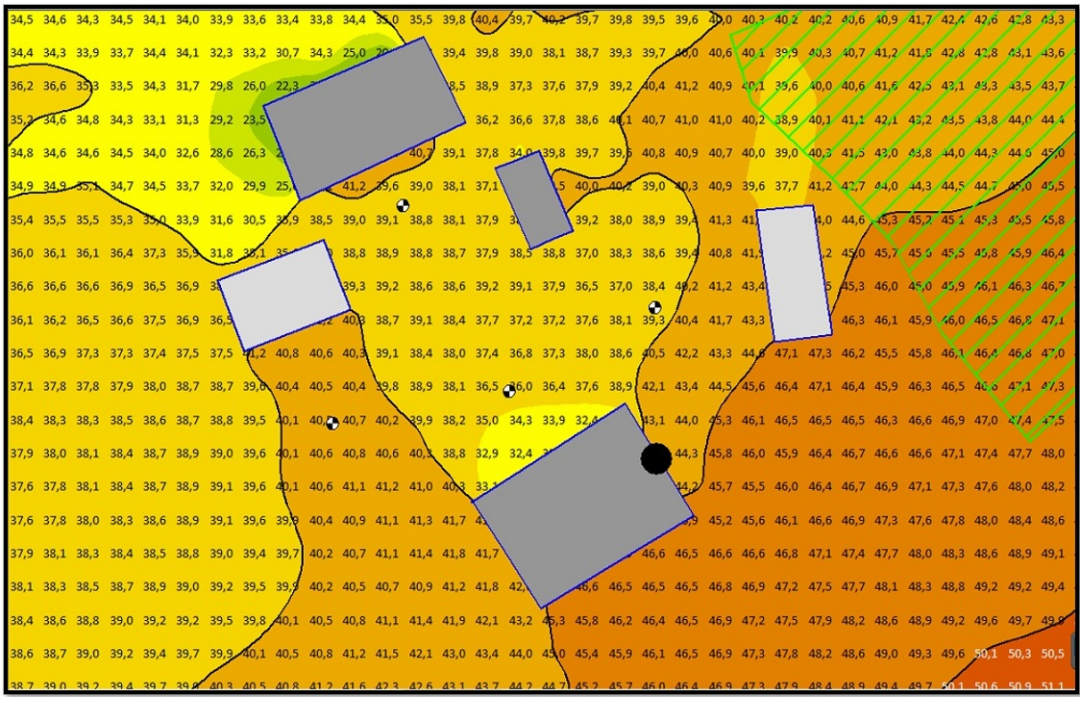

Figure B.8: Grid Noise Map based on Nord2000 for the noise indicator L_n at Solbergveien 37 in the summer.

B.1.1.3 Grid Noise Map based on Nord2000 without the building near to E18 at Solbergveien 37

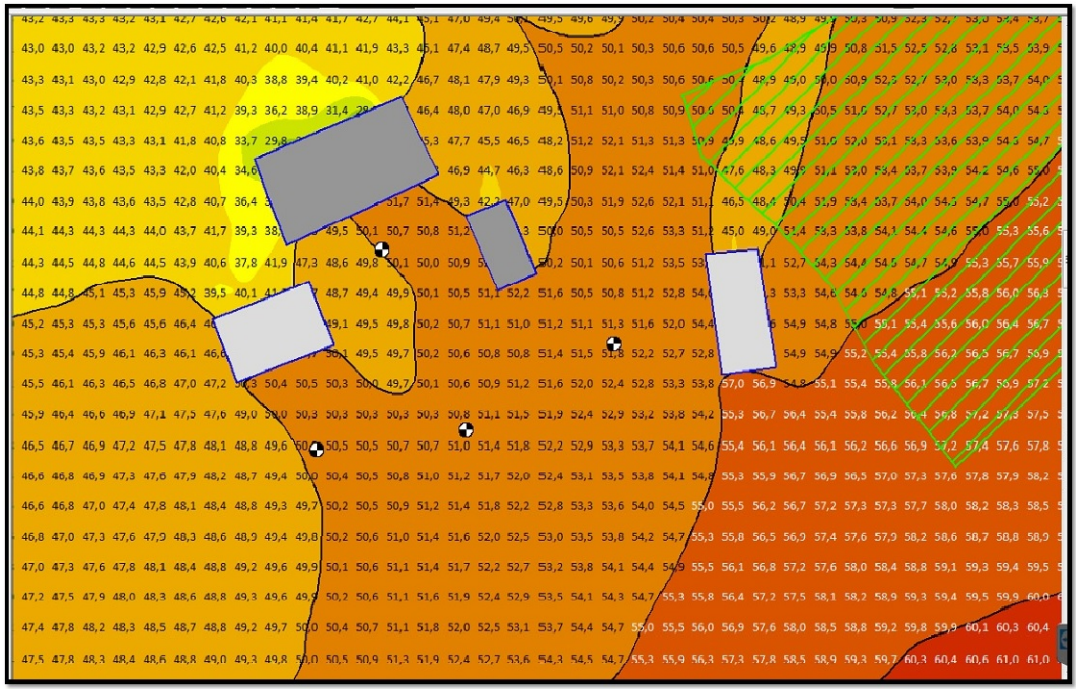

Figure B.9: Grid Noise Map based on Nord2000 for the noise indicator L_{den} without the building near to E18 at Solbergveien 37.

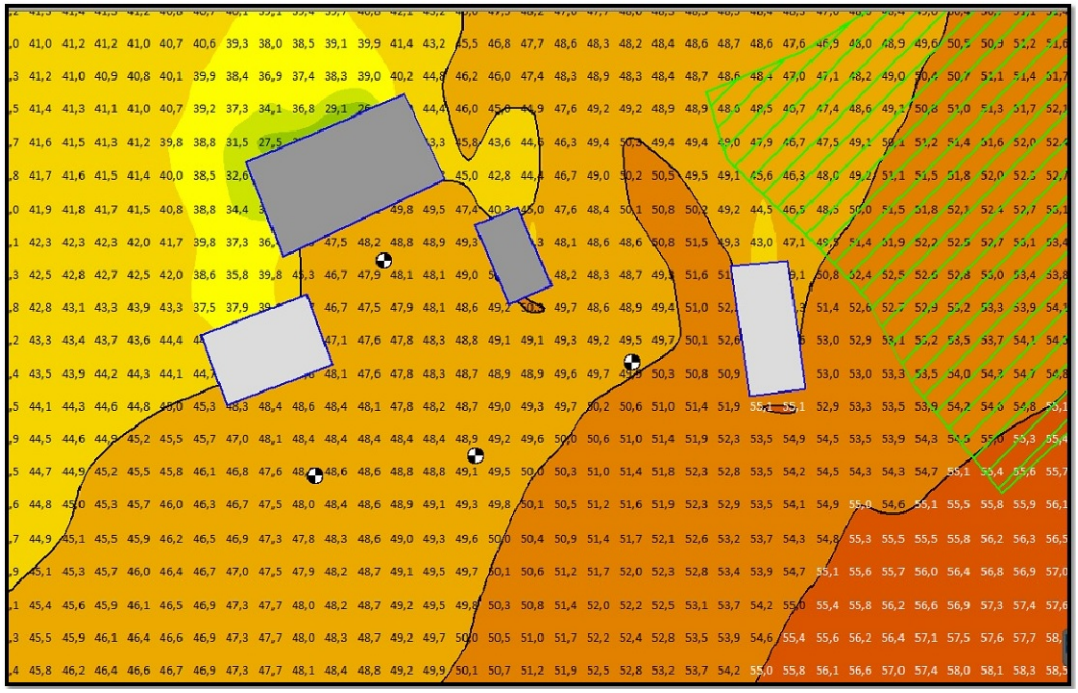

Figure B.10: Grid Noise Map based on Nord2000 for the noise indicator L_d without the building near to E18 at Solbergveien 37.

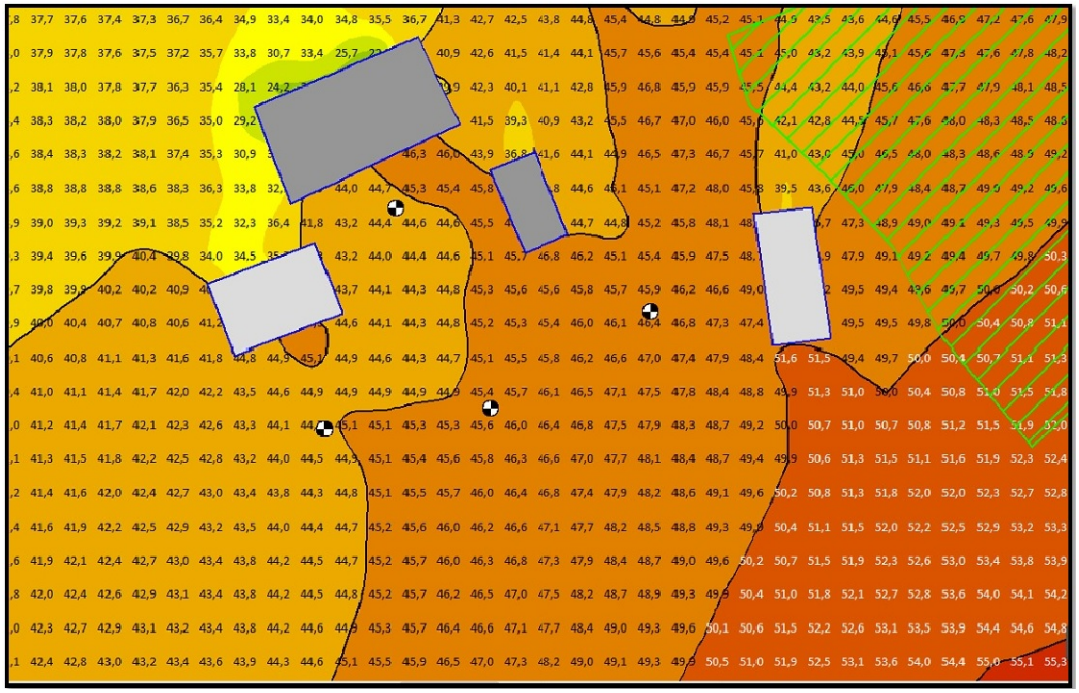

Figure B.11: Grid Noise Map based on Nord2000 for the noise indicator L_e without the building near to E18 at Solbergveien 37.

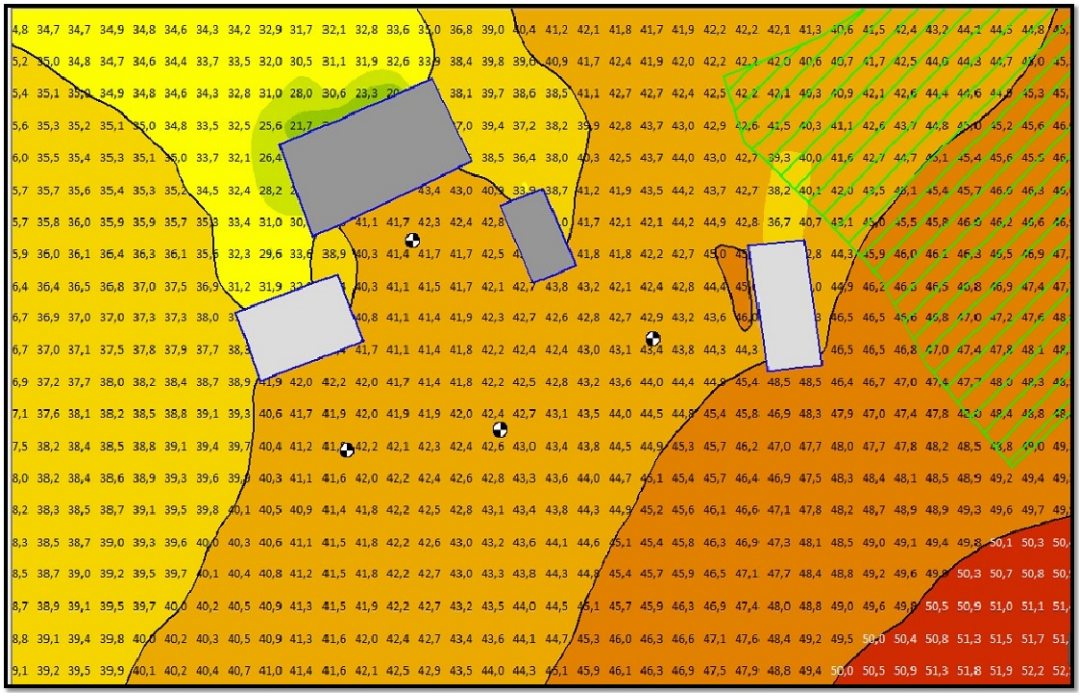

Figure B.12: Grid Noise Map based on Nord2000 for the noise indicator L_n without the building near to E18 at Solbergveien 37.

B.1.1.4 Grid Noise Map based on Nord2000 in the winter at Lånheveien 11

Figure B.13: Grid Noise Map based on Nord2000 for the noise indicator L_{den} in the winter at Lånheveien 11.

Figure B.14: Grid Noise Map based on Nord2000 for the noise indicator L_d in the winter at Lånheveien 11.

Figure B.15: Grid Noise Map based on Nord2000 for the noise indicator L_e in the winter at Lånheveien 11.

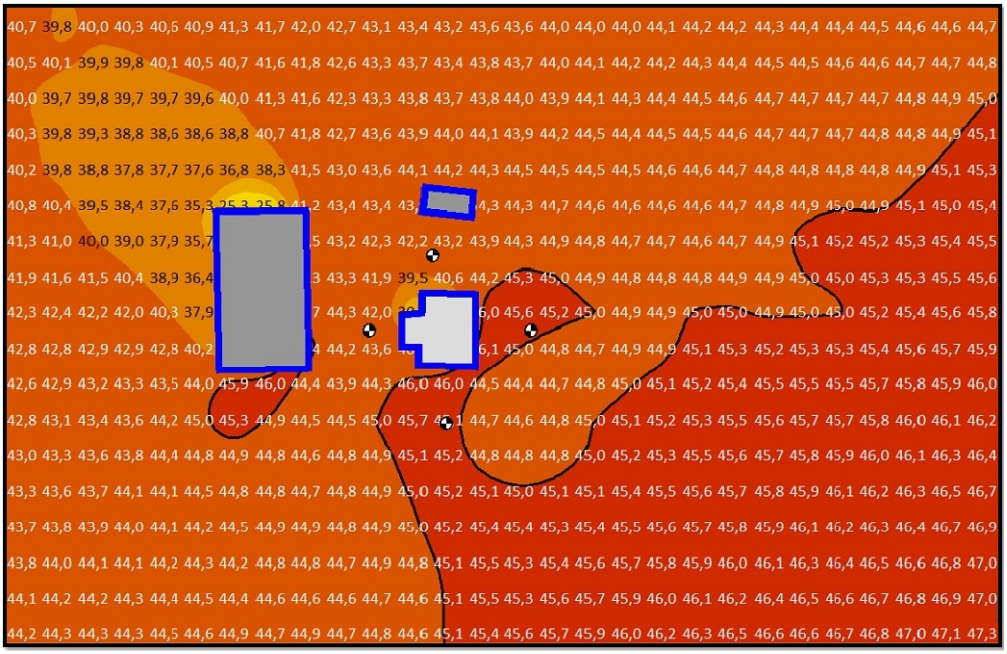

Figure B.16: Grid Noise Map based on Nord2000 for the noise indicator L_n in the winter at Lånheveien 11.

B.1.1.5 Grid Noise Map based on Nord2000 in the winter at Lånheveien 11

Figure B.17: Grid Noise Map based on Nord2000 for the noise indicator L_{den} in the summer at Lånheveien 11.

C

Appendix-Results

C.1 Results achieved with SoundPLAN 8.2

C.1.1 Non-zoomed view for the mentioned locations

C.1.1.1 Grid Noise Map based on Nord2000 in winter at Solbergveien 37

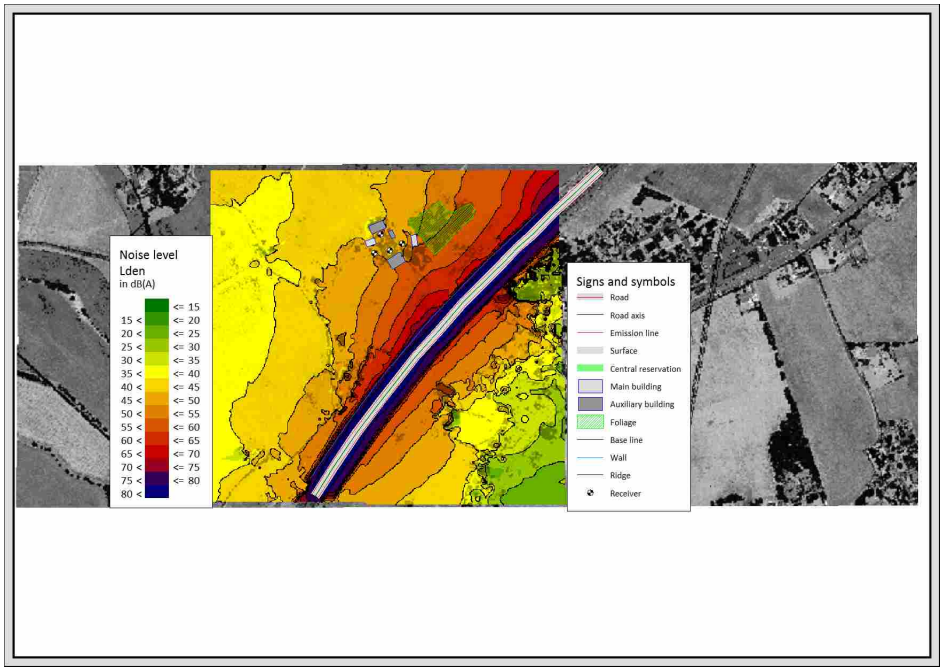

Figure C.1: Grid Noise Map based on Nord2000 for the noise indicator L_{den} at Solbergveien 37.

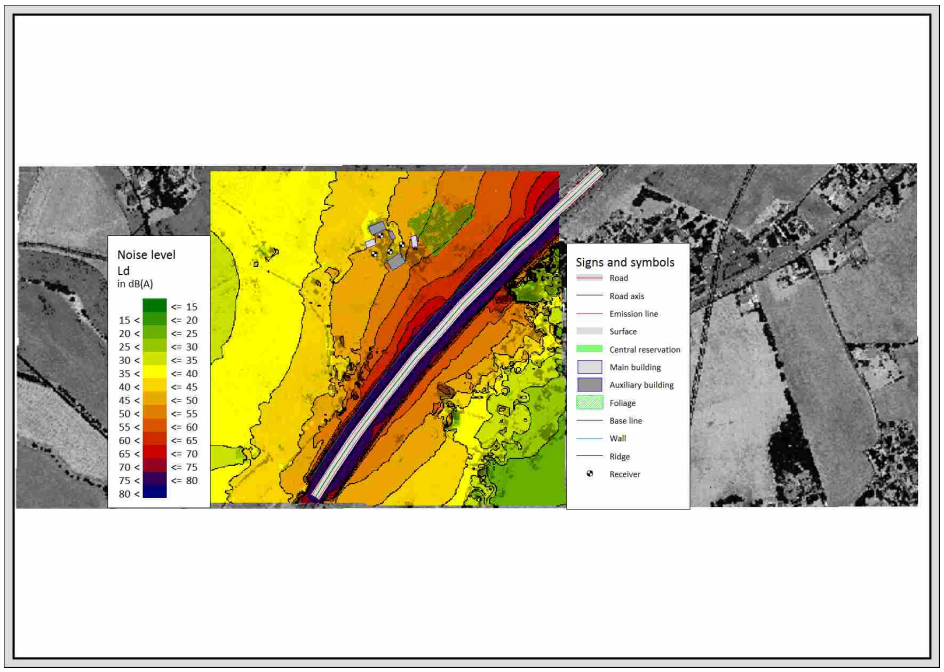

Figure C.2: Grid Noise Map based on Nord2000 for the noise indicator L_d at Solbergveien 37.

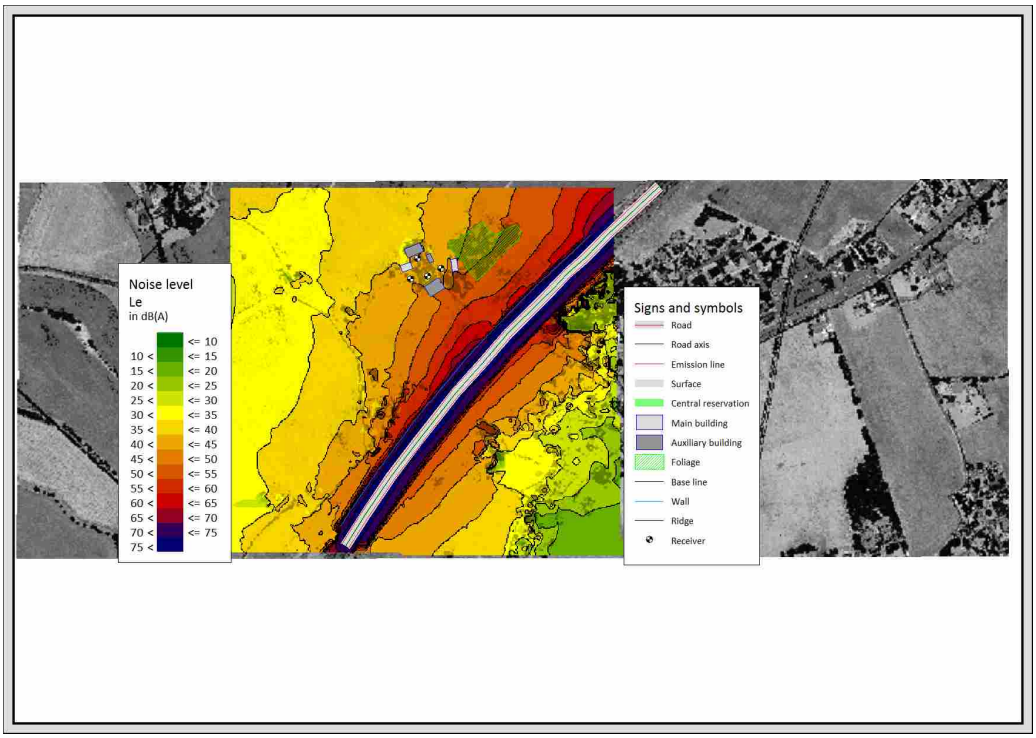

Figure C.3: Grid Noise Map based on Nord2000 for the noise indicator L_e at Solbergveien 37.

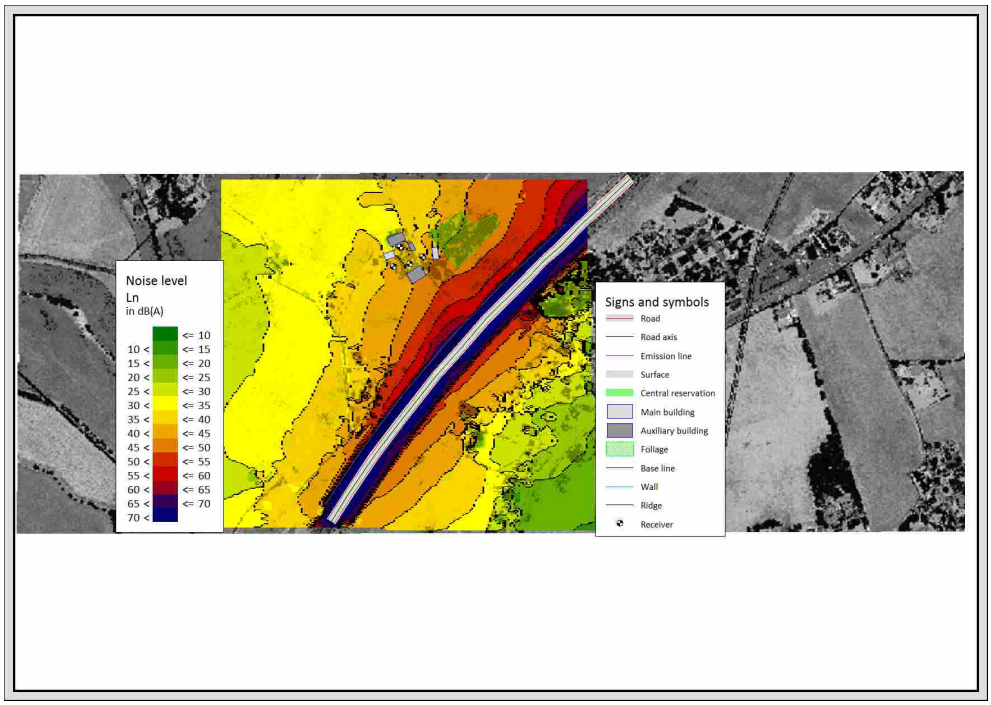

Figure C.4: Grid Noise Map based on Nord2000 for the noise indicator L_n at Solbergveien 37.

C.1.1.2 Grid Noise Map based on Nord2000 in summer at Solbergveien 37

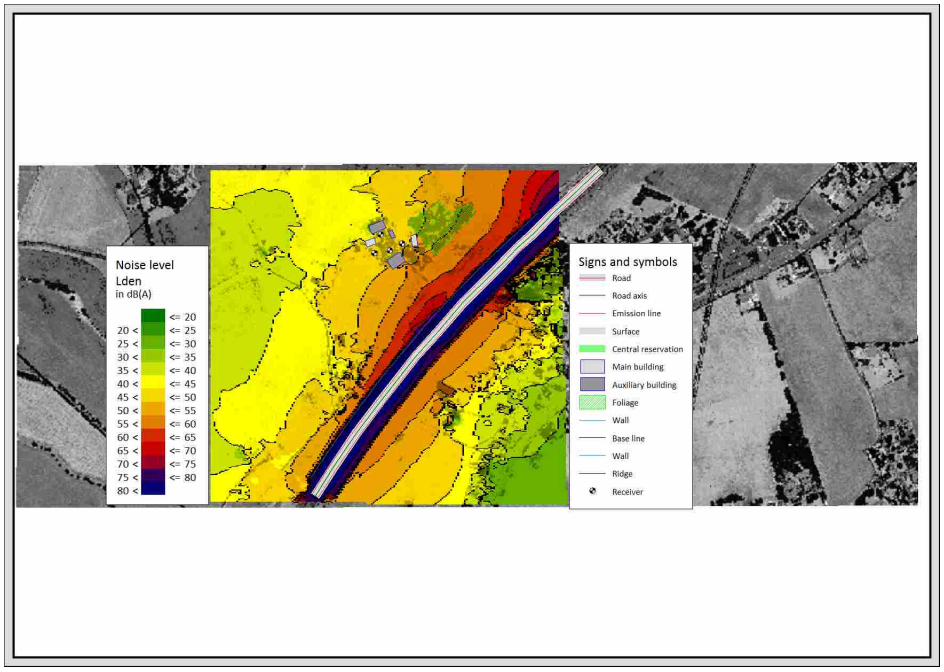

Figure C.5: Grid Noise Map based on Nord2000 for the noise indicator L_{den} in summer at Solbergveien 37.

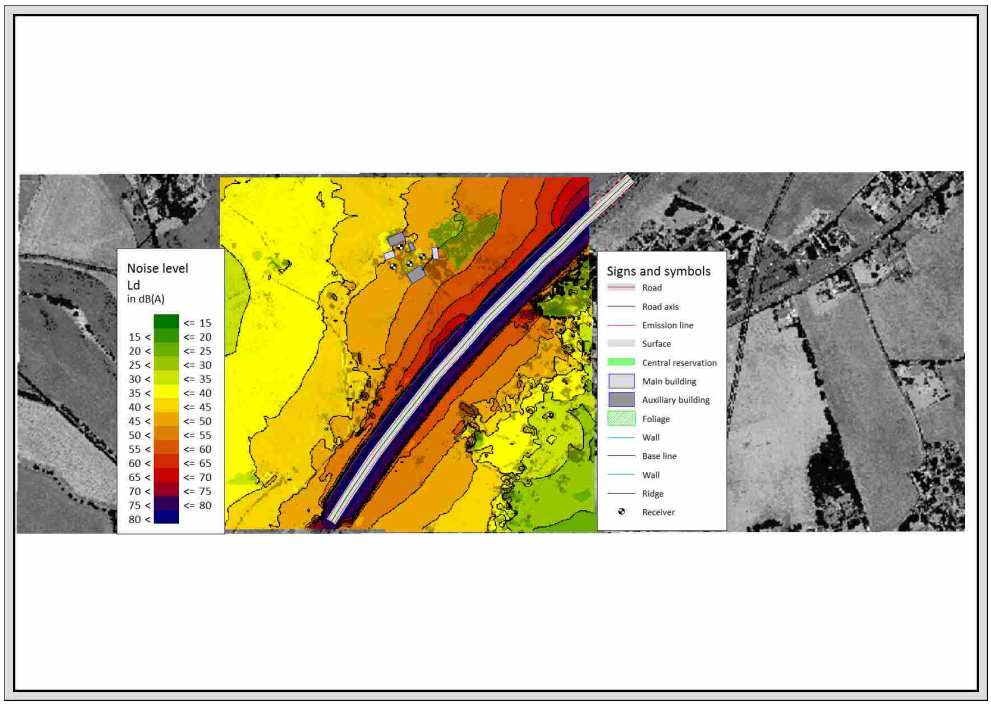

Figure C.6: Grid Noise Map based on Nord2000 for the noise indicator L_d in summer at Solbergveien 37.

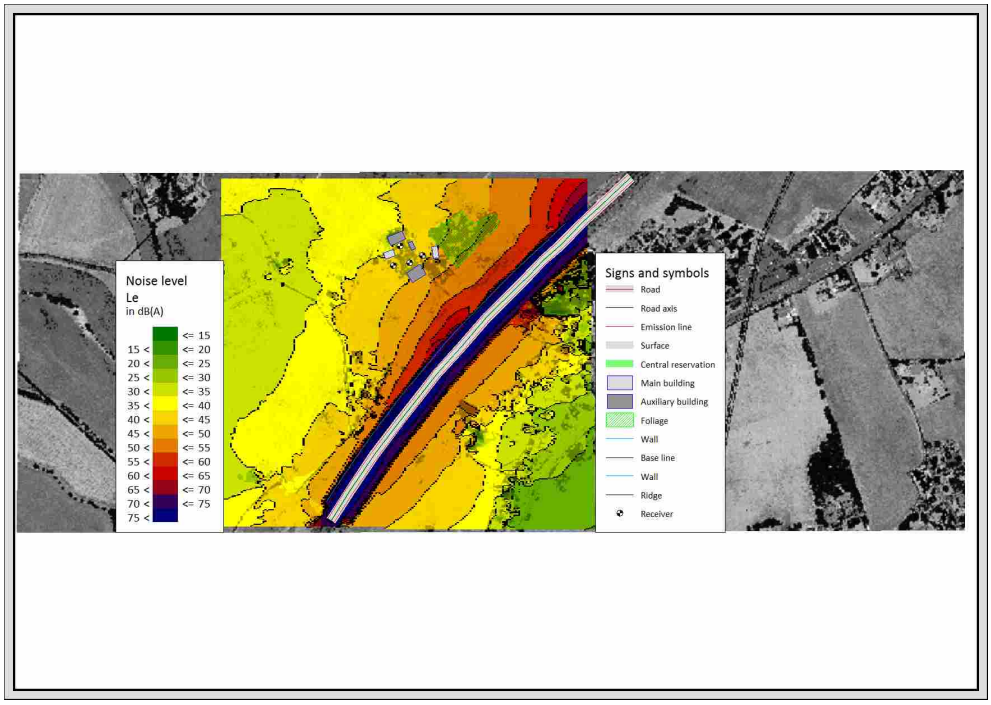

Figure C.7: Grid Noise Map based on Nord2000 for the noise indicator L_e in summer at Solbergveien 37.

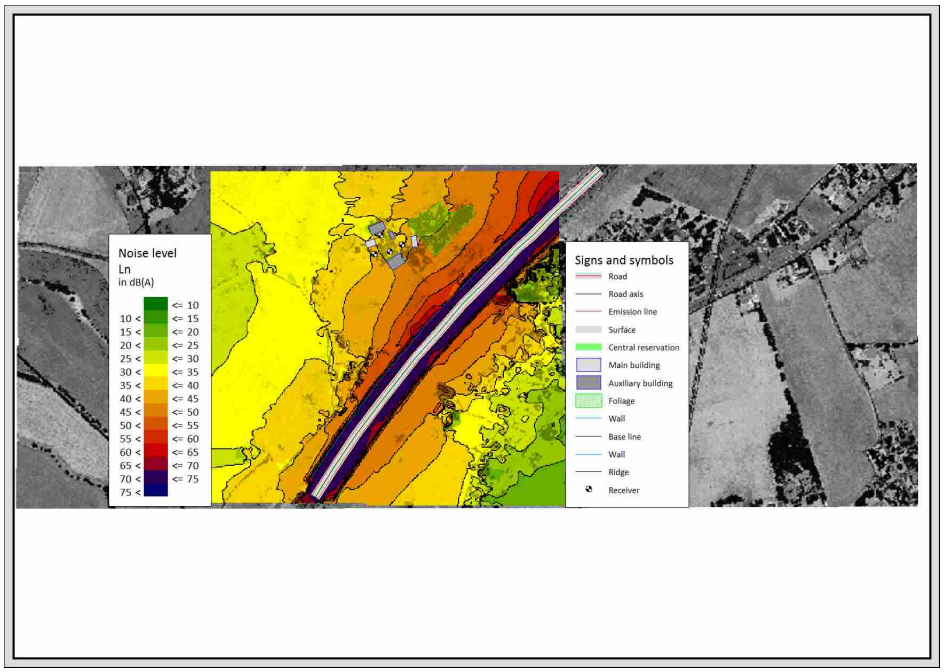

Figure C.8: Grid Noise Map based on Nord2000 for the noise indicator L_n in summer at Solbergveien 37.

C.1.1.3 The simulation based on Nord2000 at Solbergveien 37 without the nearest building to the E18

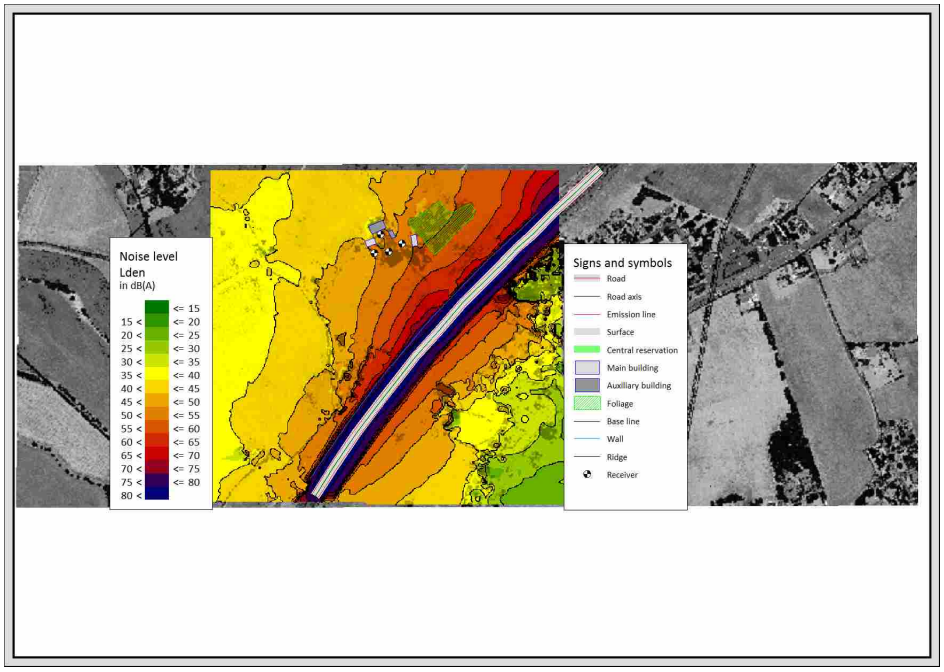

Figure C.9: Grid Noise Map based on Nord2000 for the noise indicator L_{den} without the nearest building to the E18 at Solbergveien 37.

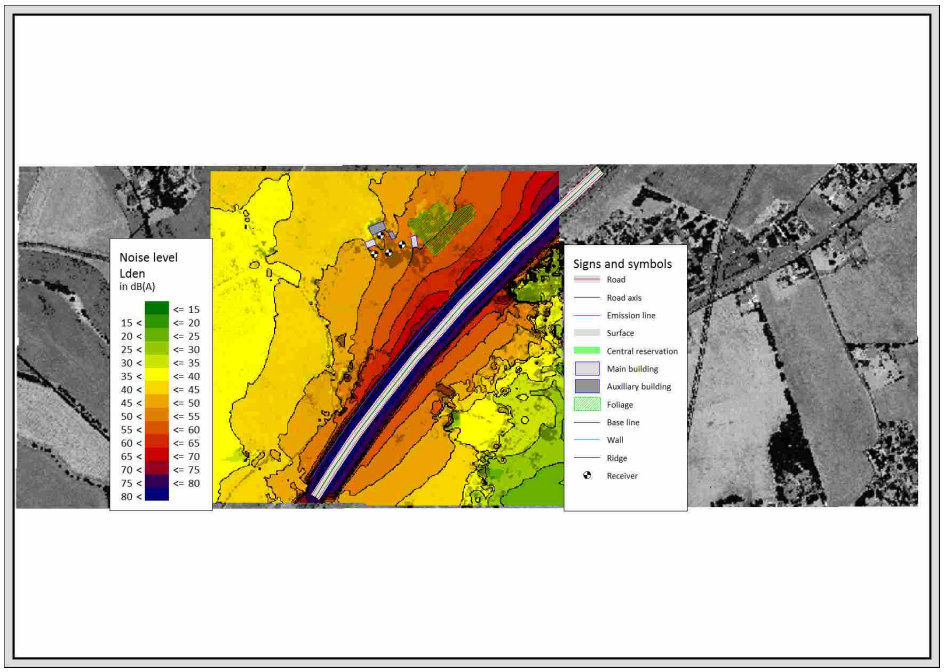

Figure C.10: Grid Noise Map based on Nord2000 for the noise indicator L_d without the nearest building to the E18 at Solbergveien 37.

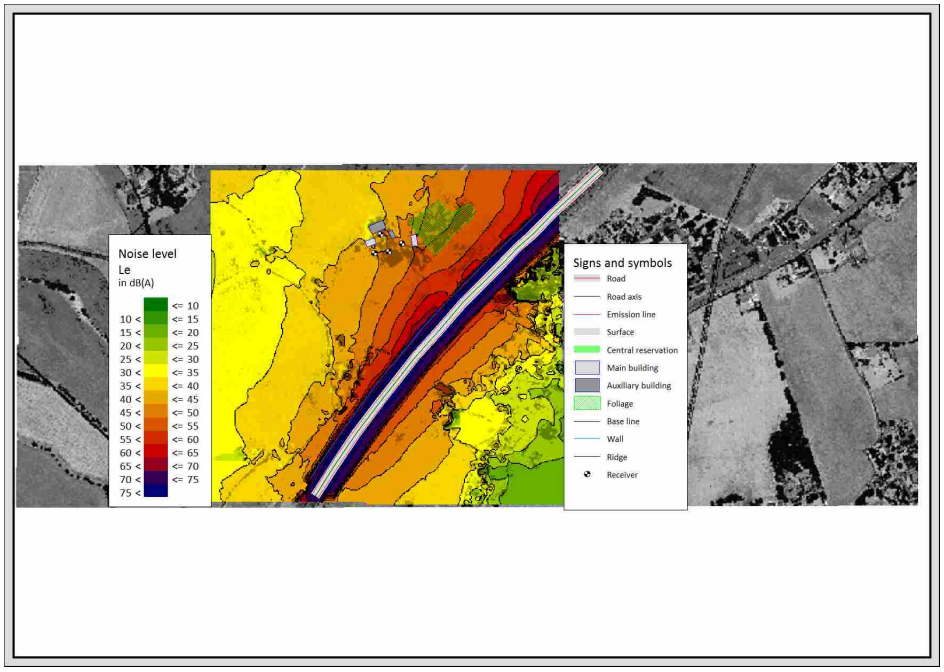

Figure C.11: Grid Noise Map based on Nord2000 for the noise indicator L_e without the nearest building to the E18 at Solbergveien 37.

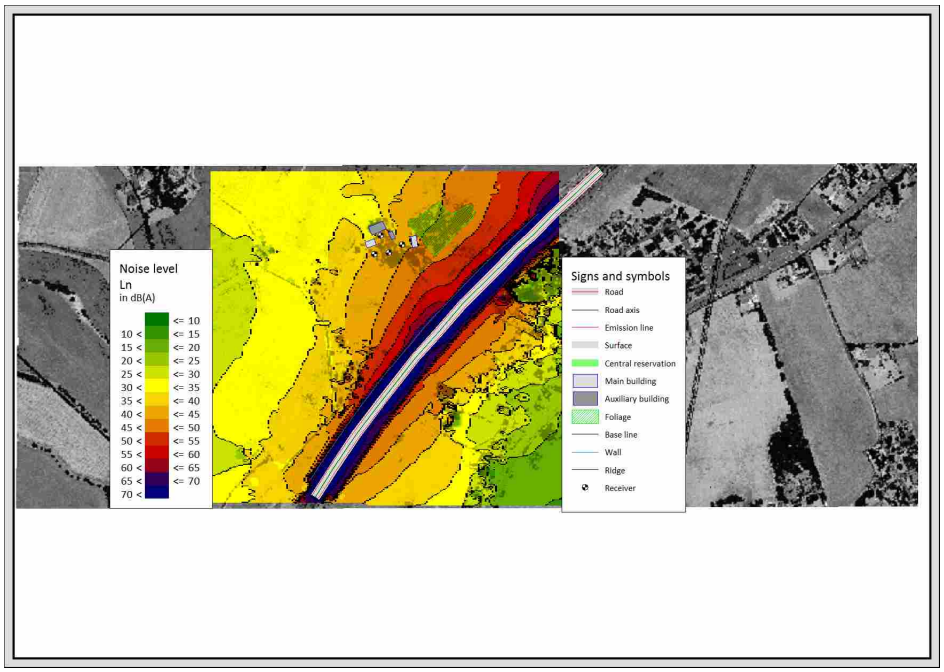

Figure C.12: Grid Noise Map based on Nord2000 for the noise indicator L_n without the nearest building to the E18 at Solbergveien 37.

C.1.1.4 Grid Noise Map based on RLS-90 at Solbergveien 37

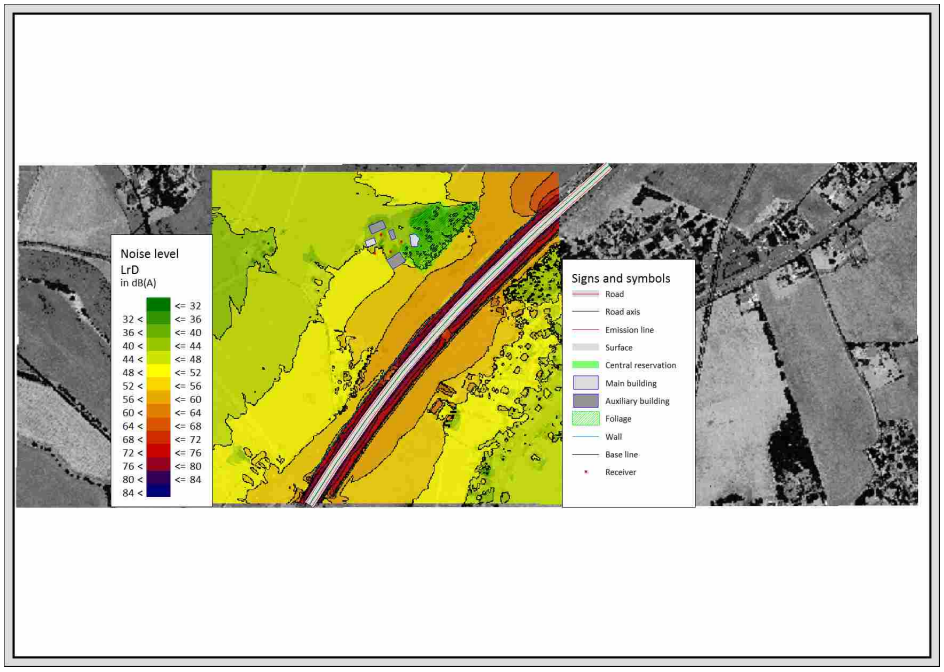

Figure C.13: Grid Noise Map based on RLS-90 for the noise indicator L_{rD} at Solbergveien 37.

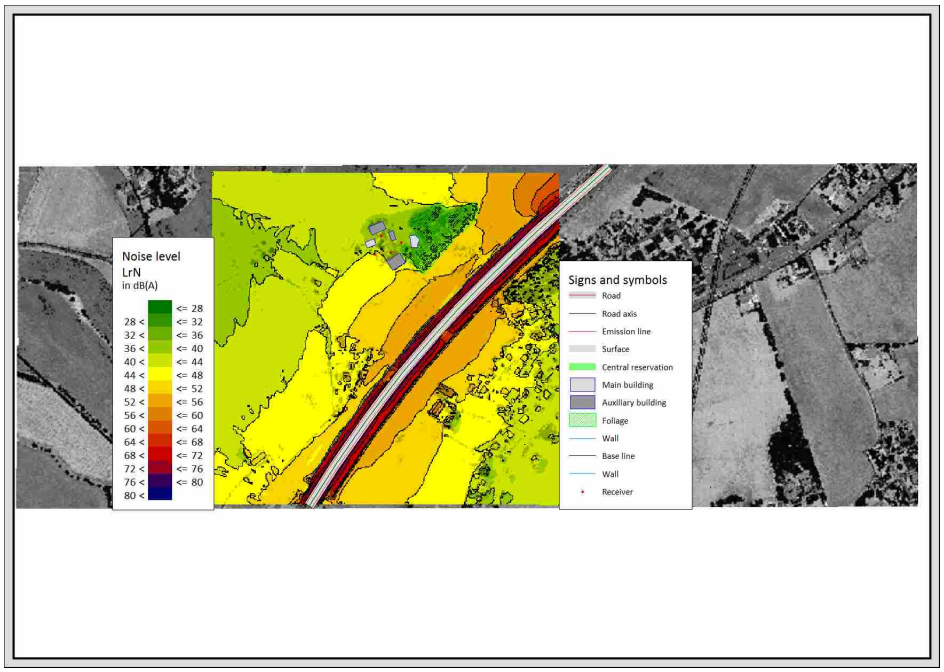

Figure C.14: Grid Noise Map based on RLS-90 for the noise indicator L_{rN} at Solbergveien 37.

C.1.1.5 Grid Noise Map based on Nord2000 at Kodalveien 31

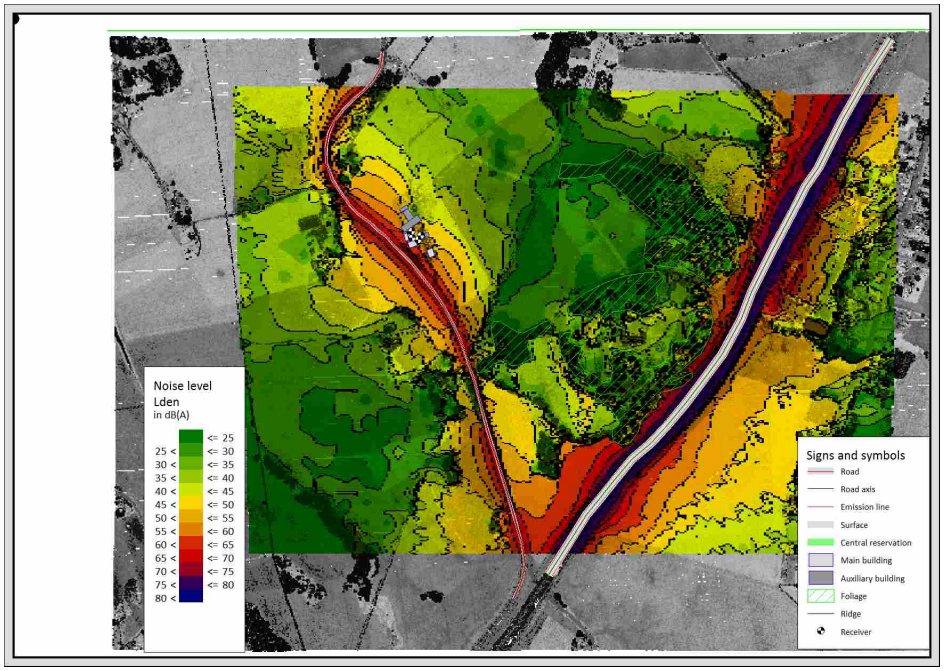

Figure C.15: Grid Noise Map based on Nord2000 for the noise indicator L_{den} at Kodalveien 31.

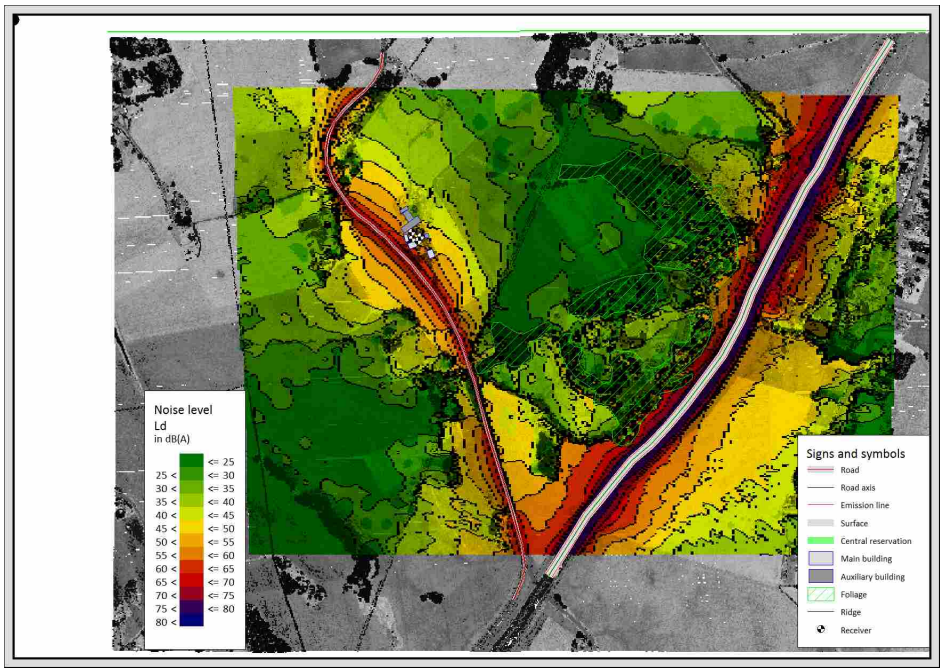

Figure C.16: Grid Noise Map based on Nord2000 for the noise indicator L_d at Kodalveien 31.

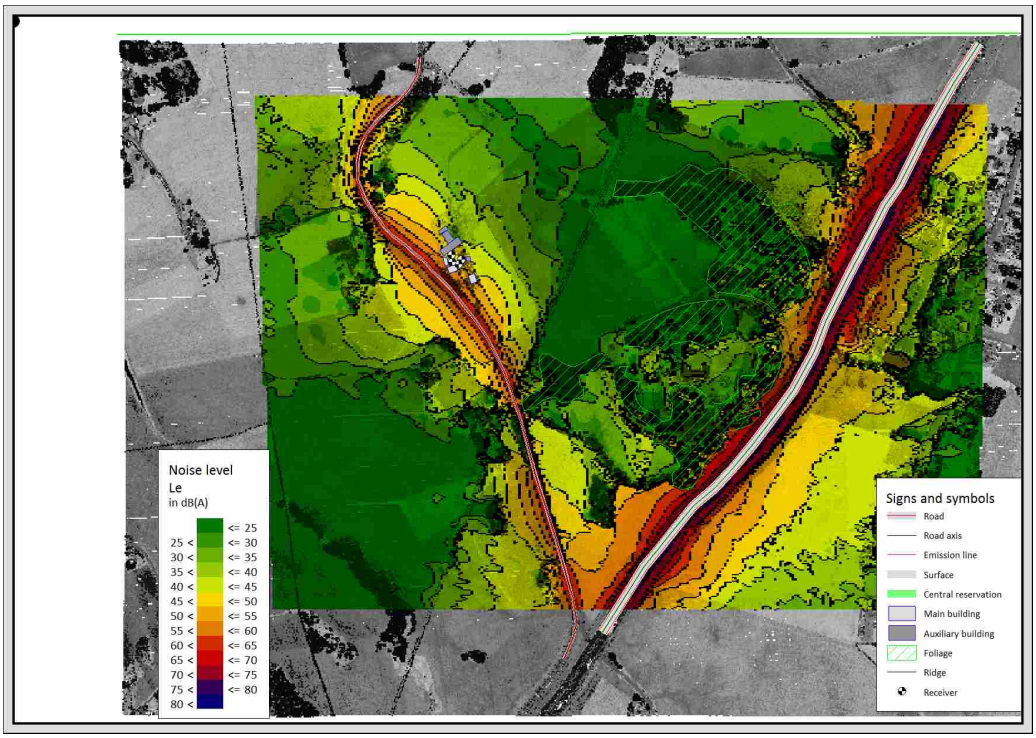

Figure C.17: Grid Noise Map based on Nord2000 for the noise indicator L_e at Kodalveien 31.

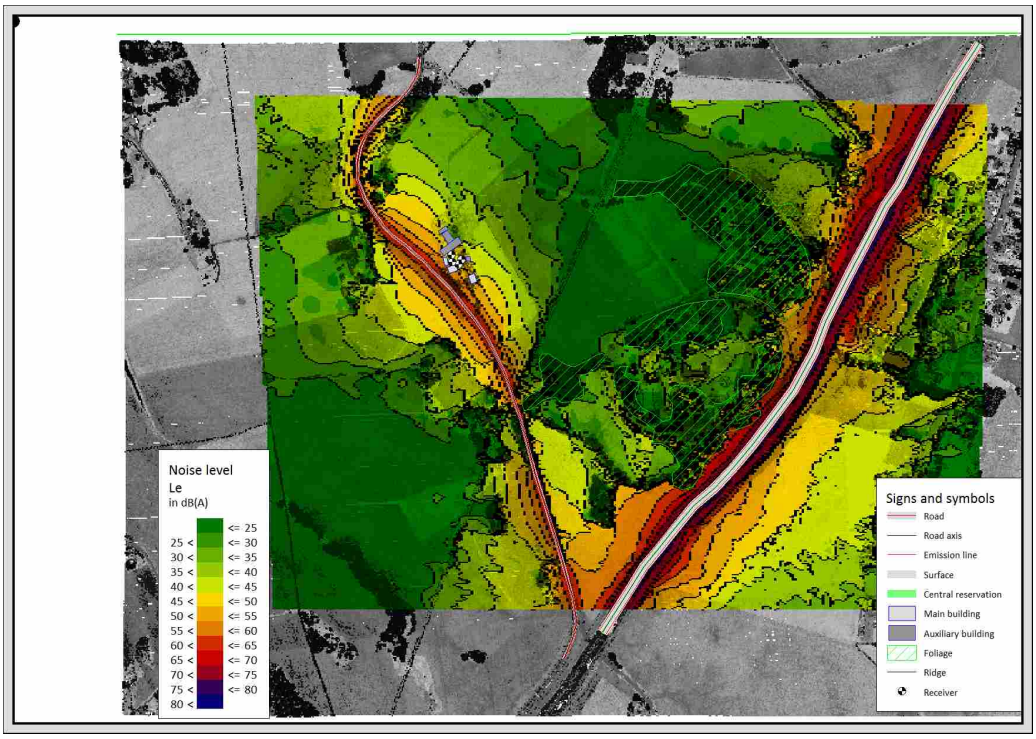

Figure C.18: Grid Noise Map based on Nord2000 for the noise indicator L_e at Kodalveien 31.

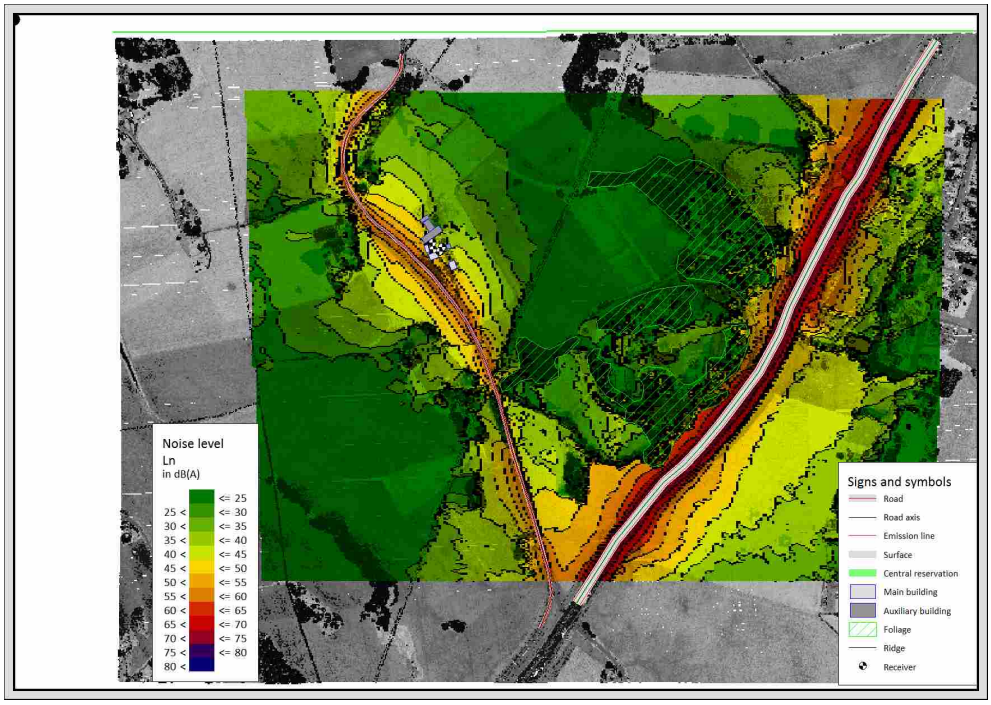

Figure C.19: Grid Noise Map based on Nord2000 for the noise indicator L_n at Kodalveien 31.

C.1.1.6 Grid Noise Map based on RLS-90 at Kodalveien 31

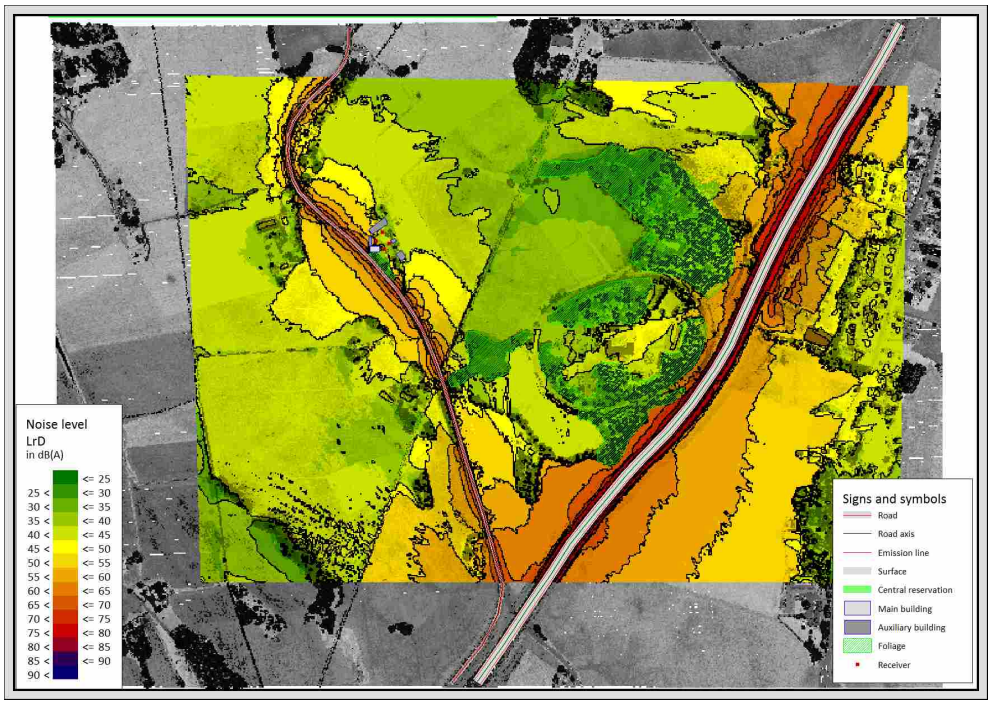

Figure C.20: Grid Noise Map based on RLS-90 for the noise indicator L_{rD} at Kodalveien 31.

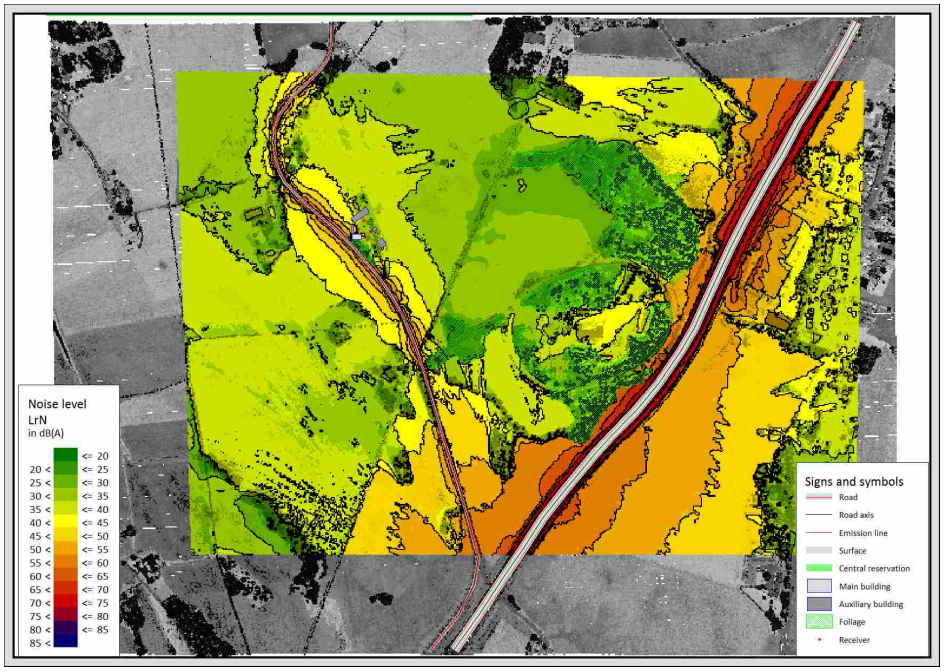

Figure C.21: Grid Noise Map based on RLS-90 for the noise indicator L_{rN} at Kodalveien 31.

C.1.1.7 Grid Noise Map based on Nord2000 in winter at Lånheveien 11

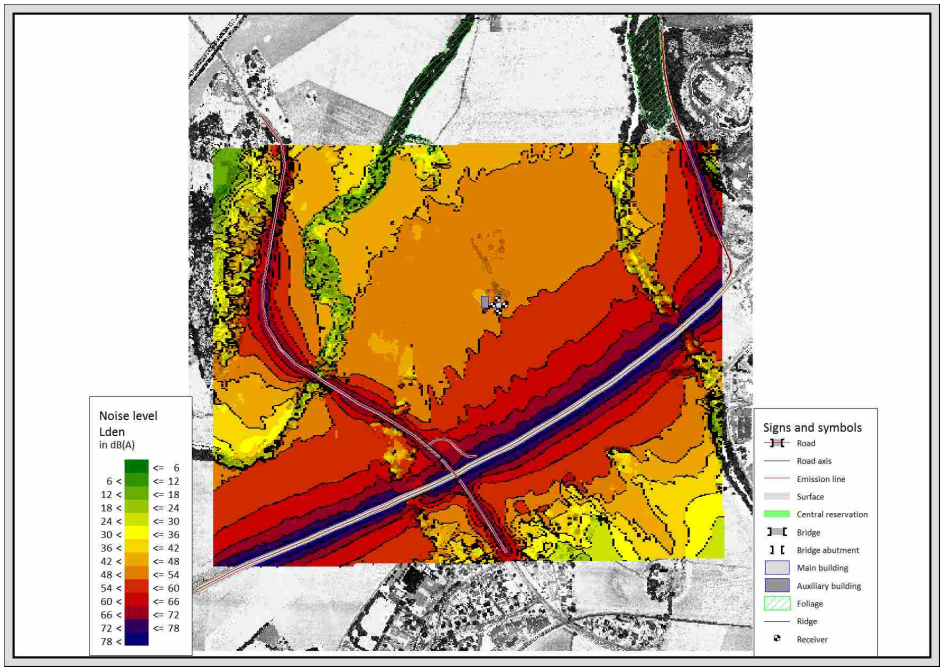

Figure C.22: Grid Noise Map based on Nord2000 for the noise indicator L_{den} in winter at Lånheveien 11.

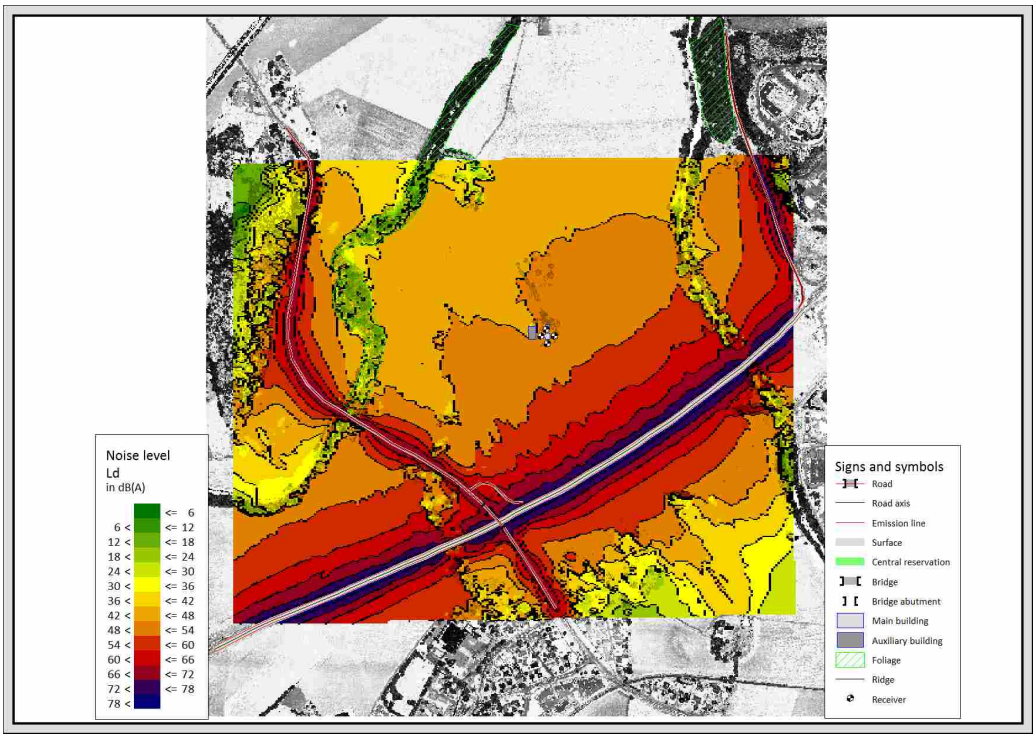

Figure C.23: Grid Noise Map based on Nord2000 for the noise indicator L_d in winter at Lånheveien 11.

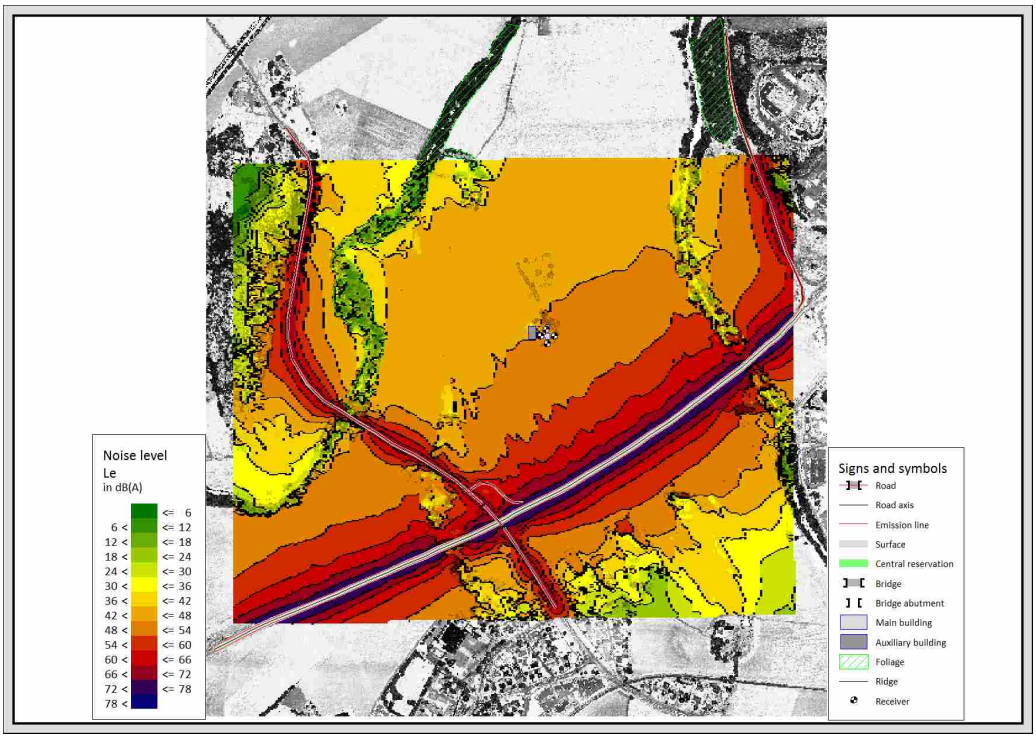

Figure C.24: Grid Noise Map based on Nord2000 for the noise indicator L_e in winter at Lånheveien 11.

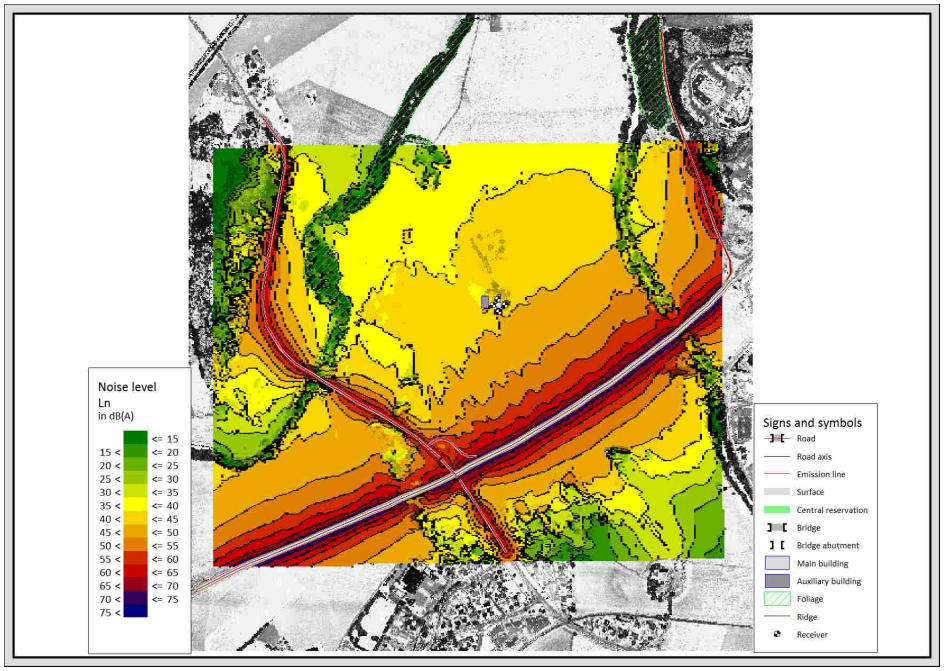

Figure C.25: Grid Noise Map based on Nord2000 for the noise indicator L_n in winter at Lånheveien 11.

C.1.1.8 Grid Noise Map based on Nord2000 in summer at Lånheveien 11

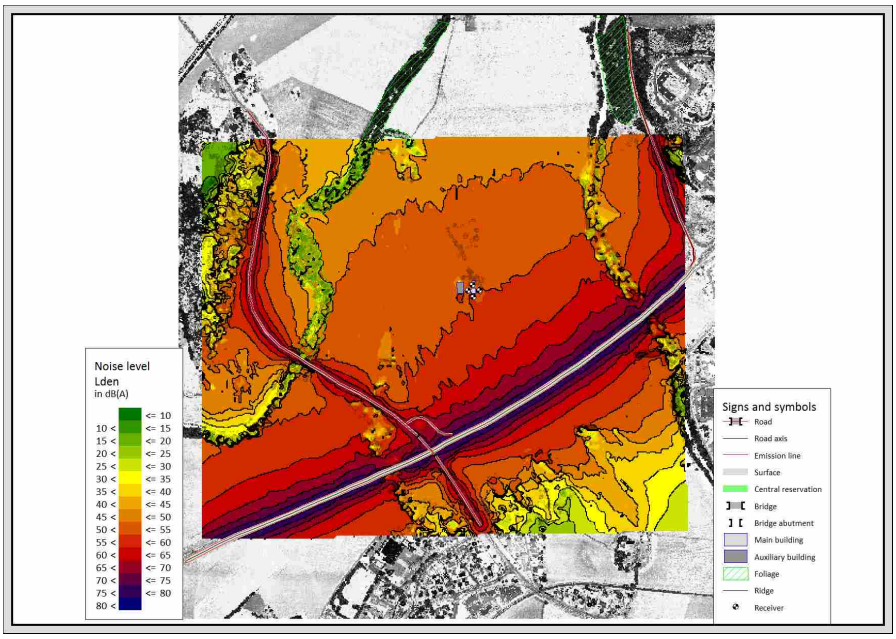

Figure C.26: Grid Noise Map based on Nord2000 for the noise indicator L_{den} in summer at Lånheveien 11.

C.1.1.9 Grid Noise Map based on RLS-90 at Lånheveien 11

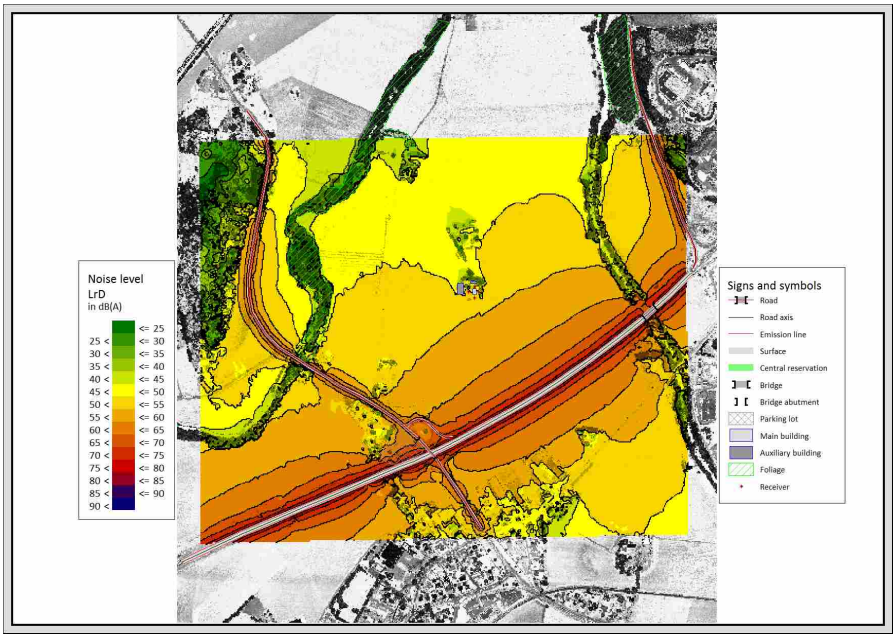

Figure C.27: Grid Noise Map based on RLS-90 for the noise indicator L_{rD} at Lånheveien 11.

D

Appendix-Results

D.1 The measured spectra on February 11th and 12th at Solbergveien 37 on an hourly basis

D.1.1 The spectra on February 11th 2021

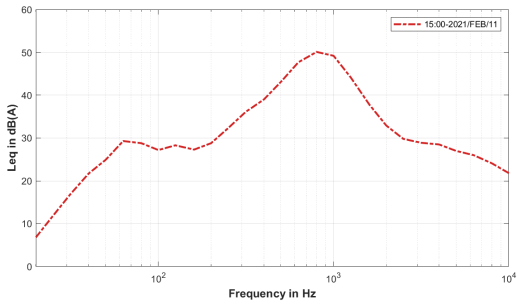

15:00

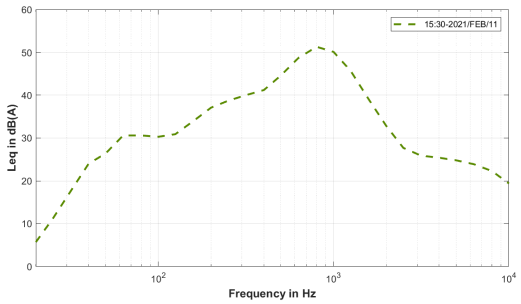

15:30

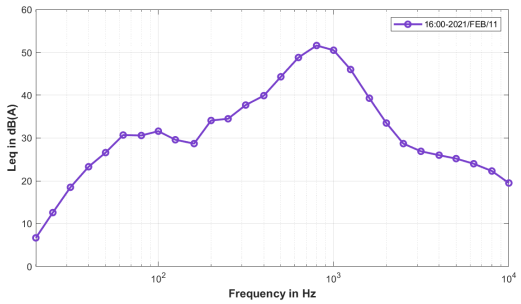

16:00

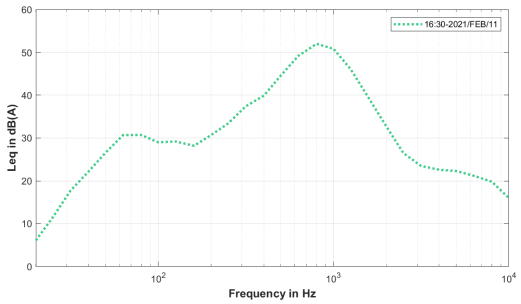

16:30

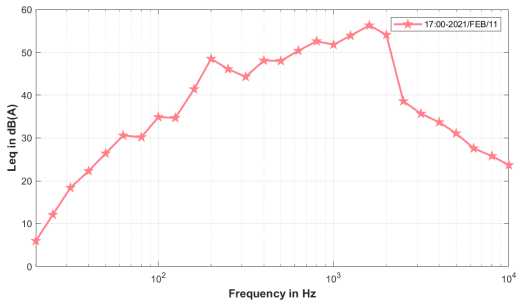

17:00

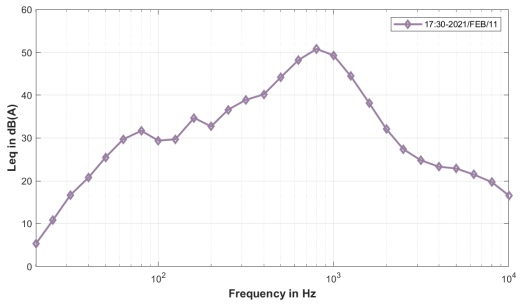

17:30

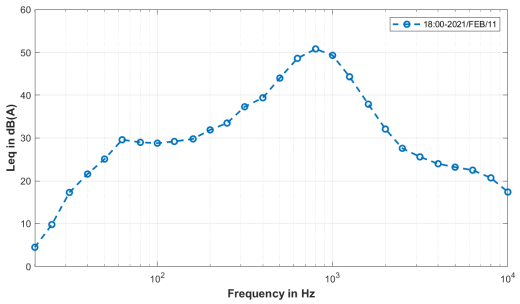

18:00

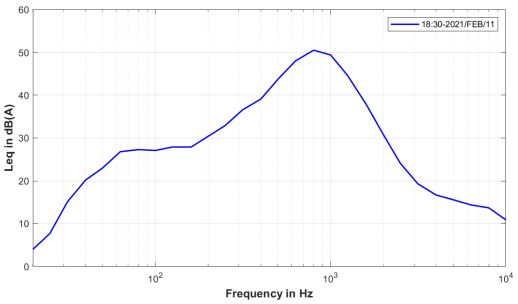

18:30

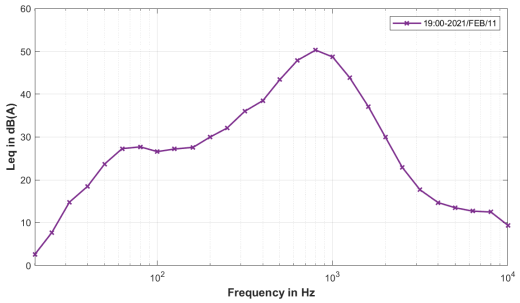

19:00

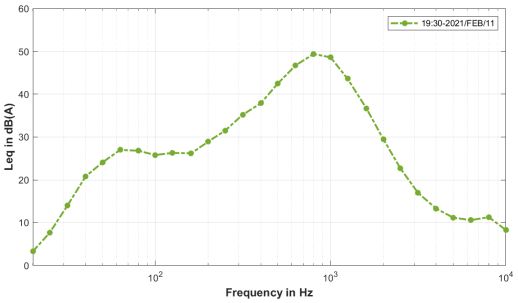

19:30

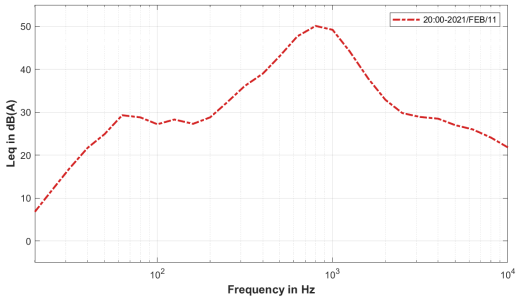

20:00

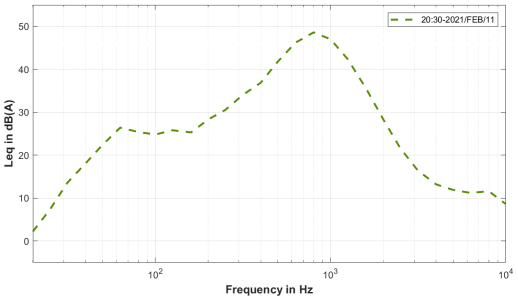

20:30

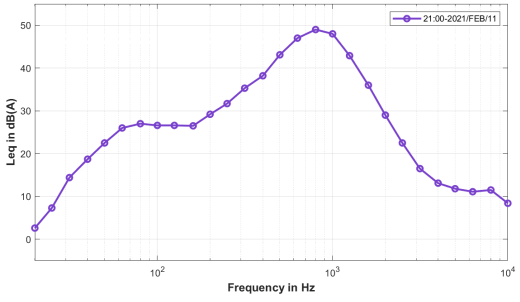

21:00

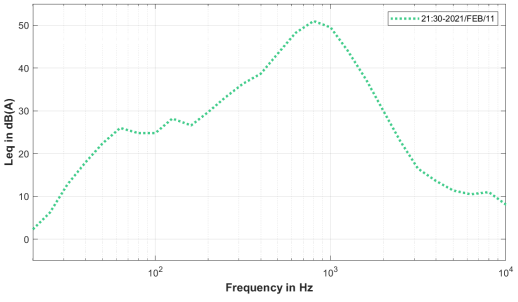

21:30

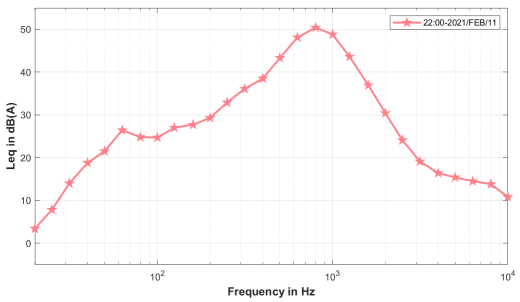

22:00

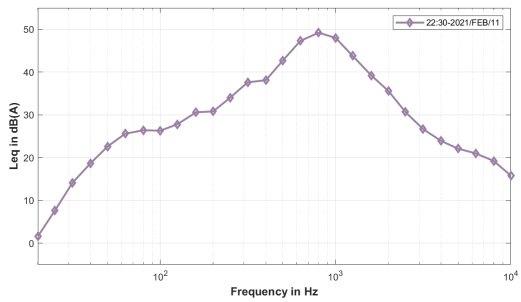

22:30

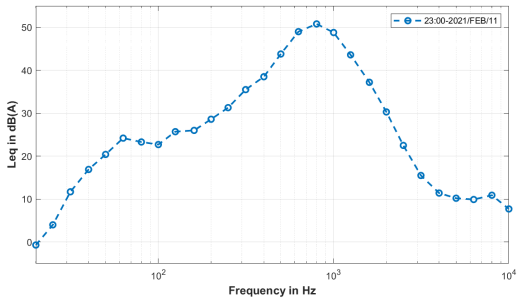

23:00

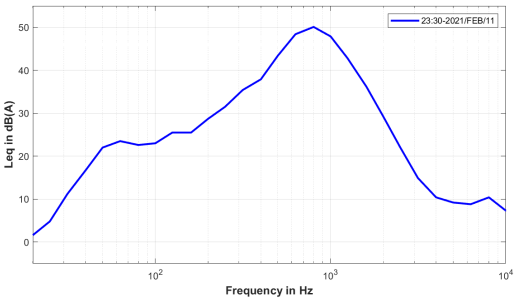

23:30

D.1.2 The spectra on February 12th 2021

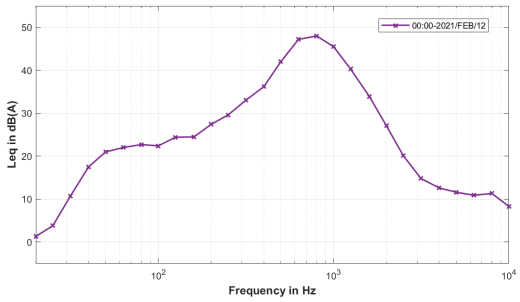

00:00

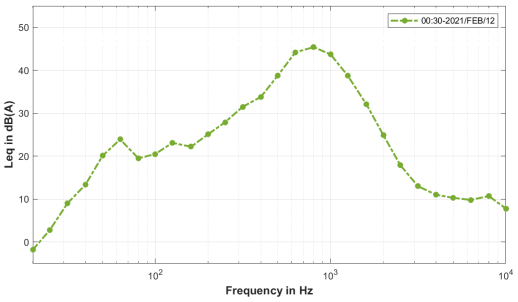

00:30

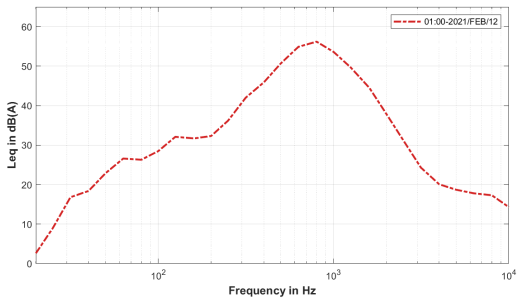

01:00

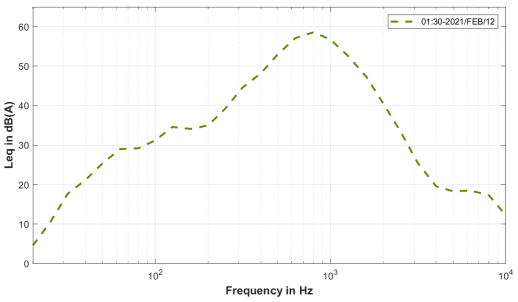

01:30

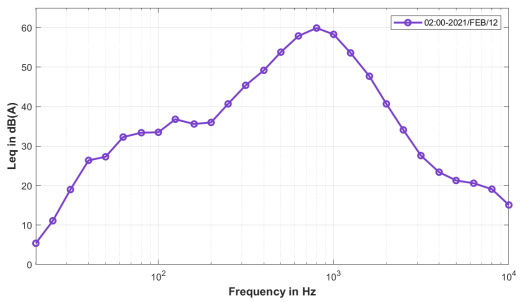

02:00

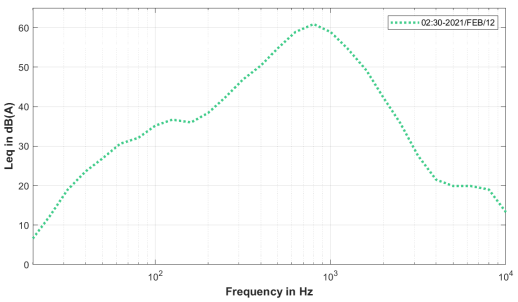

02:30

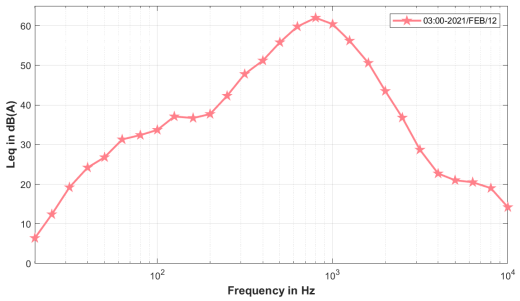

03:00

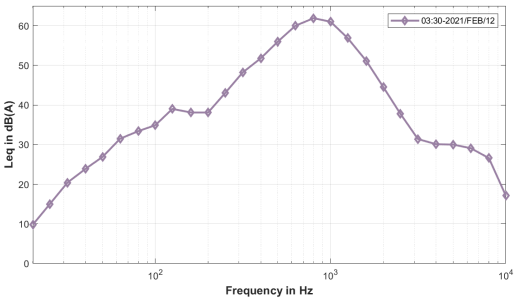

03:30

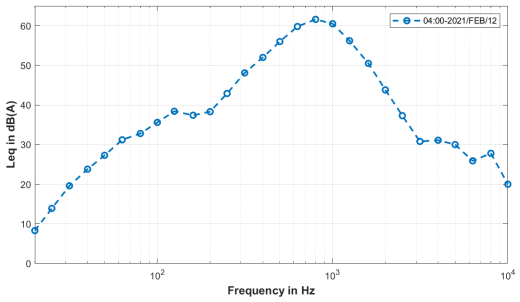

04:00

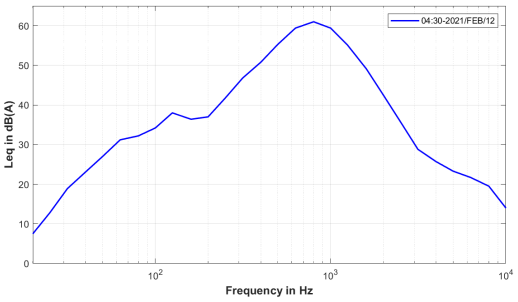

04:30

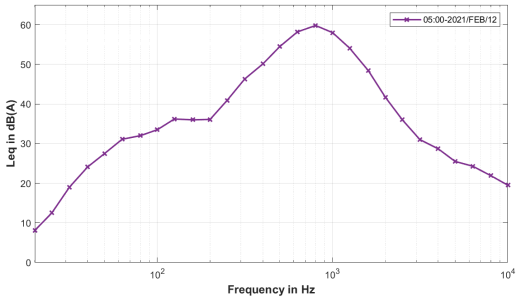

05:00

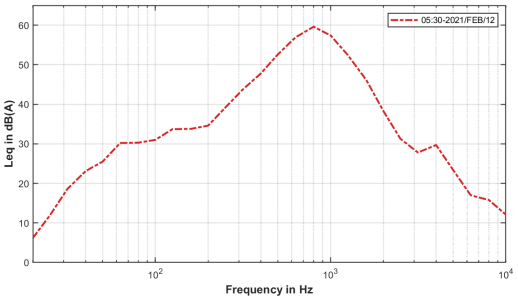

05:30

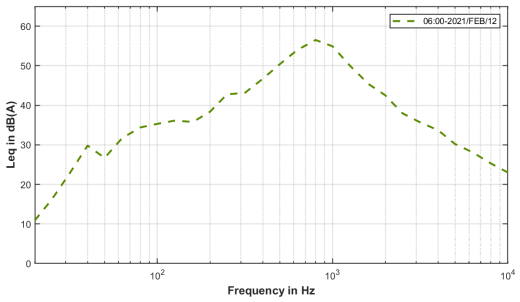

06:00

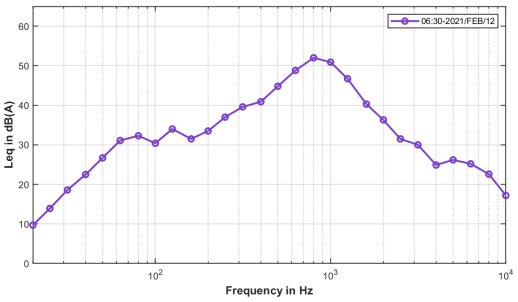

06:30

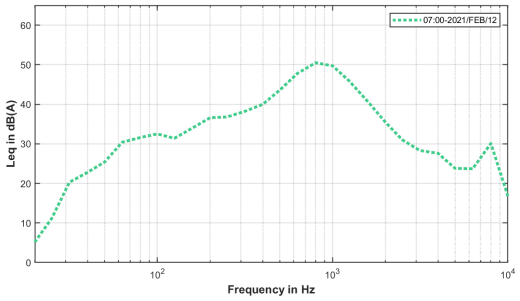

07:00

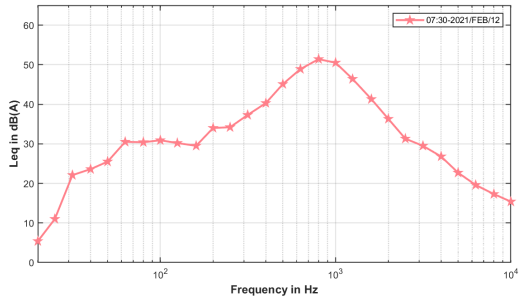

07:30

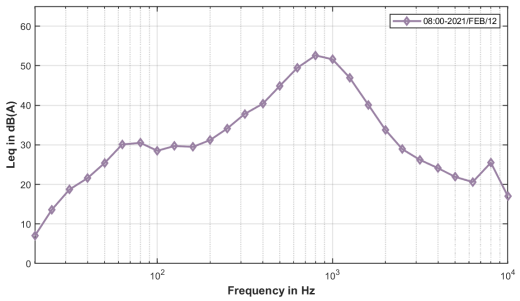

08:00

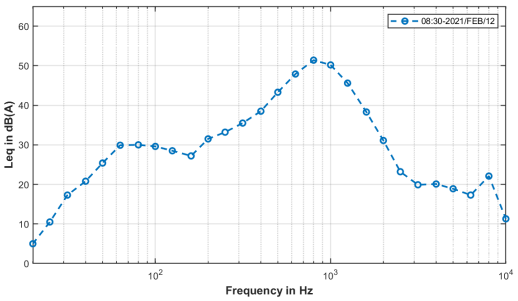

08:30

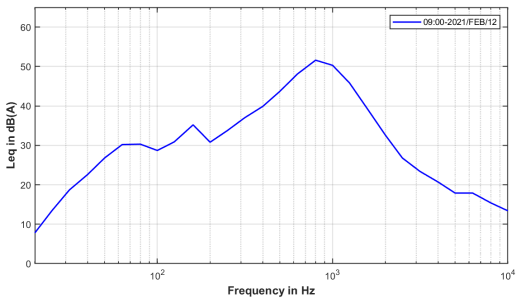

09:00

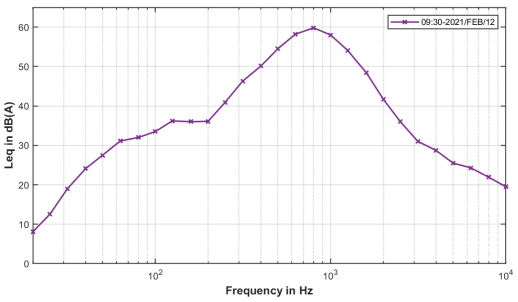

09:30

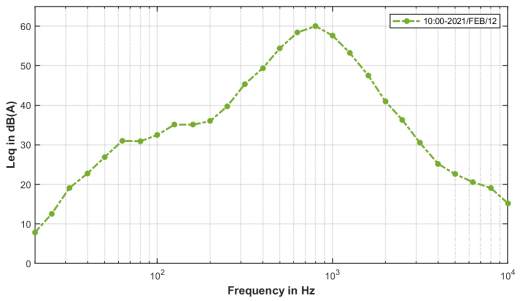

10:00

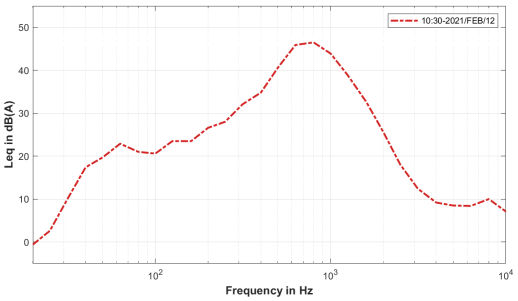

10:30

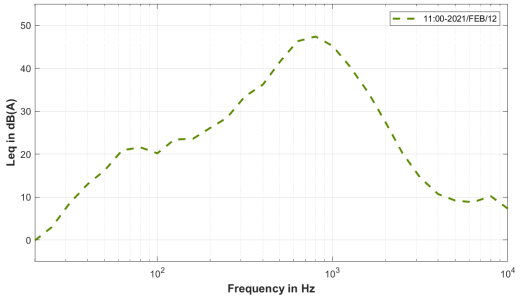

11:00

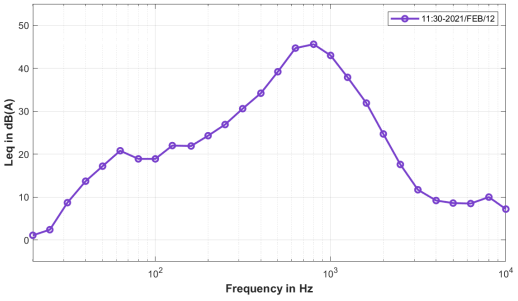

11:30

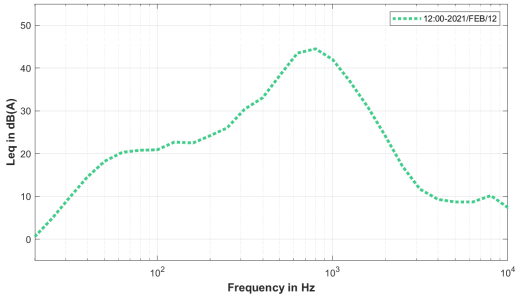

12:00

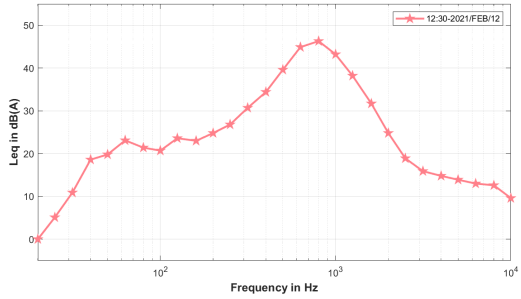

12:30

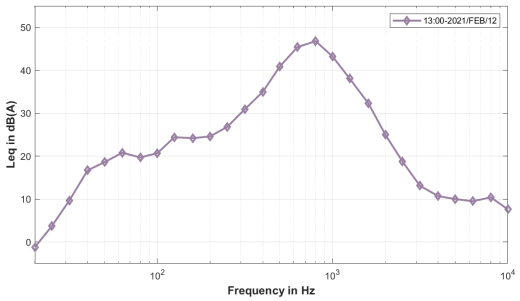

13:00

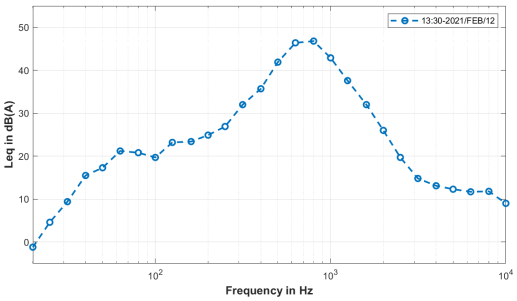

13:30

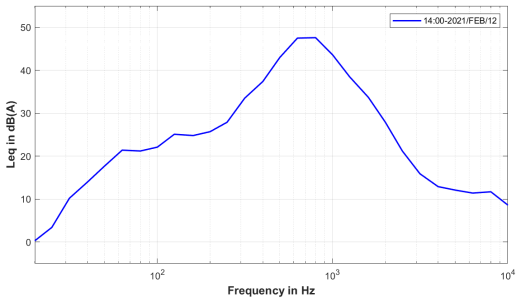

14:00

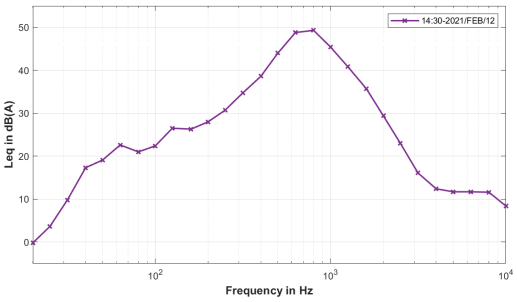

14:30

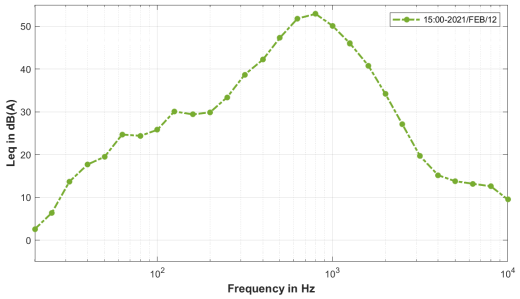

15:00